REGULATION OF NEUROTRANSMITTER SYNTHESIS IN ALZHEIMER'S DISEASE – POTENTIAL FOR NOVEL DISEASE BIOMARKERS

Fred Hudd

Department of Biological, Biomedical and Analytical Sciences,

University of the West of England, Bristol

August 2020

A thesis submitted in partial fulfilment of the requirements of the University of the West of England, Bristol for the degree of Doctor of Philosophy

Dedications and Acknowledgements

I dedicate this work to Helen Hudd and Olive Moncrieffe, you helped to make me the person I am today, and I hope that you would be proud of what I have achieved.

I would also like to acknowledge Professor Myra Conway for the exceptional support throughout my PhD and beyond, she has been instrumental in the completion of my study and furtherment of my career. Furthermore, I would like to acknowledge BRACE for their funding and support of my research.

I would like to thank Dr Tim Craig, Dr Kathryn Yuill and Dr Carolyn Morgan who have acted as second supervisors throughout my study. I additionally want to thank Dr Man-Kim Cheung for always being happy to help and for his incredible insight, Dr Tom Forshaw, Dr Matthew Harris, Dr Christopher Lee, Dr Maya El-Hindy, Dr Anna Shiel and Dr Jonathon Hull for their help and support throughout my study. I also want to thank Mai Shafei, Grace Okoro, Marcela Usmari Moraes and Jasmine Davis for the great times that we shared in the lab and making long days bearable.

Finally, I would like to thank my parents for their continued support throughout and my wonderful fiancée and soon-to-be wife, Anna, who has always been there to cheer me up through the hardest points of my work and has been more supportive than I could ever ask for, I am forever grateful for everything that she has done for me.

Research Acknowledgements

I want to acknowledge the work carried out by Dr Elizabeth Coulthard and Professor Risto Kauppinen's teams (Bryony Wood, Demi Tsivos, Alfie Wearn and Michael Knight) in the collection of blood samples and cognitive data and MRI imaging. Their collaboration helped to make this work possible.

I would also like to acknowledge Paul White for his help in statistically analysing data collected for chapter five of this thesis. Paul was invaluable in analysing this data and providing guidance to direct the analysis performed

I would like to thank Anna Shiel for her work in the processing initial samples for the development of the LC-MS method used in my work and the initial analysis of these serum samples. Additionally, I would like to thank her for teaching me these techniques.

Finally, I would like to thank Paul Bowlder for his help in the development of my isotope dilution liquid chromatography-tandem mass spectroscopy method. His help was fundamental in my learning and development in this field and in the establishment of a robust analytical tool.

Abstract

Introduction:

There currently is an unmet need for new diagnostics to monitor Alzheimer's disease (AD) and a lack of understanding of the metabolic processes, in particular leucine deprivation on disease and the autophagy pathway. It is thought that there is an altered metabolic profile related to AD that could be used to monitor the progression of patients and offer possible targets for treatment.

Findings:

The results presented show for the first time that measurement of BCATm and the amino acids increased the sensitivity and specificity of MoCA analysis in correctly identifying participants free of AD pathology (100%) but also those with the disease to 90% accuracy, with BCATm and Glutamate, significantly improve the predictive potential of MoCA, and significantly improve the predictive potential of the MRI measures.

Additionally, this research has shown that leucine and nutrient deprivation causes a significant decrease in intracellular glutamic acid and causes increased expression of markers of autophagy Beclin 1 and LC3. Metabolic analysis has additionally shown that in cases of acute leucine deprivation cellular metabolism is significantly altered.

Abbreviations:

ACh – Acetylcholine

AChE - Acetylcholinesterase

AD - Alzheimer's Disease

Aβ – Amyloid Beta

APP – Amyloid Precursor Protein

APOE – Apolipoprotein E

ArAA - Aromatic Amino Acids

BACE - β-site APP cleavage enzyme

BCAA – Branched Chain Amino Acid

BCKDC - Branched-chain Alpha-keto Acid Dehydrogenase Complex

BCAT – Branched Chain Amino Transferase

CTF – C-Terminal Membrane-Bound Fragment

CSF – Cerebral Spinal Fluid

CMA - Chaperone Mediated Autophagy

FCCP - 4-(trifluoromethoxy)phenylhydrazone

FDG – Fluoro-deoxy-d-glucose

GABA - Gamma-aminobutyric Acid

HPLC – High Performance Liquid Chromatography

HVLT - Hopkin's Verbal Learning Test Revised

hBCAT – Human Branched Chain Amino Transferase

hBCATc - Human Branched Chain Amino Transferase Cytosolic Isoform

hBCATm - Human Branched Chain Amino Transferase Mitochondrial Isoform

IEC - Ion Exchange Chromatography

ID-LC-MS/MS – Isotope Dilution Liquid Chromatography Tandem Mass Spectroscopy

LNAA – Large Neutral Amino Acids

LAT1 - Large Neutral Amino Acid Transporter

LC-MS - Liquid Chromatography Mass Spectroscopy

LC-MS/MS - Liquid Chromatography Tandem Mass Spectroscopy

LC3 - Microtubule-associated Light Chain 3 Phosphatidylethanolamine

MRI – Magnetic Resonance Imaging

mTORC - Mechanistic Target of Rapamycin Complex

MCI – Mild Cognitive Impairment

MoCA – Montreal Cognitive Assessment

MRM – Multiple Reaction Monitoring

NDMA - *N*–methyl-D-aspartate

NMDAR - N-methyl-d-aspartate Receptors

PI3KC3 - Beclin1-class III phosphatidylinositol 3-kinase

PKA - cAMP-dependent Protein Kinase

PAL - Paired Associative Learning

PIB – Pittsburgh Compound B

PET – Positron Emission Tomography

ROS – Reactive Oxygen Species

TBI – Traumatic Brain Injury

WHO - World Health Organisation

Table of Contents:

DEDICATIONS AND ACKNOWLEDGEMENTS ..... **I**

RESEARCH ACKNOWLEDGEMENTS ..... **II**

ABSTRACT ..... **III**

INTRODUCTION: III

FINDINGS: III

ABBREVIATIONS: ..... **IV**

TABLE OF CONTENTS: ..... **VI**

TABLE OF FIGURES ..... **X**

CHAPTER 1 – INTRODUCTION **1**

1.1.1 – DEMENTIA 1

1.1.2 - COGNITIVE IMPAIRMENT AND NEURODEGENERATIVE DISEASE 2

1.1.3 - DIAGNOSIS OF AD 5

1.1.4 – CURRENT AND POTENTIAL BIOMARKERS AND DISEASE MARKERS FOR ALZHEIMER'S DISEASE. 8

2.1.1 - ALZHEIMER DISEASE 13

2.1.1.1 – The Amyloid Hypothesis *15*

2.1.1.2 – Microtubule-Associated Protein Tau Hypothesis *19*

2.1.1.3 – The Cholinergic and Glutamatergic Hypothesis *21*

2.1.1.4 – Treatment of Alzheimer's Disease *23*

2.1.2 – AUTOPHAGY 24

2.1.3 - FUNCTION OF THE BRANCHED CHAIN AMINO ACIDS IN THE BRAIN 28

2.1.3.1 – Branched Chain Amino Acids in Disease *35*

2.1.3.2 - Branched Chain Amino Acid Supplementation *35*

SUMMARY 36

CHAPTER 2 – AIMS AND OBJECTIVES **38**

2.1 – HYPOTHESIS 38

2.2 – Aim One 38

2.3 - Aim Two 38

2.3 - Aim Three 38

CHAPTER 3 – MATERIALS AND METHODS 39

3.1 - Materials 40

3.2 - Antibodies 44

3.4 - Ethical Statement and Participants 45

3.5 - Methods 46

3.5.1 - Cognitive Assessment of Control, MCI and AD 46

3.5.2 – Magnetic Resonance Imaging (MRI) of Control, MCI and AD 47

3.5.3 – Blood Biomarkers for Control, MCI and AD 47

3.5.5 - Protein Estimation Using the Amido Black Assay 48

3.5.6 - Wet Transfer Western Blot Analysis 48

3.5.7 - 1D Gel Electrophoresis 49

3.5.8 - ApoE Genotyping 49

3.5.9 - PCR Amplification of ApoE Coding Region 50

3.5.10 - HhaI Restriction Digest 50

3.5.11 – Visualisation of HhaI Digested Products 50

3.5.12 - Preparation of Amino Acid Standards and Calibrators 51

3.5.13 - Serum and Fluid Sample Preparation 51

3.5.14 – Cell Sample Preparation 51

3.5.15 - Determination of Precursor Ions 52

3.5.16 - Determination of Product Ions 52

3.5.17 - Optimisation of Acquisition Parameters 53

3.5.18 - Sample Analysis for Branched Chain and Aromatic Amino Acids 53

3.5.19 - Percentage Recovery 54

3.5.20 – Sample Stability 54

3.5.21 - Statistical Analysis 54

3.5.22 - Cell Culture *55*

3.5.23 - Nutrient Deprivation *55*

3.5.24 - Leucine Deprivation *56*

3.5.25 - Leucine Supplementation *56*

3.5.26 - Protein Estimation Using Micro-Bradford Assay *56*

3.5.27 - Seahorse Assay: Cell Culture *57*

3.5.28 - Seahorse Assay *57*

3.5.29 - Crystal Violet Post Normalisation *58*

CHAPTER 4 – DEVELOPMENT OF AN ISOTOPE DILUTION LIQUID CHROMATOGRAPHY TANDEM MASS SPECTROSCOPY METHOD **60**

4.1 – INTRODUCTION 60

4.2 – SPECIFIC AIMS 62

4.3 – RESULTS 63

4.3.1 – Identification of BCAA and AAA Precursor Ions and Determination of Product Ions *63*

4.3.2 – Mass Spectrometer Source Optimisation *66*

4.3.3 – Published Chromatography and Developmental Method Chromatography Comparison *71*

4.3.4 – Chromatographic Separation of Amino Acids *73*

4.3.5 – Linearity of Amino Acids Standard Concentration *74*

4.3.6 – Intra-Run and Inter-Run Assay Variation of Analysed Samples *74*

4.3.7 – Analytical Recoveries of Amino Acid Standards, Serum and Cell Lysates *80*

4.3.8 – Serum Sample Stability *80*

4.4 – DISCUSSION 83

CHAPTER 5 – NOVEL BLOOD BIOMARKERS THAT CORRELATE WITH COGNITIVE PERFORMANCE AND HIPPOCAMPAL VOLUMETRY – POTENTIAL FOR EARLY DIAGNOSIS OF ALZHEIMER'S DISEASE DEMENTIA **88**

5.1 – INTRODUCTION 88

5.2 - SPECIFIC AIMS 91

5.3 – Results 92

5.3.1 – Clinical Data and ApoE Genotyping 92

5.3.2 – Increased BCAT Expression in Alzheimer's Disease Reflects Brain Patterns 95

5.3.3 – Increased Levels of Glutamate in AD Serum Differentiate Between Groups 95

5.3.4 – Differentiation Between Participant Groups 96

5.5 – Discussion 111

CHAPTER 6 – THE EFFECT OF LEUCINE DEPRIVATION ON CELLULAR METABOLISM 118

6.1 - Introduction 118

6.2 – Specific Aims 121

6.3 – Results 122

6.3.1 – Perturbations in the Levels of Glutamic Acid, BCAAs and AAAs in Leucine and Nutrient Deprived Conditions 122

6.3.1 – The Effect of Leucine and Nutrient Deprivation on Autophagy and the Expression of hBCATc 122

6.3. - Assessment of Mitochondrial Function in Neuronal Model SH-SY5Y under Conditions of Leucine Deprivation, Nutrient Deprivation and in Response to Leucine Supplementation 129

..... 131

6.4 Discussion 137

CHAPTER 7 – FUTURE WORK 143

7.1 – Expansion of Biomarker Data Set 143

7.2 – Evaluating the Effect of hBCAT Knockdown and Overexpression Under Leucine Deprived Conditions 143

BIBLIOGRAPHY: 145

Table of Figures

Figure 1.1 – Illustrative 11C-PIB PET-MR, Negative 11C-PIB-PET-MR and FDG-PET Imaging of Alzhiemer's disease brain. 11

Table 1.1 – Genes associated with Alzheimer's disease 17

Figure 1.2 – Autolysosome formation in autophagy 26

Figure 1.3 - Regulation of autophagy by nutrients and hormones via the mammalian target of rapamycin (mTOR) signalling pathway. 29

Figure 1.4: Transport of branched chain amino acids across the blood brain barrier and the function of hBCAT in branched chain amino acid metabolism 33

Table 4.3.1 – Composition of deuterium labelled internal standards 64

Table 4.3.2 – Precursor ions and fragmentor voltage for deuterium labelled and unlabelled amino acid standards 64

Table 4.3.3 Product ion transitions and required fragmentor voltage and collision energy for deuterium labelled and unlabelled amino acid standards 65

Table 4.3.4 Baseline and source optimised flow and compound dependent parameter values for sample analysis 66

Table 4.3.5 Comparative percentage difference of spectral count for glutamic acid, isoleucine, leucine, phenylalanine, tyrosine and valine between baseline method and source optmised method 67

Table 4.3.6 Comparative percentage difference of spectral count for deuterium labelled glutamic acid, isoleucine, leucine, phenylalanine, tyrosine and valine between baseline method and source optmised method 68

Table 4.3.7 Comparative percentage difference of absorbance for glutamic acid, isoleucine, leucine, phenylalanine, tyrosine and valine between baseline method and source optmised method 69

Table 4.3.8 Comparative percentage difference of absorbance for deuterium labelled glutamic acid, isoleucine, leucine, phenylalanine, tyrosine and valine between baseline method and source optmised method 70

Figure 4.3.1: Comparison of Chromatographic Separation using a Waters XBridge RP18 Column. 72

Figure 4.3.2: Multiple reaction monitoring chromatogram of branched chain (Ile, Leu and Val), aromatic (Tyr and Phe) amino acids and glutamic acid. 73

Table 4.3.9 - Calibration parameters for glutamic acid, isoleucine, leucine, phenylalanine, tyrosine and valine for ID-LC-MS/MS analysis. 74

Figure 4.3.3: Representative calibration curves for glutamate, isoleucine, leucine, phenylalanine, tyrosine and valine. 75

Table 4.3.10 Intra-run and inter-run method variation for control participant serum samples 76

Table 4.3.11 - Intra-run and inter-run variation for mild cognitive impairment participant serum samples 77

Table 4.3.12 Intra-run and inter-run variation for Alzheimer's disease participant serum samples. 78

Table 4.3.13 Intra-run and inter-run variation for control cell lysate samples 79

Table 4.3.14 Analytical recoveries of the LC-MS/MS method 81

Table 4.3.15 – Variation of samples stored at -80°C for a three-month and six-month period 82

Table 5.3.1 – Clinical presentation and ApoE genotype of participants 93

Figure 5.3.1: Distribution of ApoE genotypes between control, MCI, AD and all participants. 94

Figure 5.3.2 Western blot analysis of BCAT in serum from control, MCI and AD participants. 98

Table 5.3.2 – BCATc and BCATm (mean ± standard deviation) summarised by participant group 99

Table 5.3.3 – Amino acid levels (μmol/L) in the serum of control, MCI and AD participants 99

Figure 5.3.3 - Amino acid profiles of control, MCI and AD participants 100

Table 5.3.4 – Cognitive data (mean ± standard deviation) summarised by participant group 104

Table 5.3.5 – Subfield volumes for AD, MCI and control participants 105

Table 5.3.6 – Correlation analysis with MoCA 106

Table 5.3.7 - Percentage accuracy under leave one-out-out (L-O-O) cross-validation of baseline linear discriminant model (A) (MoCA (B) or Dentate Gyrus (C)) and extended model, along with p-value for inclusion of additional parameter in the baseline ordinal regression model. Optimal sensitivity and specificity for MCI and AD combined, and AD only using the ordinal logistic regression model. 107

Figure 5.3.4 - T2-weighted coronal MRI images of healthy elderly control (left) and ADD patient (right). 110

Figure 5.3.5 - Ordinal logistic model of MoCa and BCATm 110

Figure 6.3.1 – Box and whisker plots of cellular lysate Glu, Ile, Leu, Phe, Tyr and Val changes under leucine deprived, nutrient deprived and control conditions over a 72-hour period. 123

Table 6.3.1 – Pairwise comparison of Glu, Ile, Leu, Phe, Tyr and Val under control and leucine deprived condition at 12-hour and 24-hour time points. 124

Table 6.3.2 – Pairwise comparison Glu, Ile, Leu, Phe, Tyr and Val under control, leucine deprived and nutrient deprived conditions analysed at 12 hours. 125

Table 6.3.3 – Pairwise comparison Glu, Ile, Leu, Phe, Tyr and Val under control, leucine deprived and nutrient deprived conditions analysed at 24 hours. 126

Table 6.3.4 – Pairwise comparison Glu, Ile, Leu, Phe, Tyr and Val under control, leucine deprived and nutrient deprived conditions analysed at 48 hours. 127

Table 6.3.5 – Pairwise comparison Glu, Ile, Leu, Phe, Tyr and Val under control, leucine deprived and nutrient deprived conditions analysed at 72 hours. 128

Table 6.3.6 – Expression levels of BCATc, Beclin 1 and LC3 in cell maintained under control and leucine deprived conditions 130

Figure 6.3.2 – Western blot analysis of BCATc, Beclin 1 and LC3 in the cellular lysate of SH-SY5Y cells maintained under leucine deprived conditions. 131

Figure 6.3.3 – Western blot analysis of BCATc, LC3I/II, pmTOR and mTOR in the cellular lysate of SH-SY5Y cells maintained under leucine deprived conditions over 72 hours. The protein concentration of cellular lysate samples was calculated using the Schaffner and Weissmann method (Schaffner W, 1973) and separated on a NuPAGE® Novex® 4-12% Bis-Tris followed by Western blot analysis using antibodies specific for hBCATc, LC3I/II pmTOR and mTOR. Positive bands were visualised using chemiluminescent HRP substrate and an Odyssey® Fc Imaging System (LI-COR Biosciences). (n =2). 132

Figure 6.3.4 – Normalised oxygen consumption rate data from analysis of SH-SY5Y cells under normal, leucine deprived, nutrient deprived and leucine supplemented conditions. 133

Figure 6.3.5 – Normalised extracellular acidification rate data from analysis of SH-SY5Y cells under normal, leucine deprived, nutrient deprived and leucine supplemented conditions 134

TABLE 6.3.7 – PAIRWISE COMPARISON OF OXYGEN CONSUMPTION RATE AND EXTRACELLULAR ACIDIFICATION RATE OF SH-SY5Y CELLS MAINTAINED UNDER NORMAL (CONTROL), LEUCINE DEPRIVED, NUTRIENT DEPRIVED OR LEUCINE SUPPLEMENTED CONDITIONS. 135

Chapter 1

INTRODUCTION

Fred Hudd

Chapter 1 – Introduction

1.1.1 – Dementia

Dementia is defined as a chronic and progressive clinical syndrome characterised by cognitive decline resulting in interference with social or occupational functioning (Chertkow *et al.*, 2013). Syndromes include; frontotemporal dementia, Lewy body dementia, vascular dementia and Alzheimer's disease (AD). Dementia as a whole has associated social and economic costs with The World Health Organisation (WHO) estimating a spend of US$818 billion on Dementia care in 2015 (W.H.O, 2019). Current therapies fall short in significantly delaying or controlling the progressive nature of these conditions highlighting the unmet clinical need for new approaches to better understand disease pathology (W.H.O, 2019). Despite recent advances in imaging technology and cognitive assessments there are still significant challenges to better characterize disease onset. The impact of poor diagnostic and prognostic clinical tools will further delay the monitoring of effective treatment, highlighting the need for targeted research in these areas.

The pathological outcome of neurodegenerative disease is dependent on the area of the brain affected and in certain cases defined by the accumulation of specific proteins, in addition to alterations in fundamental processes associated with neuronal dysfunction and death (Dugger and Dickson, 2017). In Parkinson's disease for example, abnormal deposits of α-synuclein result in the selective death of dopaminergic neurons in the substantia nigra causing the impairment of motor function (Naoi and Maruyama, 1999). Additionally, deposits in neurons have been attributed to result in cognitive impairment and visual hallucinations as observed in Lewy body dementia (Duong *et al.*, 2017). This form of dementia

accounts for 5-15% of reported dementia cases (Canada, 2019) and can present with spontaneous parkinsonism (Zupancic *et al.*, 2011). Frontotemporal dementia encompasses disorders affecting the frontal and temporal brain lobes, where neuronal loss causes personality and behavioral changes and unlike other neurodegenerative conditions, pathological expression does not include protein deposits. Furthermore, this form of dementia can occur at a younger age compared to other forms (Duong *et al.*, 2017). Finally, cholinergic neuron loss through the deposition of neuritic plaques and neurofibrillary tangles in the hippocampus and cerebral neocortex gives rise to the typical clinical presentations of AD (Niikura *et al.*, 2006), with reduced synthesis of neurotransmitters including acetylcholine, causing loss of memory and function (Duong *et al.*, 2017). Abnormalities in autophagy, oxidative stress and neuroinflammation are also attributed to many neurodegenerative diseases, which are thought to contribute to disease pathology. However, the associated pathways present a variety of diagnostic or treatable targets.

1.1.2 - Cognitive Impairment and Neurodegenerative Disease

It is expected that a level of cognitive decline occurs with normal aging that is not classified as dementia. A key criteria for diagnosis of Mild Cognitive Impairment (MCI) is the absence of classical dementia (Albert *et al.*, 2011) whereby MCI is considered the transitional stage between normal age and education-related cognition and mild dementia (Petersen, 2007). Changes in age-related cognition with regard to assessment are divided into “crystallised” and “fluid” abilities. Crystallised abilities are defined as cumulative skills and memories from previously acquired knowledge (Murman, 2015). Fluid abilities are defined during cognitive assessment and are determined by participants problem solving ability

and their assessment and processing of new information (Murman, 2015). Educational related cognition is associated to educational attainment with higher education linked to greater cognitive performance under examination (Wilson *et al.*, 2009). Furthermore, educational attainment has been linked to reduced risk of AD and dementia (Stern *et al.*, 1994, Stern, 2009, Bennett *et al.*, 2003). However, there are issues with respect to the relationship of education-related cognition and cognitive decline. Firstly, studies have highlighted analytical differences caused by biased effect estimates through the use of regression-based approaches in early studies (Zahodne *et al.*, 2015) and this is shown to have a strong relation to variables that are associated with cognitive baseline such as years of education (Glymour *et al.*, 2005). Furthermore, in contrast to the reported reduction in cognitive decline for higher educated individuals, studies have shown that no additional years of education from the median of 11 years were associated with slower cognitive decline (Christensen *et al.*, 2004). Moreover, there is not an associated reduction in cognitive decline beyond nine years of education (Lyketsos *et al.*, 1999). Finally, there are considerations that educational attainment results in advantageous cognitive and non-cognitive experiences including intellectually demanding activities and significant use of intellectual resources through problem solving and complex decision making that can affect assessment results (Zahodne *et al.*, 2015, Parisi *et al.*, 2012). These inherent issues with analytical methods and the additional considerations for educational cognitive assessment highlights the requirement for an alternative diagnostic measure for cognitive assessment and prognostic assessment of cognitive decline including MCI.

Initially MCI was used to describe age-related progressive cognitive decline, defined as cognitive impairment of a single domain (Petersen *et al.*, 1999) whereby the domains that could be affected include memory, language, attention, visuospatial abilities and executive functioning. However, this criteria was revised to account for the preservation of functional activity (Petersen, 2004). MCI affects 19% of people age 65 and over (Lopez *et al.*, 2007), approximately 46% of those with MCI will develop dementia within three years compared with the reported 3% of age-matched controls (Tschanz *et al.*, 2006). This significant increase in disease conversion highlights the importance of developing tools to accurately predict and monitor conversion to aid clinicians with prognostic assessment and early treatment programs.

Several clinical subtypes of MCI are known, with the most recognised and researched form being amnestic MCI. Diagnostic criteria for this form include; objective memory impairment for age, referring to a subjective awareness of initial memory decline, which cannot be detected using current standardised cognitive assessment (Alegret *et al.*, 2015), preserved general cognitive function, largely intact functional domain activities including problem solving, reasoning or the ability to understand others and no presentation of dementia (Petersen, 2004). The presentation of impairment in multiple cognitive domains, including or not including memory impairment, is classified as multiple domain-MCI (Petersen, 2004). Normally affected domains in this subtype can include language, executive function and visuospatial skills (Petersen, 2004). The least common form of MCI is single non-memory domain MCI, where the domain type that is impaired in this form is the same as md-MCI.

Of those diagnosed with MCI, a specific subset, which includes those with amnestic MCI, has an increased likelihood of progression to AD (Cooper *et al.*, 2015). However, those that present may not progress to develop AD or dementia. Currently, treatment methods or prognostic outcomes for MCI are limited with neither UK nor the US health services recommending drug treatments (Cooper *et al.*, 2015). Recent investigations have found no consistent evidence of any intervention reducing the risk of dementia or cognitive decline associated with MCI (Cooper *et al.*, 2013, Cooper *et al.*, 2015). The lack of evidence in treatment efficacy and prognostic assessment indicates a significant need for the development of new and novel treatments and diagnostic/prognostic tools. Similar issues with diagnosis and treatment are seen with other neurodegenerative diseases, including Parkinson's disease and frontotemporal dementia.

1.1.3 - Diagnosis of AD

Definitive diagnosis of AD requires post-mortem examination of brain tissue to identify amyloid plaques and neurofibrillary tangles. The original criteria was established and defined by National Institute of Neurological and Communicative Disorders and Stroke - AD and Related Disorders Association for the clinical assessment of patients (McKhann *et al.*, 1984). Assessment of the disease involves categorisation of patients as having possible or probable AD. Probable AD presents with typical onset of dementia with progression and no other systemic or brain disease present that could cause progressive memory and cognitive deficit (McKhann *et al.*, 1984). Possible diagnosis is applied in cases where the presentation or disease course is considered aberrant. These criteria are based on a variety of clinical examinations including the use of a battery of cognitive tests, with the most common test applied being the Mini-Mental State

Examination (Folstein *et al.*, 1975). In addition to clinical examination other considerations are considered relating to; the number of cognitive areas affected, the progressive worsening of cognitive function including aphasia, apraxia and agnosia and the lack of disturbance in consciousness (McKhann *et al.*, 1984). Recently the introduction of a variety of imaging techniques have been included in the clinical assessment of patients with possible AD.

Imaging analysis has had a range of roles in the study and diagnosis of AD with its clinical introduction looking to reduce the uncertainty of clinical diagnosis and offer a further non-invasive form of examination. Computed tomography and magnetic resonance imaging (MRI) have been used in an exclusionary manner to rule out possible other causes of dementia or brain injury (Johnson *et al.*, 2012). However, developments and additional technology have now allowed imaging to be implemented as a diagnostic measure through the identification of characteristic signatures for both structural and functional cerebral alterations. Additionally, specific assessment of amyloid deposits can be achieved with amyloid imaging (Johnson *et al.*, 2012).

Two forms of MRI imaging are now currently utilised, the first, structural MRI, allows for the assessment of brain atrophy or changes in tissue characteristics. Cerebral atrophy is thought to arise from dendritic and neuronal losses resulting in declining cognitive function, with MRI brain volume analysis shown to be closely related to neuronal counts (Bobinski *et al.*, 2000, Jack *et al.*, 2002, Gosche *et al.*, 2002). MRI has additional utility in the assessment of the functional integrity of brain networks and an indirect measure of neuronal activity. The measurement of blood oxygen levels changes while patients perform cognitive activities involving

the processing of new information (Ogawa *et al.*, 1990, Kwong *et al.*, 1992). These are considered to reflect neuron synaptic activity with decreased hippocampal activity shown in AD patients (Rombouts *et al.*, 2000). These findings together highlight MRI assessment as a potential utility for the diagnosis of Alzheimer's, however, currently their main adoption has been investigator-initiated-add-on-studies.

Positron emission tomography (PET) has also been utilised to study cerebral metabolism with fluoro-deoxy-d-glucose (FDG) and conduct amyloid imaging studies through the use of amyloid tracers. Studies have shown that these techniques can identify characteristic changes associated with AD. The brain's reliance on glucose for an energy source has allowed for the assessment of synaptic activity using FDG-PET whereby FDG, a glucose analogue, is labelled with Fluorine-18 and monitored by PET (Johnson *et al.*, 2012). Brain uptake of FDG has been shown to strongly correlate with autopsy levels of synaptic vesicle protein synaptophysin (Rocher *et al.*, 2003) and is widely accepted as a biomarker for total brain metabolism (Magistretti, 2006). No single alteration in the metabolism has been linked to AD and instead this assessment assumes that any noted abnormalities present in AD patients are a result of the diseases pathogenesis. However, the collection of a large number of data sets using FDG-PET show a pooled sensitivity of 91% (95% confidence interval, 86%–94%) and specificity of 86% (95% confidence interval, 79%–91%) (Shivamurthy *et al.*, 2015). Furthermore, FDG-PET has been shown to differentiate AD patients from control participants with a 99% sensitivity and 98% specificity (Mosconi *et al.*, 2008). FDG-PET has additionally been found to perform better than other

available imaging techniques for the prediction of MCI to dementia conversion (Laforce *et al.*, 2010).

Estimation of brain amyloid β (Aβ) has previously been limited to post-mortem assessment, however amyloid PET has allowed for the clinical assessment of neuritic Aβ plaque density. Initial research into the use of Amyloid PET imaging used the Pittsburgh Compound B (PIB) with correlation between PIB retention and the levels of Aβ determined by immuno assay or silver staining at autopsy (Ikonomovic *et al.*, 2008, Leinonen *et al.*, 2008). Correlation has also been reported with low levels of CSF $A\beta_{42}$ in all publications that investigated the association (Fagan *et al.*, 2006, Grimmer *et al.*, 2009, Jagust *et al.*, 2009, Tolboom *et al.*, 2009, Weigand *et al.*, 2011).

The advancements in imaging methods has allowed for their inclusion in the revised criteria for AD with the acknowledgement of both neuroimaging and laboratory biomarkers as supportive criteria (Dubois *et al.*, 2010). However, their adoption into a routine clinical setting is limited due to expense, lack of expertise and relevant hardware resulting in the search for alternatives in fluid biomarkers.

1.1.4 – Current and Potential Biomarkers and Disease Markers for Alzheimer's Disease.

In 1992, one of the first biomarker studies showed that Aβ is secreted into the cerebral spinal fluid (CSF), heralding the development of quantitative immunoassays for CSF Aβ (Seubert *et al.*, 1992). Subsequent methods published in 1995 described the use of an ELISA to detect $A\beta_{42}$ with analysis showing a marked decrease in the CSF levels of $A\beta_{42}$ in AD (Motter *et al.*, 1995). This finding

has been subsequently validated in multiple published articles and shown to correlate with amyloid positive PET scans of AD patients (Olsson *et al.*, 2016). Additional combined analysis of Aβ species, $A\beta_{40}$ with $A\beta_{42,}$ demonstrated improved diagnostic accuracy (Shoji *et al.*, 1998) despite $A\beta_{40}$ remaining unchanged or only mildly changed in AD (Olsson *et al.*, 2016). The ratio of $A\beta_{42}/A\beta_{40}$ has additionally shown better correlation with amyloid PET positivity (Janelidze *et al.*, 2016).

Tau proteins have also been analysed in the CSF of AD patients, with initial identification of CSF tau obtained through Western blot analysis (Wolozin and Davies, 1987)) and the use of Alz-50 monoclonal antibody (Ksiezak-Reding *et al.*, 1988). Subsequent analysis focused on the levels of total tau and phosphorylated tau. Total CSF tau has been proposed as a marker of neurodegeneration intensity or the severity of acute neuronal damage with marked increases found in AD patients. Furthermore, combined increases in levels of total tau in addition to phosphorylated tau have be shown to be predictive of a more rapid clinical disease progression (Zetterberg *et al.*, 2013, Wallin *et al.*, 2010, Buchhave *et al.*, 2012).

Although promising data has been generated around CSF amyloid and tau analysis, these techniques are still not implemented solely for the diagnosis of AD. Instead combination assessment with routine cognitive tests and current imaging technology is used to provide a more complete clinical picture. Together with the development of CSF biomarkers there has been a drive to develop blood-based biomarkers, which are less invasive with potential for a wider clinical utility. Blood biomarkers present a range of new challenges regarding their development

and validation. Measurement of brain-derived biomarkers requires highly sensitive and specific analysis due to restricted free movement of molecules between the central nervous system and the blood by the blood brain barrier, resulting in relatively low biomarker concentrations being present (Zetterberg and Burnham, 2019). Furthermore, specific blood biomarkers with clinical utility in the diagnosis and monitoring of AD are expressed in other sites of the body and additionally present issues of analyte degradation by plasma proteases (Zetterberg and Burnham, 2019).

As previously discussed, CSF levels of $A\beta_{1-42}$ and the ratio of $A\beta_{1-42}/A\beta_{1-40}$ have some adoption in specific diagnostic profiling for AD, however plasma $A\beta_{1-42}$ and the ratio of plasma $A\beta_{1-42}/A\beta_{1-40}$ could present an alternate less invasive option to measure Aβ. Current methods for the analysis of plasma Aβ have included the application of an ultrasensitive single molecule array for Aβ42, which showed that the ratio of $A\beta_{1-42}/A\beta_{1-40}$ and plasma Aβ was reduced in the plasma of amyloid PET-positive individuals (Janelidze *et al.*, 2016). These findings follow the trend seen in analysis of the CSF ratio of $A\beta_{1-42}/A\beta_{1-40}$, however, serum analysis did not present with as distinct a separation between AD and control groups as CSF analysis of the same biomarker profile (Janelidze *et al.*, 2016). This study additionally concluded that the decreased Aβ seen in plasma indicates that changes in Aβ metabolism occur later in the periphery compared to the brain and that in specific cases of increased plasma Aβ levels there is an association with vascular disease (Janelidze *et al.*, 2016).

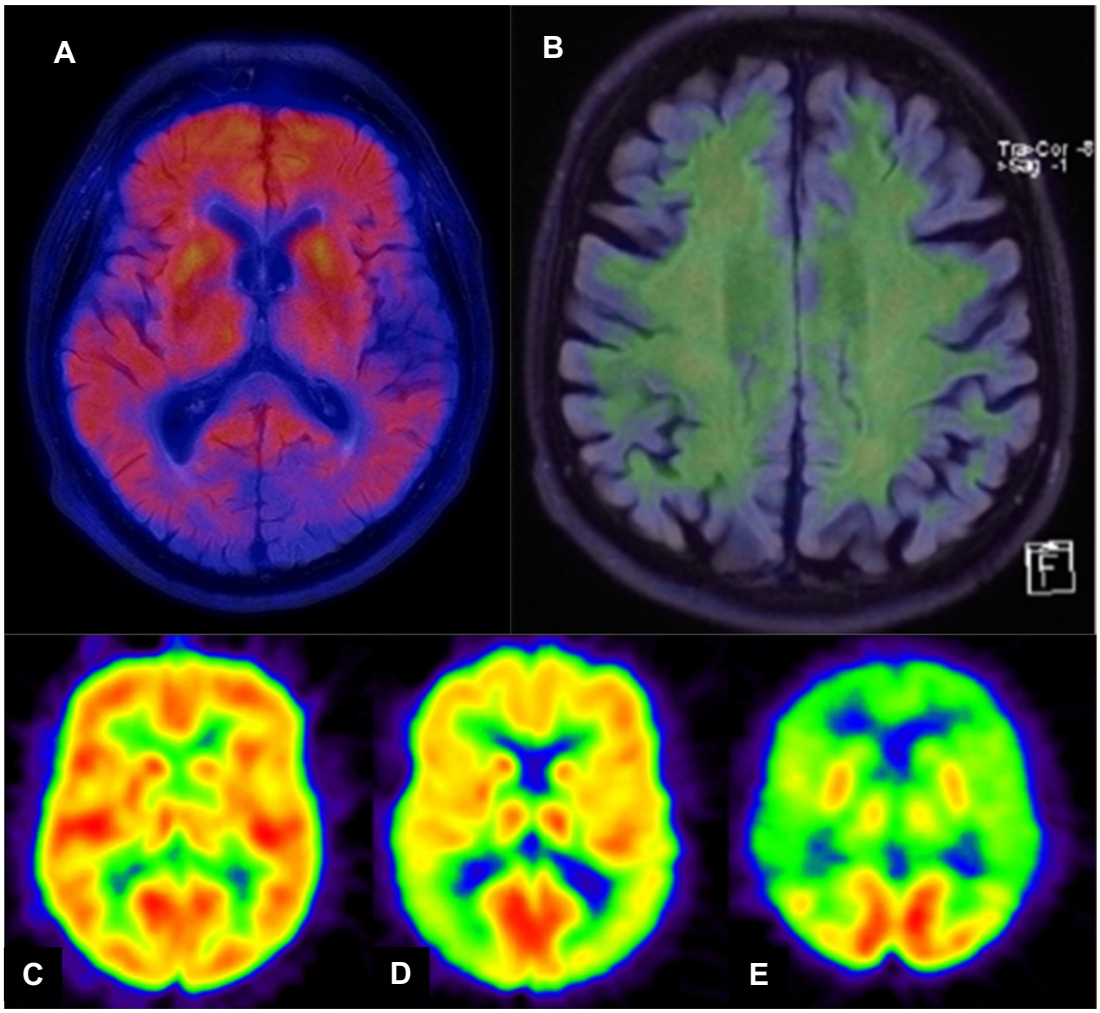

Figure 1.1 – Illustrative 11C-PIB PET-MR, Negative 11C-PIB-PET-MR and FDG-PET Imaging of Alzhiemer's disease brain.
A - Illustrative 11C-PIB PET-MR of Alzheimer's disease brain showing high tracer retention in frontal lobes with tracer signal lower in the parietal lobe and temporal cortex. **B** - Negative 11C-PIB-PET-MR from a patient with symptoms of Alzheimer's disease, showing a distinctive pattern of white matter moderate non-specific tracer uptake. **C** - FDG-PET imaging of cognitively normal subject. **D** - FDG-PET of a patient with suspected early Alzhimer's disease. **E** - FDG-PET of a patient with advanced Alzheimer's disease. Distribution shows avid cortical FDG uptake on the grey matter, the basal ganglia, and the thalami in the healthy subject. MCI patient demonstrates widespread reduction in the parietal, frontotemporal and basal ganglia glucose metabolism. The regional cerebral metabolic rate of glucose is severely impaired on the patient with advanced Alzheimer's disease (Rice and Bisdas, 2017). Reprinted from European Journal of Radiology, 94, Louise Rice,Sotirios Bisdas, The diagnostic value of FDG and amyloid PET in Alzheimer's disease—A systematic review, 16-24., Copyright (2007), with permission from Elsevier

Subsequent developments in the analysis of serum Aβ have focused on the improvement of diagnostic accuracy while still addressing the same analytical parameters. Immunoprecipitation mass spectrometry assays give around a 90% diagnostic accuracy with similar decreases in plasma $A\beta_{1-42}/A\beta_{1-40}$ ratio compared to CSF (Nakamura *et al.*, 2018, Ovod *et al.*, 2017). Although these assays present promising data for Aβ as a plasma biomarker, they do not account for non-cerebral expression of Aβ as seen in platelets (Li *et al.*, 1994) and therefore are subject to scrutiny regarding analysis specificity.

Similar developments have been made in the analysis of plasma tau, with the use of Single Molecule Array (Simoa) finding that the levels of total tau in plasma are increased in cases of cognitive decline and that these increased levels are associated with faster clinical disease progression and have an association with the incidence of AD (Mielke *et al.*, 2017, Pase *et al.*, 2019). Furthermore, the analysis of plasma phosphorylated tau using a biotinylated-AT270 capture antibody for pTau181 presented a more sensitive and specific predictor of elevated brain Aβ (Mielke *et al.*, 2018). Furthermore, levels of pTau181 were shown to be elevated in AD compared to participants classified as cognitively unimpaired (Mielke *et al.*, 2018). This increased profile is supported by analysis with both immunomagnetic reduction technology and Simoa (Tatebe *et al.*, 2017).

MicroRNA (miRNA) expression profiling for neurodegenerative disease has also gained traction with the Real-Time PCR offering both accurate and inexpensive detection of circulating miRNAs in serum and CSF (Weber JA, 2010). miRNAs selectively bind messenger RNAs, downregulating their translation into proteins, controlling key biological processes including neurogenesis and immune

response and having a fundamental role in cellular expression homeostasis (Schmiedel JM, 2015). Successful analysis of CSF miRNAs reported differential expression of miR-100, miR-146a and miR-1274a in AD (Denk *et al.*, 2015). Furthermore, discrimination analysis of these targets was able to positively classify controls and AD cases with 95.5% accuracy for AD diagnosis (Denk *et al.*, 2015). MiRNA additionally offers a potential avenue for disease monitoring with correlations seen with the levels of $A\beta_{1-42}$ and phosphorylated neurofilament heavy chain (Denk *et al.*, 2018).

Efforts have also been made to target multiple affected pathways using proteomics or metabolomics platforms to predict AD onset. These studies have focused on the generation of metabolic profiles that could be used collectively to better differentiate between MCI, AD and early disease stages (Lista *et al.*, 2013). The combination of these assays combined with high throughput mass spectroscopy analysis offer exciting new opportunities to better diagnose causes of cognitive impairment. A key focus of this thesis will aim to investigate the potential for the branched chain aminotransferase protein (BCAT) and its metabolite, glutamate to predict AD progression relative to control and MCI offering a novel biomarker to predict disease onset.

2.1.1 - Alzheimer Disease

AD is the most common form of dementia, accounting for an estimated 60-70% of dementia cases, with an estimated 46.8 million people affected worldwide and cases increasing by approximately 4.6 million each year (Irvine *et al.*, 2008, Prince *et al.*, 2016). The disease is characterised by initial presentation of cognitive dysfunction, including memory loss (determined through clinical assessment or

anecdotal evidence) disorientation with speech and language issues. The second sub-set of symptoms are deemed non-cognitive and include the presentation of psychiatric symptoms which include depression, hallucinations, delusion and in certain cases aggressive behaviour. These factors form the overall symptomatic presentation of cognitive impairment, and with regard to AD are due to the frontal, parietal, and the temporal lobe being affected.

In the majority of cases, the disease is age-related with the highest percentage of patients classified as having late onset AD with symptomatic presentation after the age of 65. Cases of AD occurring before the age of 60 are considered exceptional (Wolk and Dickerson, 2019) and classified as early onset AD (Wolk and Dickerson, 2019). Similar early presentation is observed in cases of genetic autosomal dominant forms of AD, although genetic risk factors, which play a strong role even in the development of late onset AD (Gatz *et al.*, 2006). Specific genetic factors have been seen to contribute to AD with fully penetrant mutations in Amyloid precursor protein (APP), Presenilin 1, and Presenilin 2 discovered as causes of the autosomal dominant form of AD (Van Cauwenberghe *et al.*, 2016) (Table 1.1.1).

Furthermore, the presence of the ε4 allele of Apolipoprotein E (*APOE*) has been shown to indicate strong genetic risk for both early-onset and late-onset AD (Saunders *et al.*, 1993). The *APOE* coding region encodes a polymorphic glycoprotein expressed at multiple sites in the body, including the liver, brain, macrophages, and monocytes (Van Cauwenberghe *et al.*, 2016). In the brain ApoE has a role in transport of lipids, neuronal growth and tissue response. Additionally, multiple studies have shown a relationship between ApoE and the

clearance of soluble Aβ and Aβ aggregations (Huynh *et al.*, 2017, Deane *et al.*, 2008). In the microglia, ApoE has been shown to enhance the degradation of Aβ by the zinc-dependent metalloprotease neprilysin that additionally facilitate the insulin degrading enzyme degradation of extracellular Aβ (Jiang *et al.*, 2008).

Three main allelic variations; ε2, ε3, and ε4 encode for the ApoE2, ApoE3, and ApoE4 isoforms, respectively (Corder *et al.*, 1993). The ε4 isoform is thought to be less efficient in mediating the clearance of Aβ (Corder *et al.*, 1993) and carries an associated three-fold or fifteen-fold increased risk of AD for heterozygous *APOE* ε3/4 and ε4/4 forms respectively. However, this mutation is not individually sufficient to cause the disease (Corder *et al.*, 1993, Saunders *et al.*, 1993, Farrer *et al.*, 1997). Conversely, a protective effect and delay of onset age is associated with *APOE* ε2 (Corder *et al.*, 1994).

The study of these mutations has allowed for the development of the current understanding of key pathological observations of AD. These include the key hallmarks of accumulation of extracellular Aβ plaques and intracellular accumulation of neurofibrillary tangles containing hyperphosphorylated tau, together with neurotransmitter imbalances, which result in neuronal deficit (Glenner and Wong, 2012).

2.1.1.1 – The Amyloid Hypothesis

Under normal physiological conditions Aβ is produced through APP processing by astrocytes and neurons in the brain (Puig and Combs, 2013) and is typically present as a soluble form which is secreted extracellularly for clearance by the CSF. APP can be processed in two different ways by different sets of enzymes –

the first is the non-amyloidogenic pathway and the second pathway (amyloidogenic) leads to the hallmark amyloid plaque formation in AD.

Usually around 90% of APP enters the non-amyloidogenic pathway, and 10% follows the alternative amyloidogenic path, but these ratios can change due to mutations, environmental factors, as well as the age of the individual. Through the non-amyloidgenic pathway APP is cleaved by α-secretase generating a soluble N-terminal fragment and a C-terminal (CTFα) membrane-bound fragment. CTFα undergoes further clevage by presenilin-containing γ-secretase to generate a soluble N-terminal fragment (p3) and a membrane-bound C-terminal fragment (AICD, or APP intracellular domain) (Chow *et al.*, 2010). The products from this pathway have been shown to promote memory retention through the regulation of neurite outgrowth and synaptogenesis.

Alternatively, APP may also be processed through the 'plaque forming' amylogenic pathway, generating the more commonly known toxic form of Aβ (Murphy and LeVine, 2010). In this pathway, rather than the initial cleavage by α-secretase, APP is cleaved by β-site APP cleavage enzyme 1 (BACE) (a transmembrane aspartic protease), generating a shorter sAPPβ. In this instance the remaining membrane-bound C-terminal fragment (CTFβ) is cleaved closer to the N-terminal end of APP than with α-secretase, generating a longer fragment than CTFα.

Table 1.1 – Genes associated with Alzheimer's disease

Gene	Chromosome Location	Normal Function	Inheritance	AD Pathology
Amyloid Precursor Protein	21q21	Regulation of synaptic function	Autosomal Dominant	Early onset
Apolipoprotein E	19q13.32	Cholesterol transport	Sporadic	Genetic risk factor
Presenilin 1	14q24.2	Processing of APP and formation of Aβ	Autosomal Dominant	Early onset
Presenilin 2	1q42.13	Processing of APP and formation of Aβ	Autosomal Dominant	Early onset

Table Adapted from Genetics of Alzheimer's disease and Role of glutamate and NMDA receptors in Alzheimer's disease (Bekris *et al.*, 2010, Wang and Reddy, 2017).

Although this is followed by γ-secretase cleavage forming AICD, the same as reported for the non-amyloidgenic pathway, a soluble N-terminal fragment (Aβ) that is longer than p3 is also produced. These varying lengths of Aβ include two main species, $A\beta_{1-40}$(90%) and $A\beta_{1-42}$ (10%) (Van Cauwenberghe *et al.*, 2016). The larger $A\beta_{1-42}$ fragments are those found predominantly in the plaques in AD brain and are prone to aggregation due to additional hydrophobic residues (Selkoe, 2001, Walsh and Selkoe, 2007). In contrast to the α pathway, APP processing through the β-synuclein pathway has been shown to promote memory loss and reorganisation through neuronal apoptosis and neurite retraction (Bredesen, 2009). Furthermore, the accumulation of $A\beta_{1-42}$ fragments has been shown to result in aggregate-mediated toxicity, increasing oxidative stress through the reduction of metal ions (Huang *et al.*, 1999).

Research into the role of Aβ has focused around its role in disease pathology, with less emphasis into understanding its normal physiological role. There is increasing evidence that there is an important role for soluble Aβ in synaptic plasticity and memory (Puzzo and Arancio, 2013, Morley and Farr, 2014, Brothers *et al.*, 2018). The release of Aβ into the synaptic cleft has been shown to increase the probability of neurotransmitter release from presynaptic neurons following synapse transport of APP during neuronal activity and subsequent cleavage (Kamenetz *et al.*, 2003, Cirrito *et al.*, 2005, Tampellini *et al.*, 2009).

Moreover and relating directly to the central nervous system, Aβ has shown the capability to plug ‘leaks’ in the blood brain barrier (Brothers *et al.*, 2018). The blood brain barrier describes the microvasculature of the central nervous system which regulates the transport of molecules, ions and cells to and from the blood

(Zlokovic, 2008). The highly restrictive nature of the blood brain barrier allows for tight regulation of central nervous system homeostasis and protection from any blood borne toxins or pathogens, and from inflammation and disease (Daneman and Prat, 2015). In neurological disease, neurodegenerative disorders and instances of brain trauma barrier properties are altered, causing changes to signalling, ion dysregulation and allow for immune cells entry into the central nervous system (Daneman and Prat, 2015, Zlokovic, 2008). These imbalances and entry of foreign cells can cause both neuronal dysfunction and degeneration (Daneman and Prat, 2015). Aβ has also been shown to have a definitive link with the integrity of the blood brain barrier, with study of Aβ plaques in AD showing the presence of serum albumin and collagen IV which are not found in the brain under normal conditions (Cullen *et al.*, 2006). In instances where the blood brain barrier becomes 'leaky', soluble Aβ has been shown to form an insoluble mass by binding pro-inflammatory and neuroactive compounds and stopping any further spread throughout the brain (Bishop and Robinson, 2002). Therefore, understanding the normal physiological role of Aβ will be important before further therapeutic targeting is developed.

2.1.1.2 – Microtubule-Associated Protein Tau Hypothesis

The second key pathological hallmark of AD is the accumulation of intracellular neurofibrillary tangles, which arise from abnormal hyperphosphorylation of the mature neuron microtubule protein tau (Goedert and Crowther, 1989, Goedert *et al.*, 1989). Tau promotes the assembly and stabilisation of microtubules through its interactions with tubulin (Weingarten *et al.*, 1975) with its biological function regulated through phosphorylation and alternative mRNA splicing (Stoothoff and Johnson, 2005). Through the investigation of the abnormal hyperphosphorylation

of tau studies have identified the specific phosphatases and kinases responsible for this process. Glycogen-synthase kinase-3β (GSK-3β), has been shown to have a role in both the regulation of tau splicing through the phosphorylation of the nuclear splicing element enhancer SC35 (Hernandez *et al.*, 2004) and tau phosphorylation. Phosphorylation of GSK-3β at Ser9 is recognised by the scaffolding protein 14-3-3 which forms a complex with tau in the brain (Agarwal-Mawal *et al.*, 2003). When this complex is present, GSK-3β is active leading to tau phosphorylation (Agarwal-Mawal *et al.*, 2003). The phosphorylation of tau at Thr231 and Ser400 by GSK-3β has been shown to be promoted by priming of the tau residues Ser235 and Ser404 by cyclin-dependent protein kinase 5 (cdk5) (Cho and Johnson, 2003). Tau phosphorylation is further modulated by cAMP-dependent protein kinase (PKA), through prephosphorylation promoting downstream GSK-3β phosphorylation at multiple sites including Thr181, Ser199, Ser202, Thr205, Thr217, Thr231, Ser396 and Ser422 (Liu *et al.*, 2006). Furthermore, additional modulation of tau phosphorylation by PKA is seen with cdk5 with promotion of phosphorylation at Ser396 (Liu *et al.*, 2006). Dephosphorylation of tau is modulated by protein phosphatase 2A (PP2A), which promotes dephosphorylation at multiple Ser and Thr sites by binding the tau microtubule-binding domain (Sontag *et al.*, 1996, Sontag *et al.*, 1999).

Under normal physiological conditions tubulin is present in over tenfold excess of tau, resulting in a large proportion of tau being microtubule bound (Iqbal *et al.*, 2010) with soluble tau recovered in the cytosol. However, this differs in AD brain where the protein is recovered in an additional two states, oligomeric and fibrillised (Kopke *et al.*, 1993, Grundke-Iqbal *et al.*, 1986, Bancher *et al.*, 1989). Furthermore, the levels of total tau are increased four to eight times in AD,

stemming solely from the abnormally hyperphosphorylated form of the protein (Khatoon *et al.*, 1992). Hyperphosphorylated tau does not retain the proteins normal function and cannot bind with tubulin or promote microtubule assembly. This form of tau both inhibits and disrupts microtubules (Alonso *et al.*, 1994, Li *et al.*, 2007), resulting in the sequestration of normal tau protein observed in diseased protein (Alonso *et al.*, 1996, Alonso *et al.*, 1994).

In cases of advanced AD both hallmarks are always simultaneously present (Price and Morris, 1999), however the presence of neurofibrillary tangles has been shown to more strongly correlate with AD progression compared to amyloid plaque deposition. In early disease states neurofibrillary tangles have been shown to be present in the temporal lobe with no presence of amyloid plaques (Minati *et al.*, 2009). It is also theorised that there is an intrinsic link between the production of amyloid plaques and neurofibrillary tangles with Aβ42 oligomers and plaques causing oxidation and impact upon cellular processes (Lloret *et al.*, 2011) which in turn could initiate or accelerate the hyperphosphorylation of tau.

2.1.1.3 – The Cholinergic and Glutamatergic Hypothesis

As previously mentioned, in addition to typical pathological changes observed in AD there is an increasing consideration of the role of neurotransmitters in neurodegeneration. The neurotransmitter acetylcholine (ACh) is used by cholinergic neurons, where is has a role in both peripheral and central nervous systems (Ferreira-Vieira *et al.*, 2016) and is supplied to most regions of the brain (Woolf and Butcher, 2011). The cholinergic system has been shown to have role in learning and memory including acquisition (Blokland *et al.*, 1992) and in mice models, memory retrieval (Boccia *et al.*, 2003). Studies have additionally shown

that there is significant loss of cholinergic neurons in dementia through the depletion of enzymes responsible for the generation and metabolism of ACh (Davies and Maloney, 1976) and that the loss of basal forebrain cholinergic neurons was associated with AD. These findings are the foundation for the cholinergic hypothesis of dementia, whereby the memory deficits noted in AD are related to the basal forebrain decline of the cholinergic system (Bartus *et al.*, 1982).

Cholinergic synapses have additionally been shown to be affected by the key hallmark of AD, Aβ (Bell *et al.*, 2006) in addition to a report of ACh and Aβ interaction promoting the initial formation of Aβ and its subsequent integration into Aβ -fibrils (De Ferrari *et al.*, 2001). Furthermore, there is a correlation in the severity of AD pathology and changes in synaptic transmission in the hippocampus (Selkoe, 2002).

In addition to the involvement of ACh and cholinergic receptors in the progression of AD there is also a consideration for the role of excitatory neurotransmitter glutamate. The majority of CNS neurotransmission is mediated by both glutamate and its associated receptors, the ligand gated ionotropic glutamate receptors and the metabotropic second messenger coupled receptor which have a fundamental role in in the learning and memory function by maintenance of synaptic plasticity (Riedel *et al.*, 2003). The main receptor group responsible for both the synaptic plasticity and function are the N-methyl-d-aspartate receptors (NMDAR) (Collingridge and Singer, 1990) through the enhancement of synaptic strength by a Ca2+/calmodulin-dependent protein kinase II signalling cascade (Wang and Reddy, 2017). Furthermore, NMDAR promotes neuronal survival through

suppression of the apoptosis pathway and allowing for survival gene expression by activation of cyclic-AMP response element binding protein (Wang and Reddy, 2017). The sensitivity of NMDAR to calcium signalling has been attributed to the increased stimulation of glutamatergic signaling, and glutamate excitotoxicity. Whereby, prolonged increased levels of Ca^{2+} signaling results in neuronal death and subsequent impairment of cognition (Wang and Reddy, 2017). These findings highlight both ACh and glutamate as key targets to help build a wider understanding of AD pathology and as potential diagnostic tools with expanded use in the therapeutic approach to AD.

2.1.1.4 – Treatment of Alzheimer's Disease

There is currently no cure for Alzheimer's disease, and treatment is currently focused on the temporary management symptoms and behavioural changes. The only current FDA approved treatments used are Acetylcholinesterase (AChE) inhibitors to increase brain AChE levels and inhibit ACh turnover, compensating for the reduction in cholinergic neurons in AD (Rees and Brimijoin, 2003) or the NMDA-receptor antagonist memantine.

However, there is a focus on targeted treatments for the hallmarks of AD, accumulation of Aβ plaques and hyperphosphorylated tau. For Aβ treatments have focused on targeting either the production or clearance of the peptide. Key targets include BACE1 and BACE2, where inhibition by verubecestat (MK-8931) has shown promise in clinical trials (Moraes and Gaudet, 2018). For tau therapeutic treatment options have been focused largely on PP2A stimulation and GSK-3β inhibition. The reversal of PP2A inhibition by memantine has been shown to decrease the hyperphosphorylation of tau (Mangialasche *et al.*, 2010), while a

decrease in both tauopathy and *in vivo* tau lesions has been correlated with lithium inhibition of GSK-3β (Nakashima *et al.*, 2005, Noble *et al.*, 2005).

However, in certain cases these targeted therapies have either shown little efficacy, failed at clinical trial or have normal physiological functions that if targeted could have adverse effects. This has highlighted the need for other options in both the field of treatment and diagnostics. Underlying these hallmarks and the symptomatic presentation of AD, metabolic balance and imbalance is perhaps the single most important and least understood parameter. With multiple metabolic processes are thought to be attributed to AD progression and include cellular stress, calcium overload, protein misfolding and dysregulated autophagy (discussed in Section 2: 1.2). Identifying key components in these processes may offer novel targets for both diagnosis and treatment, with the work highlighted in this thesis as focusing on the possible role of autophagy.

2.1.2 – Autophagy

Autophagy is the main pathway for the degradation of cytoplasmic components within the lysosome, to balance sources of cellular energy, during development and in response to nutrient stress (Glick *et al.*, 2010). Three key types define this pathway; chaperone mediated autophagy (CMA), macro-autophagy and micro-autophagy. In CMA protein translocation occurs through target and chaperone protein complex formation. This complex is recognised by lysosomal-membrane membrane protein 2A allowing for its transport across the membrane for unfolding and degradation to occur (Saftig *et al.*, 2008). In micro-autophagy lysosomes directly take up cytosolic components through non-selective invagination of the lysosomal membrane (Glick *et al.*, 2010). Macro-autophagy, henceforth referred

to as autophagy, however, is initiated by pre-autophagosomal structure formation, which through sequestration in the cytoplasm forming a double membrane-bound autophagosome (Axe *et al.*, 2008). The autophagosome is involved in the formation of an autolysosome by fusion with the lysosome (Glick *et al.*, 2010). Within the autolysosomes, acid hydrolases degrade the contained cellular components (Figure 1.2) (Galluzzi *et al.*, 2014). Lysosomes are reformed following substrate digestion within the autolysosome, these lysosomes mainly contain lysosomal hydrolases and are smaller and less dense (Nixon, 2007). Through this mechanism autophagy maintains normal neural function through the removal of misfolded and aggregated proteins (Glick *et al.*, 2010). This is applied directly to the generation and clearance of Aβ where autophagy is a key regulator (Nilsson and Saido, 2014).

However, in AD this clearance is shown to be affected manifesting in Aβ aggregation. The multi-step process of autophagy opens possibilities for dysfunction to occur in the regulation, formation or clearance of the autophagosome, with evidence showing that dysregulation throughout the autophagy pathway can cause aggregate accumulation or ineffective aggregate clearance. In early AD there is believed to be an autophagosome imbalance which would affect later stage, downstream clearance of aggregates (Perez *et al.*, 2015), supporting the theory that Aβ accumulation occurs in later disease states (Yang *et al.*, 1998, Cataldo *et al.*, 2000).

Furthermore, increased levels of Aβ have been found in autophagic vacuoles highlighting that APP processing can take place, with additional reports stating that in AD brain there is autophagic vacuole accumulation in dystrophic neurites

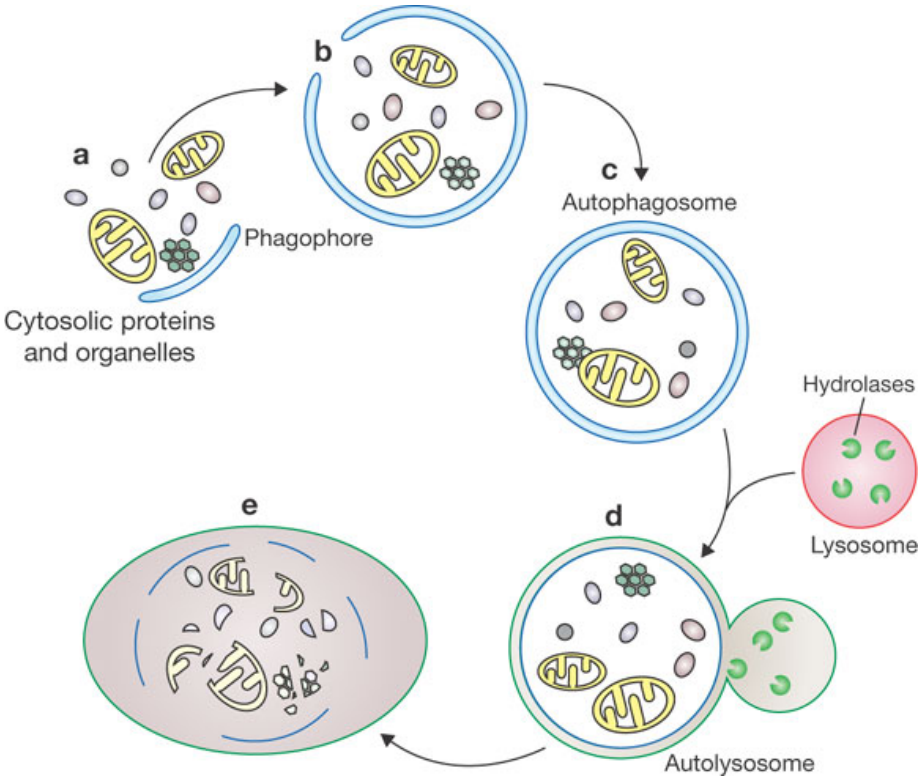

Figure 1.2 – Autolysosome formation in autophagy
Cytosolic proteins and organelles are sequestered by an expanding phagophore (a, b), resulting in double-membrane vesicle formation (c), an autophagosome; the outer membrane of the autophagosome subsequently fuses with a lysosome (d), to expose the inner single membrane of the autophagosome to lysosomal hydrolases. The cargo-containing membrane compartment is lysed, and the contents degraded (e) (Xie and Klionsky, 2007) – Reprinted by permission from Springer Nature: Springer Nature, Nature Cell Biology (Xie and Klionsky, 2007) (Autophagosome formation: core machinery and adaptations, Zhiping Xie and Daniel J. Klionsky [Copyright © 2019 Copyright Clearance Center, Inc. – Springer Nature (2007)

when compared to matched controls (Yu *et al.*, 2005, Nixon, 2007). Additionally, the endosomal trafficking protein assembly, retromer has been shown to be deficient in AD resulting in inefficient clearance of autophagic vacuole during vesicular trafficking (Small and Petsko, 2015).

Specific autophagy pathway proteins have also been shown to be dysregulated in AD, with the reduction in Beclin 1 compromising autophagosome formation in the inferior parietal lobe (Pickford *et al.*, 2008, Rohn *et al.*, 2011). Furthermore, Beclin 1 was shown to be critical in the accumulation of Aβ in mouse models, whereby depletion of the protein resulted in perturbation of clearance and formation of the autophagosome initiating the accumulation of both intracellular and extracellular Aβ (Pickford *et al.*, 2008).

Through the use of neuronal cell models our group have determined that cell signalling, and the autophagy pathway is impacted by leucine. As earlier indicated, autophagy is regulated through changes in nutrient cell signalling. Leucine, the substrate for hBCAT, controls the activity of the mechanistic target of rapamycin 1 (mTORC) complex (Figure 1.3). mTORC1 consists of five components; mTOR, regulatory-associated protein of mTOR (Raptor), GβL, PRAS40 and Deptor (Peterson *et al.*, 2009). Under normal physiological conditions, activation of mTORC1 causes the phosphorylation of autophagy related protein 13 (Atg13), preventing the formation of the ULK1 kinase complex which inhibits the pathway (Hensley and Harris-White, 2015b). However, the regulatory effect that amino acids have on mTORC1 is abolished in deprived states leading to increased autophagy (Chen *et al.*, 2014). During deprivation, ULK1 protein kinase is activated forming phagophores and inducing autophagy

(Chan *et al.*, 2009). ULK1 activation involves beclin-1, the class-III phosphatidylinositol-III kinase (PI3K), VPS34, and microtubule-associated protein 1 light chain 3 (Atg8/MAP1-LC3/LC3) or GABARAP homologs (Hensley and Harris-White, 2015a).

LC3-II and VPS34 have been used as markers for autophagy due to their involvement in ULK1 activation and have been shown to associate with amyloid β and hyperphophorlylated tau aggregates in AD (Ma *et al.*, 2010).

2.1.3 - Function of the Branched Chain Amino Acids in the Brain

The branched chain amino acids (BCAA), leucine (Leu), isoleucine (Ile), and valine (Val) are essential dietary nutrients that have a role in protein synthesis, as precursors for additional amino acids and the synthesis of brain neurotransmitter glutamate through their role as nitrogen donors (Yudkoff *et al.*, 2005), and the synthesis of amine neurotransmitter serotonin and catecholamines; dopamine and norepinephrine (Fernstrom, 1990). Serotonin, dopamine and norepinephrine are derived from the aromatic amino acids (ArAA) tryptophan (Trp), phenylalanine (Phe) and tyrosine (Tyr) (Fernstrom, 1990).

Dietary intake of BCAAs comes largely from dietary animal-based proteins which have between 15-20% amino acid content (U.S. Department of Agriculture, 2004).

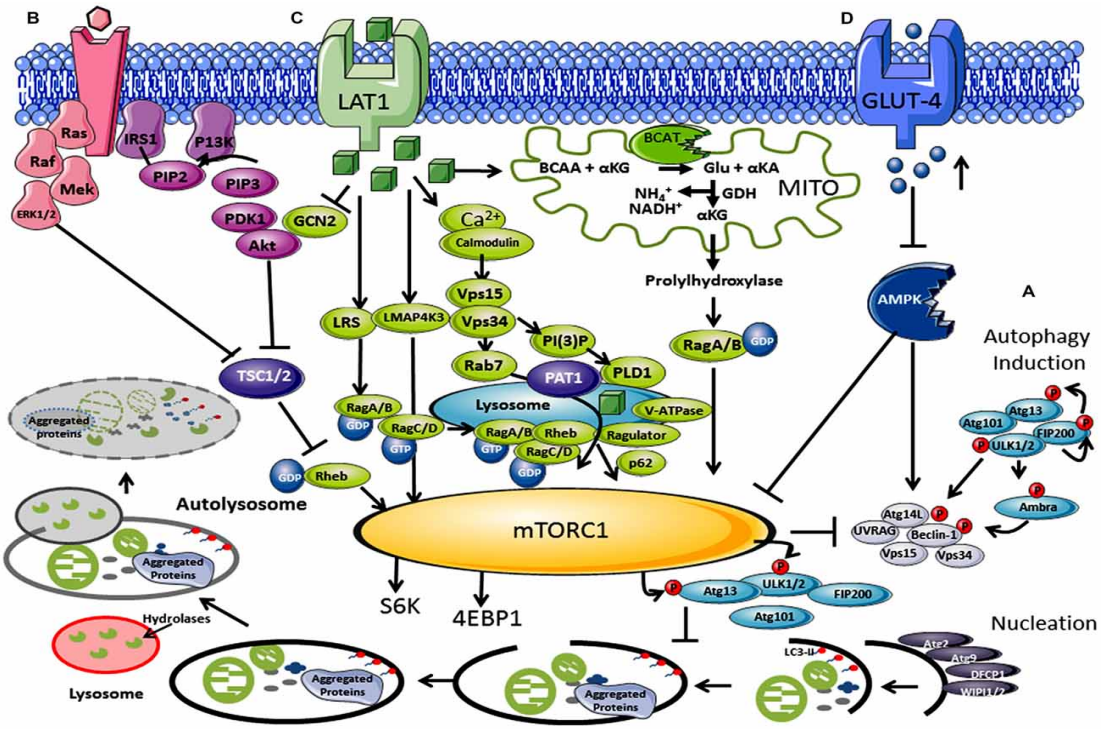

Figure 1.3 - Regulation of autophagy by nutrients and hormones via the mammalian target of rapamycin (mTOR) signalling pathway.
(A) Activation of the ULK1/2 protein kinase complex including the autophagy related proteins and the 200 kDa focal adhesion kinase family-interacting protein (FIP200) are involved in the initial induction of the autophagosome. This is followed by a class III phosphatidylinositol 3-kinase or human vacuolar protein sorting 34 (hVps34), complexed with BCL-2 interacting moesin-like coiled-coil protein 1 (Beclin 1) and Vps15 dependent nucleation step. Beclin 1 is involved in two recruitment complexes, the Atg14L and UV radiation resistance-associated gene (UVRAG) complex, which are required for phagophore formation and phagocytosis, respectively. Elongation and closure of the autophagosome requires several Atg proteins, hVps34 and microtubule-associated light chain 3 phosphatidylethanolamine (LC3), which is regulated by GTPase Rab5. The outer membrane of the autophagosome then fuses with a lysosome, exposing the inner single membrane to lysosomal hydrolases whereby the contents are degraded. (B) Hormones and growth factors such as insulin and insulin-like growth factor (IGF-1) trigger mTORC1 activity through a cascade of events resulting in recruitment and activation of Akt which induces phosphorylation and degradation of tuberous sclerosis complex protein 2 (TSC2). TSC2 degradation permits GTP-bound Rheb to directly interact and activate mTORC1. The Ras-ERK pathway also activates mTORC1 through inhibitions of TSC1 and TSC2. (C) Amino acids, in particular leucine, regulate the mTORC1 through the Rag complex (Ras-related GTPase), which recruits mTOR to the lysosomes with Rheb and hVps34. (D) Inhibition of the amp-activated protein kinase signaling pathway is triggered by high glucose levels, resulting in the decrease of AMP:ATP ratio that inhibits TSC1 and TSC2, activating mTORC1 and inhibiting autophagy.

More than 60% of ingested BCAAs are primarily metabolised extrahepatically by skeletal muscle (Gelfand *et al.*, 1986), a portion of the remaining percentage enter systemic circulation, increasing blood BCAA levels (Platell *et al.*, 2000). Peripheral BCAAs are transported into the brain across the blood brain barrier through preferential binding to the large neutral amino acid transporter (LAT1) on the central nervous system endothelial cell layer (Boado *et al.*, 1999). LAT1 transporters are almost fully saturated at normal plasma amino acid concentrations (Fernstrom, 2005), and are competitively shared by large neutral amino acids (LNAAs) which include tryptophan, tyrosine and phenylalanine (Fernstrom, 2013). Ingestion of BCAAs and LNAAs alters the uptake by LAT1 transporters. Increases in BCAA plasma or serum concentration cause LAT1 uptake of LNAAs to decrease, as shown by a fall in brain tryptophan concentrations following an injection of Ile, Leu or Val (Carlsson and Lindqvist, 1978, Fernstrom, 2013). Additionally, increases in plasma or serum LNAAs will alter the uptake of the other amino acids. Through this mechanism neurotransmitter levels in the brain can be altered, as evidenced by increases or decreases in serotonin synthesis following either tryptophan or LNAA injection, respectively resulting in altered neuronal serotonin release (Gartside *et al.*, 1992, Sharp *et al.*, 1992).

Through competitive transport by LAT1 the BCAAs enter the brain and are metabolised by the human branched chain aminotransferase (hBCAT) proteins, which are predominantly present as two isoforms, the cytosolic (hBCATc) and mitochondrial (hBCATm). The hBCAT proteins are responsible for the transamination of; Leu, Ile and Val with α-ketoglutarate (Hutson, 2001) resulting in the release of their respective branched chain α-keto acid (BCKA). The

transamination of the BCAAs supplies nitrogen to α-ketoglutarate for essential neurotransmitters glutamate and glutamine synthesis (LaNoue *et al.*, 2001).

The committed, rate limiting step in the oxidation of BCAAs is catalysed by the second enzyme in the catabolic pathway, the branched-chain alpha-keto acid dehydrogenase complex (BCKDC) (Brautigam *et al.*, 2006). BCKDC is involved in the irreversible oxidative decarboxylation of the branched chain α-keto acids into co-enzyme A derivatives (Chuang *et al.*, 2006, Hull *et al.*, 2015). The BCKD complex is composed of the three catalytic subunits; a branched chain α-keto acid decarboxylase (E1), a dihydrolipoyl transacylase (E2), and a dihydrolipoyl dehydrogenase (E3) (Harris *et al.*, 1997). At times where BCAAs are required for protein synthesis the BCKD complex is inactivated by branched chain alpha-keto acid dehydrogenase kinase (BDK) through covalent modification and phosphorylation of E1α subunits (Murakami *et al.*, 2005). Reactivation of the complex occurs, when BCAAs are in excess, through dephosphorylation by branched-chain phosphatase (Harris *et al.*, 2005).

In the brain, glutamate is a major excitatory neurotransmitter and the precursor to the major CNS inhibitory neurotransmitter gamma-aminobutyric acid (GABA) synthesis. Due to the significant impact that BCAA metabolism has on glutamate regulation, previous studies in this research group have mapped the hBCAT proteins to all areas of the human brain where hBCATc was solely expressed in neurons that were either GABAergic or glutamatergic (Hull *et al.*, 2012). Mapping of hBCATc showed significant distribution within the hippocampal region of the brain in neuronal cell bodies, implying that metabolism of BCAAs primarily contributes to the glutamate metabolic pool, rather than the excitatory glutamate

pool. Conversely, hBCATm was mapped throughout the vascular endothelial layer, demonstrating that transamination can occur in this cell type, indicating that hBCATm has a role in glutamate regulation (Hull *et al.*, 2012). Further investigation of hBCATs in AD brain has shown that expression of these proteins is increased in the frontal and temporal cortex in addition to the hippocampal region with the mitochondrial form exhibiting a 170% increase in the level of BCAT (Hull *et al.*, 2015). This finding correlated with Braak staging, the method by which the degree of AD pathology can be classified based on the distribution pattern of neurofibrillary tangles (Braak and Braak, 1991), and suggested a direct link between hBCAT levels and disease severity, and that the metabolic pathways regulated by these proteins are perturbed in AD (Hull *et al.*, 2015).

The levels of the neurotransmitter glutamate have a significant effect on protein expression and neurotoxicity. Under normal physiological conditions glutamate is essential for memory and learning, and has a role in dendrite and synapse formation (Trotti *et al.*, 2001) however, neurotoxicity can occur when extracellular glutamate levels rise at the synapses (Mattson and Chan, 2003). Increased levels of glutamate have been reported to cause short term physiological changes to neurones and neuronal degeneration in instances of extended exposure (Choi, 1985).

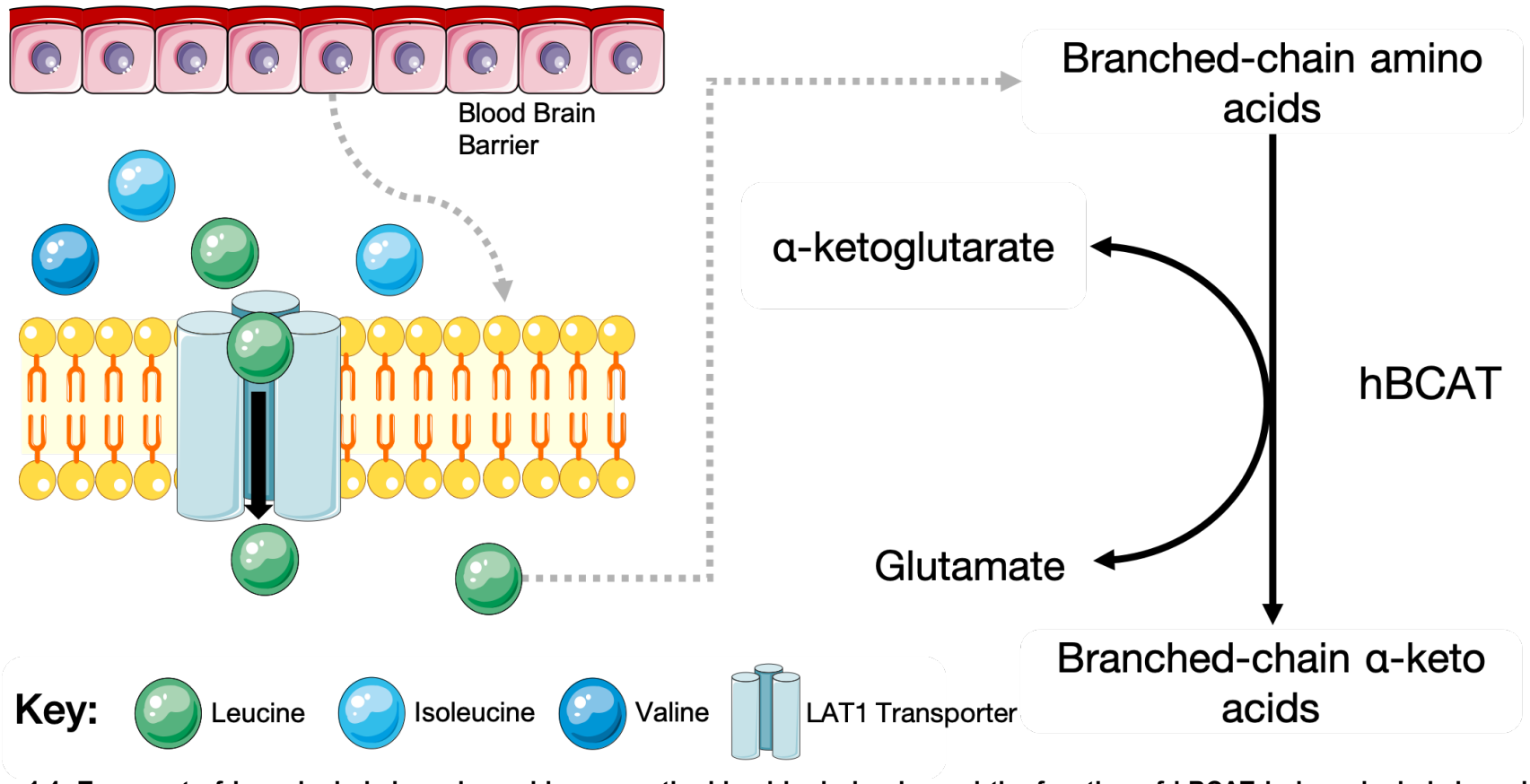

Figure 1.4: Transport of branched chain amino acids across the blood brain barrier and the function of hBCAT in branched chain amino acid metabolism.
Peripheral BCAA's isoleucine, leucine and valine are transported into the brain across the blood brain barrier through preferential binding to the large neutral amino acid transporter (LAT1) on the central nervous system endothelial layer. In the brain hBCAT catalyses the reversible transamination of BCAA's with α-ketoglutarate resulting in the release of their respective branched chain α-keto acid. The transamination of the BCAAs supplies nitrogen to α-ketoglutarate for essential neurotransmitters glutamate and glutamine synthesis. Figure created using Servier Medical Art.

The excessive release of glutamate additionally causes an intracellular influx of Ca^{2+} ions through the activation of postsynaptic membrane receptors (Sattler and Tymianski, 2000). The postsynaptic effect of glutamate is mediated by the ionotropic *N*–methyl-D-aspartate (NDMA), kainite and 2-amino-3-(3-hydroxy-5-methylisoxazol-4yl) propionate receptors (Hollmann and Heinemann, 1994), with NDMA associated with calcium dependent changes due to high Ca^{2+} permeability (Choi, 1988). Enhanced activation causes an influx of calcium ions disturbing the cellular environment and activating intracellular Ca^{2+} dependent signalling with the final result being neuronal cell death (Sattler and Tymianski, 2000). The calcium ion influx caused by excessive NDMA activation additionally activates neuronal NO synthase and generates reactive oxygen species (ROS) (Garthwaite *et al.*, 1988). The overproduction of ROS and NO free radicals contributes to cell death (Lipton and Rosenberg, 1994), and protein aggregation, indicative of neurodegenerative disease, nitrosative/oxidative stress causing post-translation changes to proteins (Zhang and Kaufman, 2006). The observed metabolic changes in AD have an impact on brain neurotransmitter levels, which result in the cognitive impairment of AD. These impairments can range between the early clinical symptoms of depression to impaired communication, disorientation and behavioural changes in later stage disease (Alzheimer's, 2015).

2.1.3.1 – Branched Chain Amino Acids in Disease

Serum BCAA levels are altered in several neurological disorders. Increased and toxic levels of BCAA and branched chain α-keto-acids are observed in maple syrup urine disease (Menkes, 1962). Symptoms at clinical presentation include neurological dysfunction and seizures, in some cases resulting in infant death (Chuang *et al.*, 2006, Chuang and Chuang, 2000). Conversely, in traumatic brain injury (TBI) the serum amino acid profile show reduced levels of BCAAs and increased ArAAs, with excessive glutamate release following the initial injury (Vuille-Dit-Bille *et al.*, 2012). Changes in net synaptic efficacy and neuronal destruction, similar to that reported in AD occurs, with damage to the limbic hippocampus also observed. This contributes to cognitive impairment and a regional shift in network excitability in both the CA1 and dentate gyrus (Witgen *et al.*, 2005), areas which have been shown to dye heavily populated by hBCATc labelled neurones (Hull *et al.*, 2015), which contribute to glutamate production.

2.1.3.2 - Branched Chain Amino Acid Supplementation

Amino acid supplementation has been trialled with respect to improving cognition in conditions which present with deregulated glutamate levels. Supplementation with BCAAs in TBI models, brain injured mice, showed improved cognition and restored synaptic ability (Cole *et al.*, 2010). In these models, expressional changes for BCATc, BCKDC, glutamate dehydrogenase and glutamic acid decarboxylase were induced post-trauma suggesting a role for BCAA and neurotransmitter metabolism disturbance in this model. Additional investigation has shown new findings for the role of BCAA supplementation to improve cognition and in some cases improved recovery from a vegetative or minimally conscious state (Aquilani *et al.*, 2008). In patients with hepatic encephalopathy,

where similar amino acid profiles to TBI are observed, supplementation with BCAA restored their Fischer ratio (ratio BCAA relative ArAA) to normal (Itou *et al.*, 2009). The altered BCAA and ArAA profile from these reports indicate how changes in BCAA metabolism can impact neurotransmitter synthesis and how supplementation can correct these changes. It is therefore important to understand how serum BCAA levels influence brain glutamate in AD models and more importantly if supplementation can alleviate the potential dysregulation.

Summary

The limited knowledge of the metabolic imbalances that present in AD, and involvement of BCAAs, in particular leucine, offer an important diagnostic and prognostic factor. Diagnosis of MCI and the determination of those who will develop AD is currently dependent on clinical assessment and cognitive ability testing, with no guarantee of accurately determining a patient's prognosis. Understanding the role and profile of the BCAAs in both MCI and AD offers and will enable earlier and more accurate diagnostic and prognostic assessment. Additionally, BCAAs supplementation have been shown to improve cognition in neurological conditions where glutamate levels are deregulated, as seen in AD. This work aimed to expand the understanding of the role of leucine deprivation and supplementation on glutamate levels, and further explore the role of leucine in autophagy and metabolism.

Chapter 2

AIMS AND OBJECTIVES

Fred Hudd

REGULATION OF NEUROTRANSMITTER SYNTHESIS IN ALZHEIMER'S DISEASE – POTENTIAL FOR NOVEL DISEASE BIOMARKERS | 2019

Chapter 2 – Aims and Objectives

2.1 – Hypothesis

The hypothesis for this research is that extracellular leucine directly regulates glutamate levels, and that deprivation contributes to glutamate toxicity and protein aggregation, hallmarks of AD pathology. Moreover, the concentration of the BCAAs will be significantly lower in patients with AD relative to controls and will progressively decrease from the early onset of MCI to progressive disease forms.

2.2 – Aim One

To develop a liquid chromatography tandem mass spectroscopy method for the analysis of serum amino acids, to establish an amino acid 'signature' profile for patients with AD and monitor the BCAA profile in the serum of patients with MCI. These finding will be correlated with brain imaging using MRS and cognitive assessments

2.3 - Aim Two

To investigate the impact of leucine deprivation on cellular amino acid levels, metabolism and markers of autophagy.

2.3 - Aim Three

To investigate the effect of short-term and long-term supplementation on reversing leucine-deprived autophagy and balancing glutamate in AD models.

Chapter 3

MATERIALS AND METHODS

Fred Hudd

Chapter 3 – Materials and Methods

3.1 - Materials

The following materials were obtained from the listed manufacturers.

Abcam plc

Address: Discovery Drive, CB2 0AX, Cambridge, United Kingdom

Materials: Ab7291 - Alpha-Tubulin Mouse Antibody

Agilent Technologies UK Limited

Address: Winnersham Triangle, RG41 5DZ, Wokingham, United Kingdom

Materials: 5182-0716 - Vial, screw top, amber, write-on spot, certified, 2 mL, 100/pk, 5182-0717 - Cap, screw, blue, PTFE/red silicone septa, 100/pk, 959993-902 - ZORBAX Eclipse Plus 95Å C18, 4.6 x 150 mm, 5 µm, 103015-100 - Seahorse XF Cell Mito Stress Test Kit, 102340-100 Seahorse XFe24 FluxPaks, 103577-100 – Seahorse XF 1 M Glucose Solution, 103579-100 Seahorse XF 200 mM Glutamine Solution, 103578-100 Seahorse XF 100 mM Pyruvate Solution.

CK Isotopes Limited

Address: Desford, LE9 9FL, Leicestershire, United Kingdom

Materials: DLM-3725-0.5 - L-Glutamic Acid (2,4,4-D3, 97-98%), DLM-141-0.1 - L-Isoleucine (D10, 98%), DLM-1259-1 – L-Leucine (5,5,5-D3, 99%), DLM-1258-1 –

L-Phenylalanine (Ring-D5, 98%), DLM-451-0.5 – L-Tyrosine (Ring-D4, 98%), DLM-488-0.5 – L-Valine (D8, 98%)

Eurofins Genomics Germany GmbH

Address: Anzigner Str. 7a, 8556, Ebersberg, Germany

Materials: Custom oligonucleotides (Section 3.3 – Table 3.3.1)

Fisher Scientific Ltd

Address: Bishop Meadow Road, LE11 5RG, Loughborough, United Kingdom

10001334 - Acetonitrile, Optima™ LC/MS Grade, Fisher Chemical, 10505904 - Water, Optima™ LC/MS Grade, Fisher Chemical, 10188164 - Water with 0.1% Formic Acid (v/v), Optima™ LC/MS Grade, 26623 - Spectra™ Multicolour Broad Range Protein Ladder, NP0002 - NuPAGE™ MES SDS Running Buffer (20X), 61965059 - DMEM, high glucose, GlutaMAX™ supplement, A3160802 - Fetal Bovine Serum, qualified, One Shot™ format, Brazil, K0781 - Thermo Scientific™ GeneJET™ Whole Blood Genomic DNA Purification Mini Kit, 10338442 - Invitrogen™ Novex™ NuPAGE™ 4-12% Bis-Tris Protein Gels, 1.0mm, 15 well, Thermo Scientific™ 10X TBE Buffer (Tris-borate-EDTA), 10544773 Alexa Fluor 568 Goat Secondary (Anti-Rabbit)

Insight Biotechnology

hBCATc and hBCATm Custom Synthesised Antibodies

New England BioLabs (UK) Ltd

Address: 75-77 Knowl Piece, SG4 0TY, Hitchin, United Kingdom

R0139S – HhaI (20000 units/ml), N3233S - Low Molecular Weight DNA Ladder (500 µg/ml)

Cell Signalling Technologies antibodies – Beclin-1, mTOR and Phospho-mTOR were obtained from New England BioLabs.

Sigma Aldrich Co

Address: The Old Brickyard, New Road, SP8 4XT, Gillingham, United Kingdom

D9443-500ML Dulbecco's Modified Eagle's Medium – Low Glucose (SILAC), LAA21-1KT – L-Amino Acids, GE10600003 - Amersham™ Protran® Premium Western blotting membranes, nitrocellulose pore size 0.45 µm, roll W × L 300 mm × 4 m, WHA7141104 -Whatman® nitrocellulose membrane filters white gridded, pore size 0.45 µm, diam. 47 mm, sterile

---

Waters UK

Address: 610 Centennial Park, Centennial Avenue Elstree, WD6 3TJ, Hertz, United Kingdom

186003038 - XBridge BEH Shield RP18 Column, 130Å, 3.5 µm, 2.1 mm X 150 mm, 1/pkg, WAT097958 - 2.1x1 mm Holder Kit for Cartridges and Guard Columns, 186003068 - XBridge Shield RP 18, 2.1x10 mm, 3.5 µm

---

3.2 - Antibodies

Antibodies were used at the concentrations listed below and obtained from the respective suppliers.

Antibody	Source	Dilution	Supplier	Code
Alpha-tubulin	Mouse	1:5000	Abcam plc	Ab7291
Beclin-1	Rabbit	1:1000	Cell Signalling Technologies	3738S
hBCATc	Rabbit	1:3000	Insight Biotechnology	Custom Synthesis
hBCATm	Rabbit	1:3000	Insight Biotechnology	Custom Synthesis
MAP LC3β	Mouse	1:500	Santa Cruz	SC-376404
mTOR	Rabbit	1:1000	Cell Signalling Technologies	2972S
P-mTOR (S2448)	Rabbit	1:1000	Cell Signalling Technologies	2971S
Alexa Fluor 568 Secondary (Anti-Rabbit)	Goat	1:500	Invitrogen	10544773

3.3 - Primers:

Primer	Sequence
ApoE Upstream	5'-TCC AAG GAG CTG CAG GCG GCG CA-3'
ApoE Downstream	5'-ACA GAA TTC GCC CCG GCC TGG TAC ACT GCC A-3'

3.4 - Ethical Statement and Participants

The study was approved by North Somerset and South Bristol Research Ethics Committee, Bristol, UK. All experiments were carried out in accordance with ethical and NHS governance guidelines and approvals. University of Bristol agree in principle to anonymised data sharing with external researchers and each data request is assessed individually. Participants with the capacity to consent were recruited from the following local and national volunteer registers: Join Dementia Research, BRACE charity, Avon and Wiltshire Mental Health Partnership Trust, ReMemBr group research database and North Bristol NHS Trust. A total of 118 participants were recruited, where 71 were healthy aged individuals and 30 people had a recent diagnosis of MCI (both amnesic and multi-domain MCI) and 17 people with a diagnosis of probable AD. MCI was diagnosed at the Dementia Research Clinic and other local memory services using standard criteria and, for inclusion, all MCI had to have had memory complaints and/or score more than 1 SD below expected for age on a test of memory. Inclusion criteria: All participants had capacity to consent to research and were either drug-free or on stable treatment. In summary: 1) Patients diagnosed with Alzheimer's disease with a Mini-Mental State Examination (MMSE) or Montreal Cognitive Assessment (MoCA) score of greater than 10/30 and have memory deficits demonstrated on at least one of their clinical cognitive assessments. 2) Patients diagnosed with MCI who have either symptoms of amnesia or >1 SD impairment below expected for age performance in episodic memory clinical cognitive tests. 3) Healthy participants age-matched to patients above. Exclusion criteria 1) patients with dementia likely to be of a different aetiology; 2) participants taking medication likely to interfere significantly with cognitive function (except cholinesterase inhibitor and memantine used routinely in dementia) 3) participants with physical

limitations such that they will not be able to carry out the requirements of the study; 4) participants with a history of significant claustrophobia or previous panic or claustrophobia while in an MRI scanner; 5) participants with significant other neurological or psychiatric illnesses likely to interfere with performance on the task. All participants underwent a screening interview to assess demographic factors thought to impact on cognitive decline (IQ, history of head trauma, epilepsy, smoking and alcohol intake) (Table 1). There was no significant difference between AD, MCI and control groups with respect to most parameters, however, there was a significant difference with respect to years of education and IQ score. For blood analysis a number of people were unable to provide a sample, therefore a total of 46 controls, 17 MCI and 15 AD were recruited for this aspect of the study.

3.5 - Methods

3.5.1 - Cognitive Assessment of Control, MCI and AD

A battery of assessments designed to probe hippocampal function as well as tests of wider cognitive function was implemented (Conducted by The ReMemBer group at The University of Bristol). Tests that were performed as part of the experimental procedure included: 1) Montreal cognitive assessment (MoCA, as a global cognitive screen). 2) Paired Associate Learning from CANTAB as a pattern/spatial memory task widely used and thought to be a "hippocampal" task - used as an early marker of AD. 3) Adapted verbal learning task (similar to Hopkins Verbal Learning Task) testing memory over 30 minutes, 24 hours, 2, 7 and 14 days (Dillon *et al.*, 2017).

3.5.2 – Magnetic Resonance Imaging (MRI) of Control, MCI and AD

MRI imaging was performed at the Clinical Research and Imaging Centre (CRiC Bristol), University of Bristol.

All participants were scanned using a Siemens Magnetom Skyra 3T MRI system using a 32Ch head coil. The MRI protocol was as follows: 3D T1-weighted MRI was collected with MPRAGE: coronal, TR 2200 ms, TE 2.42 ms, TI 900 ms, flip angle 9°, resolution 0.34 x 0.34 x 1.60 mm3 (after 2-fold interpolation in-plane), matrix size 540 x 640 x 144 (after 2-fold interpolation in-plane), GRAPPA factor 2, time 5:25. Quantitative T2 images were acquired with a multi-contrast spin-echo sequence: coronal, TR 4500, TE 12 ms, number of echoes 10, echo spacing 12 ms, resolution 0.34 x 0.34 x 1.7 mm3 (after 2-fold interpolation in-plane, and inclusive of 15% slice gap), matrix size 540 x 640, 34 slices, GRAPPA factor 2, time 11:07.

Total brain, gray matter, white matter and CSF space volumes were determined using FSL routines (http://www.fmrib.ac.uk/fsl). Morphometry of hippocampus and its sub-regions were determined from T2 images using the manual protocol by (Wood *et al.*, 2015). This protocol provides volumes for 6 subfields as follows: CA1, CA2, CA3, dentate gyrus, subiculum and lumped stratum moleculare, stratum lacunosum and stratum radiatum (SM/SL/SR).

3.5.3 – Blood Biomarkers for Control, MCI and AD

Whole blood samples were provided by participants grouped into control, presentation of Alzheimer's disease or mild cognitive impairment. Samples were

fractionated by centrifugation at 1,300 x g for 10 minutes at 4°C. Serum was aliquoted and subsequently stored at -80°C until analysed.

3.5.5 - Protein Estimation Using the Amido Black Assay

A purified BSA protein standard was prepared to a concentration of 0.1 µg/µL and diluted to produce a standard curve (0, 1, 2.5, 5, 7.5, 10, 12.5, 15, 17.5 and 20 µg). Unknown samples were diluted to a concentration approximately within the range of the standard curve with 18 MΩ water. For all samples, 30 µL of Tris-HCl buffer (1M trichloroacetic acid, 35 mM sodium dodecyl sulphate, pH 7.4) and 60 µL of 60% trichloroacetic acid were added and the samples incubated at room temperature for 5 minutes. Samples were pipetted onto a 0.45 µm nitrocellulose membrane periodically hydrated with 6% trichloroacetic acid and pulled through under gentle vacuum (16.9 kPa). The membrane was subsequently stained in staining buffer (1g/L Amido black powder, 45% methanol, 10% acetic acid in diH_2O) for 2 minutes, washed with diH_2O and destained in buffer (90% methanol, 2% acetic acid in diH_2O) for 1 minute. Destaining was repeated to remove excess background staining and protein spots excised from the membrane and incubated in eluent (25 mM sodium hydroxide, 50 µM ethylenediaminetetraacetic acid, 50% ethanol in diH_2O) for 10-20 minutes. Eluent absorbances were measured at 620 nm using a FLUOstar Omega microplate reader (BMG Labtech). Samples concentration was calculated against the BSA standard curve.

3.5.6 - Wet Transfer Western Blot Analysis

Serum samples were diluted to a concentration of 10 µg in LDS sample buffer (4x) with 5% β-mercaptoethanol and denatured at 95°C for 10 minutes. Samples were vortexed and centrifuged prior to loading onto a 4-12% Bis-Tris gradient gel. Proteins were separated in parallel with broad range ladder at 150 V for 1 hour in

MES electrophoresis buffer. The proteins were then transferred overnight onto a PVDF membrane at 50 V in transfer buffer (20% methanol, 25 mM Tris, 190 mM glycine, pH 8.3). The membrane was washed in TBST (0.1% Tween, 200 mM NaCl, 2 mM Tris, pH 7.5) and subsequently blocked with 5% BSA in TBST for 1 hour. Primary antibody was prepared in 5% BSA (1:1000 for hBCATc and hBCATm) and added to the membrane for 1 hour. Several washes in TBST were performed and the membrane incubated for a further 1 hour with appropriate dilutions of HRP-linked secondary antibody. After further washes the positive bands were visualised with chemiluminescent HRP substrate on an Odyssey® Fc Imaging System (LI-COR Biosciences) and results normalised against the appropriate loading controls.

3.5.7 - 1D Gel Electrophoresis

Serum samples were diluted to a concentration of 5 µg in LDS samples buffer (4x) with 5% β-mercaptoethanol. Samples were treated and separated in the same manner detailed in Wet Transfer Western Blot. Gels were subsequently stained with InstantBlue Coomassie Dye and incubated at room temperature for 1 hour on a rocking mixer. After 1-hour gels were washed in deionised water and imaged using an Odyssey® Fc Imaging System (LI-COR Biosciences).

3.5.8 - ApoE Genotyping

Genomic DNA was extracted from whole blood or lysed white blood cells using a GeneJET Whole Blood Genomic DNA Extraction Kit. Two hundred microlitres of whole blood or WBC were aliquoted and 20 µL of proteinase K and 400 µL of lysis buffer added. Samples were mixed by vortex and incubated at 56°C for 10 minutes in a thermo mixer at 1000 RPM. Subsequently, 200 µL of 100% ethanol

was added, the sample transferred to a GeneJET spin column and centrifuged for 1 minute at 6,000 x g. The flow through was discarded and 500 µL of Wash Buffer I added before centrifuging for 1 minute at 8,000 x g. The flow through was once again discarded, 500 µL of Wash Buffer II added and the column centrifuged again at 17,000 x g for 3 minutes. The column was subsequently transferred to a new collection tube and 200 µL of elution buffer added. The column was incubated in elution buffer for 2 minutes at room temperature before being centrifuged at 17,000 x g for 2 minutes. Eluted DNA was stored at -20°C.

3.5.9 - PCR Amplification of ApoE Coding Region

The ApoE coding region of extracted genomic DNA was amplified by PCR using oligonucleotide primers (Eurofins Genomics; upstream primer: 5'- TCC AAG GAG CTG CAG GCG GCG CA -3', downstream primer: 5'- ACA GAA TTC GCC CCG GCC TGG TAC ACT GCC A - 3'). The PCR mix consisted of 10 µL of GC Taq 5x buffer, 2 µL of ApoeE23 and ApoE31 primers (2 pmol), 2 µL of dNTPs mix, 0.2 µL of One Taq polymerase and made to a final volume of 50 µL with nuclease free water. Amplification was performed in an PTC-200 Peltier Thermal Cycler.

3.5.10 - HhaI Restriction Digest

PCR product was digested with HhaI restriction enzyme, 26 µL of product was added to 1 µL of HhaI and 3 µL of NEB CutSmart Buffer (10x). The solution was incubated at 37°C overnight in a thermomixer.

3.5.11 – Visualisation of HhaI Digested Products

HhaI digested PCR products were visualised on a 2.5% Metaphor agarose gel supplemented with ethidium bromide at 2.5%. Samples were separated at 80v for

2 hours in TBE buffer and imaged using an Odyssey® Fc Imaging System (LI-COR Biosciences).

3.5.12 - Preparation of Amino Acid Standards and Calibrators

Powdered amino acid standards for glutamic acid, isoleucine, leucine, phenylalanine, tyrosine and valine were used to prepare individual 1 mM stock solutions in 0.1% formic acid in water and stored at -80°C until required. Deuterium labelled isotope internal standards for each amino acid were prepared in the same manner and combined and diluted to a concentration of 500 µM. Mixed amino acid calibrators of 1 µM, 5 µM, 10 µM, 20 µM, 30 µM, 40 µM, 50 µM, 60 µM, 70 µM, 80 µM, 90 µM and 100 µM were prepared by dilution with 0.1% formic acid in water and the addition of 50 µM internal standard.

3.5.13 - Serum and Fluid Sample Preparation

Serum samples were thawed unassisted at room temperature and vortexed before analysis. One hundred microlitres was added to 350 µL of 0.1% formic acid in acetonitrile and 50 µL of mixed deuterium labelled internal standard to give a final concentration of 50 µM. Samples were vortexed and centrifuged at 3,200 g for 10 minutes at room temperature. Fifty microlitres of supernatant was aliquoted into sample vials and evaporated to dryness under a stream of nitrogen gas. The sample residue was reconstituted in 200 µL of 0.1% formic acid in water.

3.5.14 – Cell Sample Preparation

SH-SY5Y cells were grown to confluence and treated before the media was removed and the cells washed with ice cold PBS. Cells were subsequently extracted by scraping in RIPA buffer (10 mM Tris, 150 mM NaCl) with protease inhibitor cocktail. Cells were incubated in RIPA buffer for 30 minutes before

sonication for 2 minutes (10 seconds on, 10 seconds off) at 10 microns. Lysates were clarified by centrifugation at 13,000 x g for 10 minutes and the supernatant aliquoted into separate tubes and stored at -80 until required. Cell media was filtered through a 0.45 µM membrane to remove any remaining cells and stored at -80. Both cell lysates and media were prepared for analysis in the same manner as serum samples.

3.5.15 - Determination of Precursor Ions

Mass spectrometry scanning was used to determine each amino acid and labelled isotopes precursor ion value. Ten microlitre of sample was analysed with no chromatographic separation. Samples were positively ionised by an electrospray ionisation source with Agilent JetStream technology. Nitrogen was used as both nebuliser and collision gas at a pressure of 45 psi, with sample injection time set to 0.50 minutes. Ion mass was analysed between a detection range of 100-300, at a fragmentor voltage of 135 V and cell accelerator voltage of 4 V.

3.5.16 - Determination of Product Ions

Product ion transitions were determined through the use of the Agilent MassHunter Optimiser program (Ver. B.07.01 Build. 7.1.7112.0). Precursor ion values were input from previous mass spectroscopy data and optimised for amino acid mass with the addition of a single hydrogen atom. Ten microlitres of 1 mM amino acid and internal standard stock solution was analysed and precursor ion intensity optimised through automated alteration of fragmentor voltage. Tandem mass spectroscopy was used to determine the most suitable product ions, and detection sensitivity optimised through automated alteration of collision energy.

3.5.17 - Optimisation of Acquisition Parameters

Acquisition parameters for the source were optimised using Agilent MassHunter Source Optimiser and iFunnel software. Flow dependent parameters (nebuliser pressure, drying gas temperature and flow rate, sheath gas flow (SGF)), and compound dependent parameters (capillary voltage (CV), sheath gas temperature (SGT) and nozzle voltage (NV)) were optimised through the injection of 10 µL of 1 mM mixed amino acid and internal standard. Spectral count and abundance were monitored for beneficial alterations for each amino acid and internal standards product ion.

3.5.18 - Sample Analysis for Branched Chain and Aromatic Amino Acids

Chromatographic separation was performed using an Agilent 1260 Series LC system, coupled with an Agilent 6460 triple quadrupole mass spectrometer for tandem mass spectroscopy and multiple reaction monitoring. Sample was injected at onto an Agilent ZORBAX Eclipse Plus C18 column (4.6 mm x 150 mm, 5 µm) maintained at 20°C. Glutamic acid, isoleucine, leucine, tyrosine and valine were eluted with a mobile phase of 0.01% formic acid in water – acetonitrile (98:2). Phenylalanine was eluted with a mobile phase of 0.01% formic acid in water – acetonitrile (80:20). Mobile phase was set to a flow rate of 0.3 mL/minute for all analysis. For all sample runs blanks of 0.1% formic acid were injected between triplicate sample runs and the system and column cleaned with 80% acetonitrile after 5 sample runs.

Sample data was analysed with Agilent MassHunter Quantitative Analysis and Qualitative analysis software (Ver. B.07.00 Service Pack 1) and normalised against total protein for each sample.

3.5.19 - Percentage Recovery

Serum, cell samples and prepared amino acid standards were spiked with a 50 μM mixed amino acid in 0.1% formic acid in water and prepared in the same manner as analysis samples without the addition of an internal standard before drying. Dried samples were reconstituted in 200 μL of mixed deuterium labelled internal standard and analysed in the same manner as participant samples.

3.5.20 – Sample Stability

Serum amino acid stability when stored at -80°C was assessed over a three-month and six-month period from sample collection. Samples were analysed as described in 3.5.17 upon collection with subsequent analysis three and six months after this date. Intra-run and total coefficients of variation were calculated for each run.

3.5.21 - Statistical Analysis

The data was screened for its accuracy and validity and for any potentially influential or outlying observations which may otherwise unduly impact results. A between-participants analysis of variance for a one-way design, with a post-hoc application of Tukey's HSD pairwise test was used to assess for differences between Control/MCI/AD for BCATc, BCATm, amino acids, brain sub-volumes, and the cognitive data. Residuals under each ANOVA were examined to ensure they did not grossly deviate from the assumption of errors being independent identically distributed normal deviates. Pearson's correlation coefficient was used to assess the strength and direction of correlations between quantitative measures.

MoCA scores were used in a linear discriminant analysis to develop a baseline model to discriminate between Control/MCI/AD. We sought to extend this baseline model to determine whether the inclusion of BCATc, BCATm, the amino acids and brain sub-volumes would improve the discrimination between groups. Accuracy of discrimination was determined using leave-one-out cross-validation. To account for the putative ordering of outcome (Control/MCI/AD) we further used MoCA scores in an ordinal logistic regression model. We sought to extend this baseline ordinal logistic regression model to determine whether the inclusion of BCATc, BCATm, the amino acids and brain sub-volumes would improve the predictive capability of the baseline model. This modelling utilising linear discriminant analysis and ordinal logistic regression using MoCA as a baseline model was repeated using Dentate Gyrus volume in replace of MoCA. We further sought to investigate the utility of the blood markers in isolation and repeated the modelling with BCATm as the baseline marker. Optimal sensitivity and specificity for predicting MCI or AD, and for AD was determined using the ordinal logistic regression model through the maximisation of Youden's Index.

3.5.22 - Cell Culture

SH-SY5Y cells were grown in Dulbecco's modified Eagle's medium (DMEM) supplemented with 10% foetal bovine serum (FBS). Cells were maintained at 37°C in a saturated humidity atmosphere of 95% oxygen and 5% carbon dioxide. Cells were grown to 70-80% confluence before sub-cultured.

3.5.23 - Nutrient Deprivation

SH-SY5Y cells were maintained in nutrient deprived conditions through culture in EBSS for time periods of 12, 24 and 48 hours. Cells were maintained at 37°C in a saturated humidity atmosphere of 95% oxygen and 5% carbon dioxide.

3.5.24 - Leucine Deprivation

SH-SY5Y cells were deprived of leucine over period of 12, 24 and 48 hours. Maintenance cell media was changed to Sigma SILAC media supplemented with L-arginine hydrochloride (0.4 mM) and L-lysine hydrochloride (0.8 mM). Cells were maintained at 37°C in a saturated humidity atmosphere of 95% oxygen and 5% carbon dioxide.

3.5.25 - Leucine Supplementation

Leucine deprived SH-SY5Y cells were maintained in Sigma SILAC media, supplemented with L-arginine hydrochloride (0.4 mM) and L-lysine hydrochloride (0.8 mM), for 12, 24 or 48 hours before supplementation with 2 mM or 5 mM L-leucine. Cells were subsequently extracted at 12, 24, 48 or 72 hours. Cells were maintained at 37°C in a saturated humidity atmosphere of 95% oxygen and 5% carbon dioxide.

3.5.26 - Protein Estimation Using Micro-Bradford Assay

A concentrated stock dye of Coomassie blue G was prepared by dissolving 300 mg Coomassie blue G dye in 100 mL phosphorus acid/ethanol (2:1). For protein estimation this was diluted to a working due (3% stocky dye, 3.8% ethanol, 8% phosphoric acid) prior to experimentation. A purified bovine serum albumin (BSA) protein standard was prepared to a concentration of 1 µg/mL and aliquoted into 1 mL volumes and stored at -20°C.

Samples were diluted to an approximate concentration within the standard curve range, and 5 µL pipetted in triplicate into a 96 well plate. BSA protein standard was prepared to concentration between 0.2 µg/µL and 1 µg/µL and pipetted in

triplicate, before the addition of 200 µL of working dye to both standard and sample. Absorbance was measured at λ620 nm on an Odyssey spectrophotometer and a standard curve generated using the BSA dilution.

3.5.27 - Seahorse Assay: Cell Culture

SH-SY5Y cells were seeded in triplicate or quadruplicate at a density of 60,000 cells per 100 µL of DMEM supplemented with 10% FBS. Cells were allowed to adhere at 37℃ for 2 hours and 150 µL of media added to each well to bring the final volume to 250 µL. Cells were either leucine deprived (3.5.22), maintained in nutrient deprived conditions (3.5.21), leucine deprived and subsequently supplemented with leucine (3.5.23) or maintained under normal control conditions (3.5.20)

3.5.28 - Seahorse Assay

The day prior to performing the assay, the Seahorse sensor cartridge was hydrated with 1 mL of Seahorse XF Calibrant per well and incubated overnight at 37°C in a non-CO_2 incubator.

Assay medium was prepared by supplementing Seahorse XF Base Minimum DMEM with 1 mM pyruvate, 2 mM glutamine and 10 mM glucose and adjusting the pH to 7.4 with 0.1 N NaOH. The prepared media was subsequently sterile filtered and incubated at 37°C until used.

Kit reagents for the Seahorse XF Cell Mito Stress Kit were prepared on the day of analysis with assay medium from powdered stocks of oligomycin, FCCP and rotenone/antimycin A to final concentrations of 100 µM, 100 µM and 50 µM, respectively. Stock solutions were diluted to a working

concentration of 1 μM in assay media and pipetted into the sensor cartridge injection ports.

Prior to analysis, cells were washed twice in assay media and 500 μL of media subsequently added to each well. The plate was subsequently incubated at 37°C in a non-CO_2 incubator for 1 hour.

The Seahorse sensor cartridge was loaded in the Seahorse Xfe24 analyser and initially calibrated. The hydrated utility cartridge was subsequently removed, and the incubated cell plate inserted for analysis.

Data from the Seahorse was analysed with Agilent Seahorse Wave Software (Version 2.6.1) and values normalised against values obtained from Crystal Violet staining (3.5.28).

3.5.29 - Crystal Violet Post Normalisation

Cells were fixed in 100 μL of 4% paraformaldehyde for 20 minutes at room temperature. Cells were washed in 200 μL of PBS three times and stained with 0.2% Crystal Violet solution for 30 minutes at room temperature on a shaker. Crystal Violet solution was removed, and the cells washed again in 200 μL of PBS three times. Cells were solubilised in 100 μL of SDS per well and incubated for 1 hour at room temperature on a shaker. The absorbance of the solution was read at 595 nm using a FLUOstar Omega microplate reader (BMG Labtech).

Chapter 4

DEVELOPMENT OF AN ISOTOPE DILUTION LIQUID CHROMATOGRAPHY TANDEM MASS SPECTROSCOPY METHOD FOR THE MEASUREMENT OF SERUM AND CELL LYSATE BRANCHED CHAIN AND AROMATIC AMINO ACIDS

Fred Hudd

REGULATION OF NEUROTRANSMITTER SYNTHESIS IN ALZHEIMER'S DISEASE – POTENTIAL FOR NOVEL DISEASE BIOMARKERS | 2019

Chapter 4 – Development of an Isotope Dilution Liquid Chromatography Tandem Mass Spectroscopy Method

4.1 – Introduction

Amino acids are routinely analysed from whole blood by dried blood spots, serum, urine and CSF (French, 2017). Initial quantitative analysis was routinely carried out by ion exchange chromatography (IEC) coupled with optical detection (Sandlers, 2019). This method allowed the automated separation using a polystyrene resin column (Moore *et al.*, 1958) and quantitative and qualitative analysis of amino acids by IEC after ninhydrin post column derivatisation (Moore *et al.*, 1958). IEC is still adopted in a number of clinical settings with post-column derivatisation and UV detection used for sample analysis (Sandlers, 2019). Successive techniques have since been adopted, including reverse-phase high performance liquid chromatography (HPLC), gas chromatography, liquid chromatography mass spectroscopy (LC-MS) and gas chromatography mass spectroscopy for the measurement of amino acids. When compared to IEC, sample impurities have a greater effect on analysis of amino acids by HPLC and therefore sample clean up through pre-column or post-column derivatisation is required (Csapó *et al.*, 2008). Furthermore, as with IEC, HPLC offers high sensitivity, however, the specificity of analysis is solely determined by retention time of the analyte which can lead to false findings as with the falsely elevated levels of phenylalanine due to coelution with ampicillin and amoxicillin (Sandlers, 2019).

The use of ion-exchange chromatography and high-performance liquid chromatography both require extended chromatography run times (Yang *et al.*,

2013). The use of higher-pressure and smaller particle size allowed ultra-high-performance liquid chromatography for increased sample throughput with comparable results to IEC (Narayan *et al.*, 2011). In addition to these typical methods of chromatographic analysis gas chromatography can be used in place of IEC and presents results in agreement with IEC analysis (Zumwalt *et al.*, 1987). However, as with both HPLC and IEC gas chromatography requires derivatisation prior to analysis.

Overcoming this requirement, the combined techniques of chromatographic separation and mass spectroscopy methods offer both highly selective and sensitive analysis while negating the need for pre-column derivatisation. Liquid chromatography tandem mass spectroscopy (LC-MS/MS) has shown utility in analysing individual or small groups of amino acids and their metabolites (Walker and Mills, 1995) analysis of branched chain and aromatic amino acids for diabetes screening (Yang *et al.*, 2013) and the analysis of underivatised amino acids for the diagnosis of inborn errors of amino acid metabolism (Piraud *et al.*, 2005).

I developed and validated an isotope dilution liquid chromatography tandem mass spectroscopy method for the analysis of serum and cellular lysate glutamic acid, isoleucine, leucine, phenylalanine, tyrosine and valine. The method requires minimal sample preparation with no requirement for sample derivatisation and allows for the complete chromatographic separation of each amino acid.

4.2 – Specific Aims

Specific Aim 1: Develop an isotope dilution liquid chromatography tandem mass spectroscopy method for the analysis of glutamic acid, isoleucine, leucine, phenylalanine, tyrosine and valine.

Specific Aim 2: Validate and optimise the isotope dilution liquid chromatography tandem mass spectroscopy (ID-LC-MS/MS) method for the analysis of glutamic acid, BCAAs and ArAAs in human serum

4.3 – Results

4.3.1 – Identification of BCAA and AAA Precursor Ions and Determination of Product Ions

To identify BCAA and AAA, deuterium labelled (Table 4.3.1) and unlabelled standards of glutamic acid, isoleucine, leucine, phenylalanine, tyrosine and valine were prepared to a concentration of 1 mM in 0.01% formic acid (Yang *et al.*, 2013). Each amino acid was analysed separately by MS1 scan to determine the quasi-molecular ion (M-H+) with scanning range of 100-300 m/z by introduction of the sample into an Agilent 6460 QQQ mass spectrometer via an Agilent 1260 Infinity series HPLC. These ions were subsequently entered into Agilent MassHunter Optimiser software (Ver. B.07.01 Build. 7.1.7112.0). Select ion monitoring of precursor ions at various at course and fine stepped fragmentor voltages were used to find the optimum field ionisation for each amino acid (Table 4.3.2). Product ions scans at multiple collision energies were used to establish product ions values, with subsequent multiple reaction monitoring of these ions at various collision energies used to determine the optimum collision energy for each ion. Product ions scans at the optimal fragmentor voltage and collision energy were used to fine tune the exact mass of each product ion.

Isoleucine and leucine share the transitions of m/z 132.10 $\rightarrow$ 69.10 and m/z 132.10 $\rightarrow$ 86.10 which presented the highest peak are ratios compared to other transitions. Deuterium labelled variants of these amino acids did not share transitions due to the difference in label size between isoleucine and leucine.

Table 4.3.1 – Composition of deuterium labelled internal standards

Internal Standards	Internal Standard Labelling
Glutamic acid	L-Glutamic Acid (2,4,4-D3, 97-98%)
Isoleucine	L-Isoleucine (D10, 98%)
Leucine	L-Leucine (5,5,5-D3, 99%)
Phenylalanine	L-Phenylalanine (Ring-D5, 98%)
Tyrosine	L-Tyrosine (Ring-D4, 98%)
Valine	L-Valine (D8, 98%)

Table 4.3.2 – Precursor ions and fragmentor voltage for deuterium labelled and unlabelled amino acid standards

Amino Acids	Precursor Ion	Fragmentor Voltage (V)
Glutamic acid	148.10	90
Isoleucine	132.10	90
Leucine	132.10	90
Phenylalanine	166.10	94
Tyrosine	182.10	86
Valine	118.10	90
Deuterium Labelled Amino Acids	**Precursor Ion**	**Fragmentor Voltage**
Glutamic acid	151.08	76
Isoleucine	142.17	76
Leucine	135.12	76
Phenylalanine	171.12	76
Tyrosine	186.11	76
Valine	126.14	76

Table 4.3.3 Product ion transitions and required fragmentor voltage and collision energy for deuterium labelled and unlabelled amino acid standards

Amino Acids	Ion Transitions (m/z)	Fragmentor Voltage (V)	Collision Energy (V)
Glutamic acid	148.10 → 56.10	90	20
	148.10 → 84.10	90	20
Isoleucine	132.10 → 69.10	90	20
	132.10 → 86.10	90	20
Leucine	132.10 → 69.10	90	20
	132.10 → 86.10	90	8
Phenylalanine	166.10 → 103.10	94	32
	166.10 → 120.10	94	20
Tyrosine	182.10 → 91.10	86	29
	182.10 → 165.10	86	5
Valine	118.10 → 55.10	90	24
	118.10 → 72.10	90	20
Deuterium Labelled Amino Acids	**Ion Transitions (m/z)**	**Fragmentor Voltage (V)**	**Collision Energy (V)**
Glutamic acid (Glu-D3)	151.08 → 86.70	76	17
	151.08 → 133.10	76	5
Isoleucine	147.17 → 48.10	76	29
	147.17 → 78.20	76	21
	147.17 → 96.20	76	9
Leucine	135.12 → 46.10	76	25
	135.12 → 89.20	76	9
Phenylalanine	171.12 → 106.10	76	33
	171.12 → 125.10	76	13
Tyrosine	186.11 → 93.80	29	33
	186.11 → 140.10	76	9
	186.11 → 169.10	76	5
Valine	126.14 → 62.10	76	25
	126.14 → 80.20	76	9

4.3.2 – Mass Spectrometer Source Optimisation

Flow dependent and compound dependent parameters were optimised using Agilent Source and iFunnel Optimisation software (Ver. B.07.01 Build. 7.1.7112.0) to reduce final serum sample injection volume and increase detector response. The baseline settings for analysis before optimisation and the chosen analytical settings achieved from source optimisation are presented in Table 4.3.4 – 4.3.8. Parameter alteration yielded spectral count increased between 24.11% and 104.38% and absorbance reading increased between 23.22% and 154.36% for glutamic acid, leucine, phenylalanine, tyrosine and valine. Conversely, a 9.35% decrease in absorbance for unlabelled isoleucine was reported.

Table 4.3.4 Baseline and source optimised flow and compound dependent parameter values for sample analysis

Method	Capillary Voltage	Drying Gas Flow Rate	Drying Gas Temperature	Nebuliser Pressure	Nozzle Voltage	Source Gas Flow Rate	Source Gas Temperature
Baseline	3500 V	5 L/min	300°C	45 psi	500 V	11 L/min	250°C
Source Optimised	2500 V	4 L/min	350°C	30 psi	0 V	12 L/min	400°C

Values for source and compound dependant optimisation parameters for the baseline method used for initial standard analysis and the source optimised method used for subsequent calibrator and sample analysis.

Table 4.3.5 Comparative percentage difference of spectral count for glutamic acid, isoleucine, leucine, phenylalanine, tyrosine and valine between baseline method and source optmised method

	Glutamic Acid				Isoleucine				Leucine			
	Transition (56.1)	Difference	Transition (84.1)	% Difference	Transition (69.1)	Difference	Transition (86.1)	% Difference	Transition (69.1)	Difference	Transition (86.1)	Difference
Baseline Spectral Count	825000	24.11	2655709	23.23	1505914	104.38	1855746	98.52	1505692	104.95	10757172	81.06
Optimised Spectral Count	1023869		3272701		3077774		3683935		3085942		19477428	

	Phenylalanine				Tyrosine				Valine			
	Transition (103.0)	% Difference	Transition (120.1)	% Difference	Transition (91.1)	Difference	Transition (165.1)	% Difference	Transition (55.1)	% Difference	Transition (72.1)	% Difference
Baseline Spectral Count	4026381	59.70	8183411	60.38	959484	29.30	1110251	29.36	2747845	74.43	3055751	4026381
Optimised Spectral Count	6430065		13124604		1240629		1436199		4792939		5252702	6430065

Table 4.3.6 Comparative percentage difference of spectral count for deuterium labelled glutamic acid, isoleucine, leucine, phenylalanine, tyrosine and valine between baseline method and source optmised method

	Glutamic Acid (Deuterium)				Isoleucine (Deuterium)				Leucine (Deuterium)			
	Transition (86.7)	**% Difference**	**Transition (133.1)**	**% Difference**	**Transition (48.1)**	**% Difference**	**Transition (78.2)**	**% Difference**	**Transition (96.2)**	**% Difference**	**Transition (46.1)**	**% Difference**
Baseline Spectral Count	41617	32.57	62045	28.59	126969	105.40	94053	102.51	762710	102.62	288878	90.36
Optimised Spectral Count	55173		79783		260793		190465		1545389		549904	

	Phenylalanine (Deuterium)				Tyrosine (Deuterium)				Valine (Deuterium)			
	Transition (106.1)	**% Difference**	**Transition (125.1)**	**% Difference**	**Transition (93.8)**	**% Difference**	**Transition (140.1)**	**% Difference**	**Transition (169.1)**	**% Difference**	**Transition (62.1)**	**% Difference**
Baseline Spectral Count	161277	58.21	913704	52.45	20651	29.91	66132	29.62	76532	27.59	1662965	75.36
Optimised Spectral Count	255150		1392973		26827		85723		97647		2916212	

Table 4.3.7 Comparative percentage difference of absorbance for glutamic acid, isoleucine, leucine, phenylalanine, tyrosine and valine between baseline method and source optmised method

	Glutamic Acid				Isoleucine				Leucine			
	Transition (56.1)	Difference	Transition (84.1)	% Difference	Transition (69.1)	Difference	Transition (86.1)	% Difference	Transition (69.1)	Difference	Transition (86.1)	Difference
Baseline Absorbance	21873.32	24.11%	70264.84	23.22%	27174.59	-9.35%	125986.97	51.52%	12775.3	150.05	96966.02	154.36%
Optimised Absorbance	27146.91		86582.63		24633.15		190894.34		31944.78		246640.09	

	Phenylalanine				Tyrosine				Valine			
	Transition (103.0)	% Difference	Transition (120.1)	% Difference	Transition (91.1)	Difference	Transition (165.1)	% Difference	Transition (55.1)	% Difference	Transition (72.1)	% Difference
Baseline Absorbance	8370.9	33.92	17268.97	33.89	19707.21	29.32	22798.1	29.32	56630.09	35.91	62886.28	33.93
Optimised Absorbance	11210.33		23121.24		25484.78		29481.46		76963.57		84224.32	

Table 4.3.8 Comparative percentage difference of absorbance for deuterium labelled glutamic acid, isoleucine, leucine, phenylalanine, tyrosine and valine between baseline method and source optmised method

	Glutamic Acid (Deuterium)				Isoleucine (Deuterium)				Leucine (Deuterium)			
	Transition (86.7)	% Difference	Transition (133.1)	% Difference	Transition (48.1)	% Difference	Transition (78.2)	% Difference	Transition (96.2)	% Difference	Transition (46.1)	% Difference
Baseline Absorbance	1136.07	58.58	1901.02	42.33	3684.91	70.11	2742.58	67.46	21890.41	68.81	8312.45	89.62
Optimised Absorbance	1801.55		2705.72		6268.37		4592.60		36954.16		15762.23	

	Phenylalanine (Deuterium)				Tyrosine (Deuterium)				Valine (Deuterium)			
	Transition (106.1)	% Difference	Transition (125.1)	% Difference	Transition (93.8)	% Difference	Transition (140.1)	% Difference	Transition (169.1)	% Difference	Transition (62.1)	% Difference
Baseline Absorbance	2143.48	56.86	11947.99	52.21	534.96	-7.69	1628.8	-8.34	1885	0.71	43331.5	60.79
Optimised Absorbance	3362.3		18186.19		493.82		1492.89		1898.72		69671.27	

Percentage differences were calculated using values obtained from analysis of amino acid standards using the baseline source parameter settings and the chosen optimised parameters summarised in Table 4.3.4.

4.3.3 – Published Chromatography and Developmental Method Chromatography Comparison

Early multiple reaction monitoring (MRM) analysis showed that separation of mixed amino acid standards could not be achieved using a Waters XBridge Shield RP18 3.5 µm 2.1 x150 mm column, with co-elution of all amino acids occurring in under 0.3 minutes. All amino acids were present in a singular peak, determined through ion transition analysis, where retention times for each amino acid showed significant overlap and no distinct individual peak area. Figure 4.3.1 shows the reported chromatographic separation in Yang *et al* (2013) and the separation achieved through from my analysis using the same column and mobile phase.

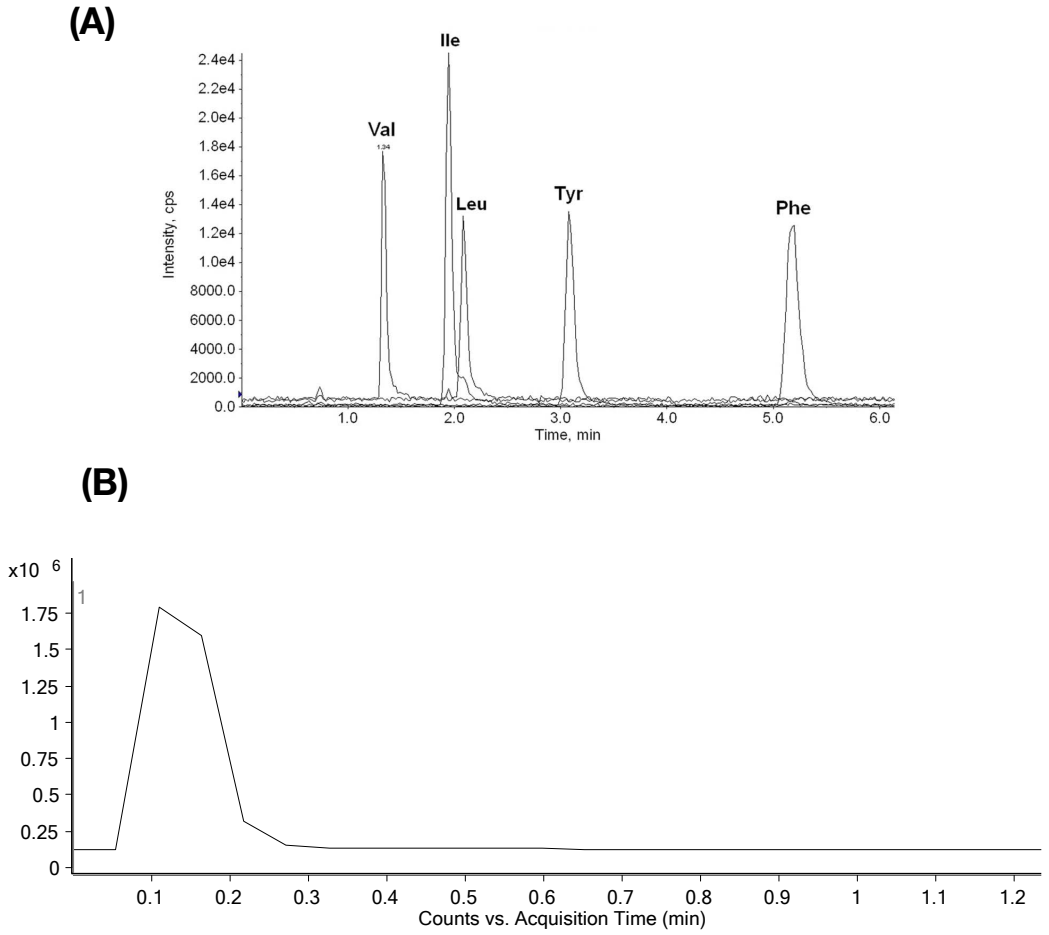

Figure 4.3.1: Comparison of Chromatographic Separation using a Waters XBridge RP18 Column.
(A) Chromatographic separation of Val, Ile, Leu, Tyr and Phe reported by Yang (2013) using a Waters XBridge Shield RP18 3.5 µm 2.1 x150 mm column, eluted using a mobile phase of 98:2 0.01% formic acid in water and acetonitrile. Full separation was achieved in under 6 minutes. (B) Chromatographic separation achieved during ID-LC-MS/MS method development, of Glu, Val, Ile, Leu, Tyr and Phe using the same column type and mobile phase. No individual separation was recorded, and all amino acids were eluted in under 0.3 minutes.

4.3.4 – Chromatographic Separation of Amino Acids

Representative spectral count peaks for each amino acid with all amino acids eluted from the column in under 21 minutes (Figure 4.3.2). Glutamic acid, valine, isoleucine, leucine, tyrosine and phenylalanine were retained on the column for 4.90 ± 1.02 mins, 6.06 ± 0.79 mins, 9.13 ± 1.60 mins, 9.95 ± 2.39 mins, 11.02 ± 2.70 mins and 19.84 ± 3.07 mins, respectively. To decrease total run time the percentage of acetonitrile was increased from 2% to 20% at fourteen minutes to reduce the elution time of phenylalanine.

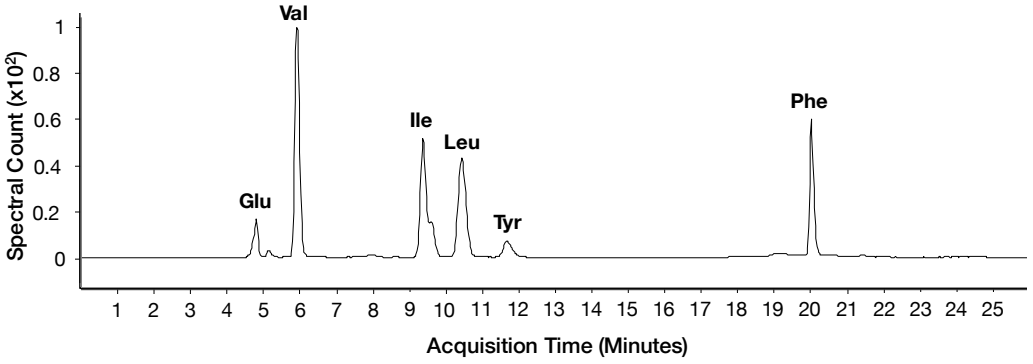

Figure 4.3.2: Multiple reaction monitoring chromatogram of branched chain (Ile, Leu and Val), aromatic (Tyr and Phe) amino acids and glutamic acid.
Samples were eluted from an Agilent ZORBAX Eclipse Plus C18 column (4.6 x 150 mm, 5 μm) with a mobile phase of 0.01% formic acid in water – acetonitrile at a ratio of either 98:2 for Glu, Val, Ile, Leu, Tyr or 80:20 for Phe.

4.3.5 – Linearity of Amino Acids Standard Concentration

Linear regression between peak area ratio and amino acid concentration was used to establish calibration functions for each amino acid (Representative curves Figure 4.3.3). Table 4.3.9 summarises the regression coefficient, intercept, and correlation coefficient for each amino acid.

Table 4.3.9 - Calibration parameters for glutamic acid, isoleucine, leucine, phenylalanine, tyrosine and valine for ID-LC-MS/MS analysis.

Amino Acid	Regression Coefficient (a)	Intercept (b)	Standard Error of the Estimate (y)	Correlation Coefficient (r^2)
Glutamic acid	1.88	0.032	-0.01 ± 0.47	0.9994
Isoleucine	0.95	0.111	-3.33 ± 3.94	0.9912
Leucine	0.96	0.019	-1.26 ± 1.37	0.9989
Phenylalanine	0.63	0.033	-3.43 ± 4.27	0.9907
Tyrosine	0.72	0.020	-0.69 ± 0.69	0.9997
Valine	0.12	0.001	0.48 ± 0.99	0.9969

4.3.6 – Intra-Run and Inter-Run Assay Variation of Analysed Samples

Intra-Run variation was determined through analysing four randomly selected serum samples from each participant group used in the biomarker study and analysed independently in triplicate. The CV's for control, MCI and AD participants are summarised in Table 4.3.10, 4.3.11 and 4.3.12, respectively with cell lysate CV's summarised in Table 4.3.13.

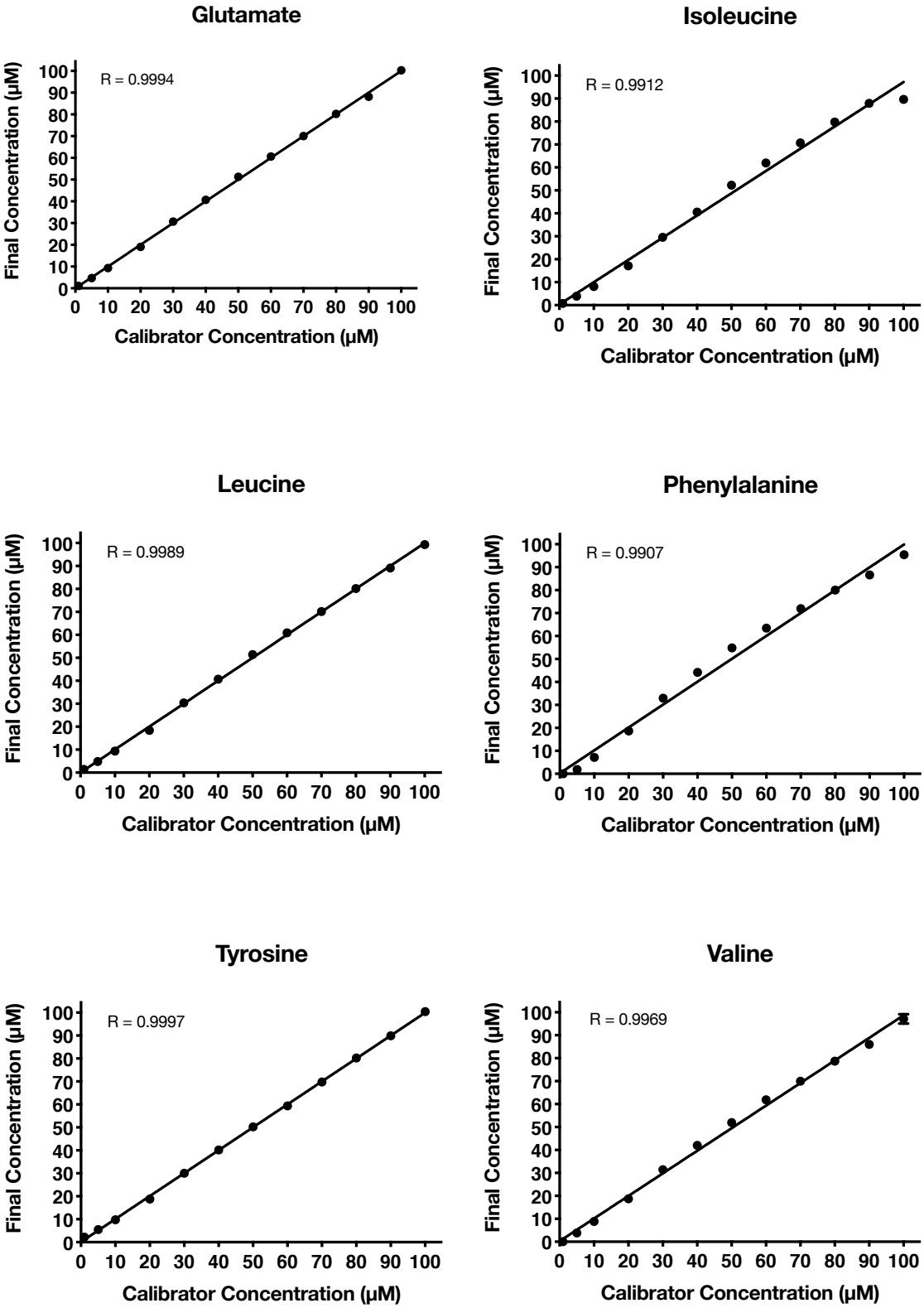

Figure 4.3.3: Representative calibration curves for glutamate, isoleucine, leucine, phenylalanine, tyrosine and valine.
Calibration functions for each amino acid were calculated using the linear regression between peak area ratio and amino acid concentration. All functions were calculated against a 50 µM deuterium labelled internal standard.

Table 4.3.10 Intra-run and inter-run method variation for control participant serum samples

Control Participants

Results	Serum Sample 1 – Amino Acids Glutamic Acid	Isoleucine	Leucine	Phenylalanine	Tyrosine	Valine
Mean (μM)	13.05	21.21	40.26	15.22	20.67	65.53
Intra-Run CV (%)	3.32	0.45	0.26	6.62	0.68	0.87
Inter-Run CV (%)	2.53	0.73	0.43	9.32	0.99	1.31
Results	**Serum Sample 2 – Amino Acids Glutamic Acid**	**Isoleucine**	**Leucine**	**Phenylalanine**	**Tyrosine**	**Valine**
Mean (μM)	14.29	13.56	24.74	9.74	11.63	45.19
Intra-Run CV (%)	2.45	6.69	0.27	3.15	0.44	0.37
Inter-Run CV (%)	2.04	6.94	0.26	2.59	0.36	0.39
Results	**Serum Sample 3 – Amino Acids Glutamic Acid**	**Isoleucine**	**Leucine**	**Phenylalanine**	**Tyrosine**	**Valine**
Mean (μM)	8.42	7.42	13.07	6.10	11.39	25.83
Intra-Run CV (%)	1.46	3.05	0.58	2.34	0.64	0.28
Inter-Run CV (%)	0.71	1.73	0.30	1.34	0.51	0.16
Results	**Serum Sample 4 – Amino Acids Glutamic Acid**	**Isoleucine**	**Leucine**	**Phenylalanine**	**Tyrosine**	**Valine**
Mean (μM)	8.20	10.10	19.03	8.86	10.03	30.70
Intra-Run CV (%)	2.40	1.97	1.12	5.29	0.40	0.74
Inter-Run CV (%)	1.15	1.52	0.85	4.40	0.28	0.53

Table 4.3.11 - Intra-run and inter-run variation for mild cognitive impairment participant serum samples

Mild Cognitive Impairment Participants

Results	Serum Sample 1 – Amino Acids					
	Glutamic Acid	**Isoleucine**	**Leucine**	**Phenylalanine**	**Tyrosine**	**Valine**
Mean (μM)	12.46	20.68	38.27	16.84	21.11	59.69
Intra-Run CV (%)	1.16	4.37	1.39	3.73	1.03	0.77
Inter-Run CV (%)	2.39	3.03	0.99	2.48	0.73	0.62
Results	**Serum Sample 2 – Amino Acids**					
	Glutamic Acid	**Isoleucine**	**Leucine**	**Phenylalanine**	**Tyrosine**	**Valine**
Mean (μM)	6.35	23.67	38.88	17.34	20.48	64.28
Intra-Run CV (%)	1.63	0.60	1.03	6.09	0.64	2.13
Inter-Run CV (%)	2.45	0.36	0.72	3.93	0.47	1.60
Results	**Serum Sample 3 – Amino Acids**					
	Glutamic Acid	**Isoleucine**	**Leucine**	**Phenylalanine**	**Tyrosine**	**Valine**
Mean (μM)	79.90	9.95	22.16	6.61	10.65	40.84
Intra-Run CV (%)	0.92	0.55	1.22	1.75	0.53	0.40
Inter-Run CV (%)	2.45	0.80	1.50	2.96	0.75	0.47
Results	**Serum Sample 4 – Amino Acids**					
	Glutamic Acid	**Isoleucine**	**Leucine**	**Phenylalanine**	**Tyrosine**	**Valine**
Mean (μM)	33.55	8.13	18.63	5.86	11.85	35.84
Intra-Run CV (%)	1.49	0.83	0.72	2.93	0.76	0.12
Inter-Run CV (%)	2.45	1.46	1.06	5.60	0.96	0.16

Table 4.3.12 Intra-run and inter-run variation for Alzheimer's disease participant serum samples.

Alzheimer's Disease Participants

Results	Serum Sample 1 – Amino Acids Glutamic Acid	Isoleucine	Leucine	Phenylalanine	Tyrosine	Valine
Mean (μM)	4.44	5.11	11.75	6.17	13.23	20.53
Intra-Run CV (%)	1.32	0.15	0.51	0.43	1.00	0.72
Inter-Run CV (%)	2.45	0.28	0.94	0.59	1.08	0.72
Results	**Serum Sample 2 – Amino Acids Glutamic Acid**	**Isoleucine**	**Leucine**	**Phenylalanine**	**Tyrosine**	**Valine**
Mean (μM)	30.12	5.43	13.41	8.41	16.03	26.98
Intra-Run CV (%)	2.59	2.13	2.12	5.84	2.31	2.24
Inter-Run CV (%)	2.45	3.82	3.41	5.93	2.05	2.24
Results	**Serum Sample 3 – Amino Acids Glutamic Acid**	**Isoleucine**	**Leucine**	**Phenylalanine**	**Tyrosine**	**Valine**
Mean (μM)	66.15	12.71	27.62	11.38	12.78	52.37
Intra-Run CV (%)	13.46	1.89	0.23	5.37	0.73	0.61
Inter-Run CV (%)	2.45	1.45	0.18	4.03	0.82	0.61
Results	**Serum Sample 4 – Amino Acids Glutamic Acid**	**Isoleucine**	**Leucine**	**Phenylalanine**	**Tyrosine**	**Valine**
Mean (μM)	76.43	5.44	15.26	5.90	9.53	31.83
Intra-Run CV (%)	2.15	0.91	0.39	1.55	0.44	1.69
Inter-Run CV (%)	2.45	1.63	0.55	2.24	0.66	1.69

Table 4.3.13 Intra-run and inter-run variation for control cell lysate samples
Cell Lysate

Results	Lysate Sample 1 – Amino Acids Glutamic Acid	Isoleucine	Leucine	Phenylalanine	Tyrosine	Valine
Mean (μM)	117.09	23.15	26.50	16.43	16.86	30.96
Intra-Run CV (%)	1.14	1.51	1.44	1.26	1.96	4.91
Inter-Run CV (%)	0.98	0.91	0.98	1.80	1.79	3.24
Results	**Lysate Sample 2 – Amino Acids Glutamic Acid**	**Isoleucine**	**Leucine**	**Phenylalanine**	**Tyrosine**	**Valine**
Mean (μM)	244.25	80.38	2.54	80.50	70.76	113.54
Intra-Run CV (%)	3.24	4.72	3.06	0.89	0.93	2.98
Inter-Run CV (%)	4.25	3.95	3.25	1.71	2.45	3.52
Results	**Lysate Sample 3 – Amino Acids Glutamic Acid**	**Isoleucine**	**Leucine**	**Phenylalanine**	**Tyrosine**	**Valine**
Mean (μM)	33.86	20.05	1.05	14.29	13.48	23.82
Intra-Run CV (%)	2.45	1.85	1.23	2.25	1.67	0.14
Inter-Run CV (%)	2.05	1.55	2.51	2.44	2.30	1.32
Results	**Lysate Sample 4 – Amino Acids Glutamic Acid**	**Isoleucine**	**Leucine**	**Phenylalanine**	**Tyrosine**	**Valine**
Mean (μM)	124.87	20.19	21.03	14.15	14.46	21.19
Intra-Run CV (%)	2.19	1.61	1.86	2.48	2.37	1.97
Inter-Run CV (%)	2.35	1.23	1.22	2.14	1.93	1.67

4.3.7 – Analytical Recoveries of Amino Acid Standards, Serum and Cell Lysates

Absolute recoveries were tested through spiking with a known concentration of each amino acid and analysed in triplicate. Table 4.3.14 summarises the average analysed concentration of amino acid standard, serum sample and cell lysate and percentage recovery. Analytical recoveries of all amino acids were close to 100% for both standards and serum.

4.3.8 – Serum Sample Stability

Serum amino acid stability when stored at -80°C was assessed over a three-month and six-month period from sample collection. Total coefficients of variation were 2.12%, 1.54%, 1.29%, 2.01%, 1.40% and 1.42% for glutamic acid, isoleucine, leucine, phenylalanine, tyrosine and valine respectively. Intra-run and total coefficient of variation are summarised in Table 4.3.15.

Table 4.3.14 Analytical recoveries of the LC-MS/MS method

Results	***Spiked Standard* – Amino Acids**					
	Glu	**Ile**	**Leu**	**Phe**	**Tyr**	**Val**
Initial Concentration (µM)	51.30	52.28	51.40	54.81	50.23	51.95
Final Concentration *(µM)*	102.61	104.56	102.80	109.62	100.47	103.89
Spiked Standard (µM)	51.30	52.28	51.40	54.81	50.23	51.95
Recovery %	104.31	95.30	99.05	94.02	102.77	100.11
Results	**Spiked Serum – Amino Acids**					
	Glu	**Ile**	**Leu**	**Phe**	**Tyr**	**Val**
Initial Concentration (µM)	12.02	16.91	31.77	11.90	15.04	48.93
Concentration (µM)	62.97	65.29	81.74	63.19	66.09	105.25
Spiked Standard (µM)	51.30	52.28	51.40	54.81	50.23	51.95
Recovery %	98.96	94.08	98.39	94.80	101.00	103.83
Results	**Spiked Cell Lysate – Amino Acids**					
	Glu	**Ile**	**Leu**	**Phe**	**Tyr**	**Val**
Initial Concentration (µM)	135.40	44.82	50.15	32.84	30.04	29.38
Concentration (µM)	196.9	96.12	105.68	84.41	83.48	84.41
Spiked Standard (µM)	51.30	52.28	51.40	54.81	50.23	51.95
Recovery %	105.33	98.77	104.17	96.37	103.77	103.16

Table 4.3.15 – Variation of samples stored at -80°C for a three-month and six-month period

Analysis Time	Amino Acids					
	Glu	Ile	Leu	Phe	Tyr	Val
Fresh Sample CV (%)	1.22	1.38	1.06	1.23	0.66	1.22
Three Months CV (%)	2.36	1.20	2.06	2.02	0.74	1.97
Six Months CV (%)	2.77	2.03	0.76	2.77	2.80	1.07
Total CV (%)	2.12	1.54	1.29	2.01	1.40	1.42

4.4 – Discussion

The focus of this chapter was to develop and validate an LC-MS method to analyse serum glutamic acid, the branched chain acids and the aromatic amino acids. This method will be subsequently utilise to determine the clinical utility of these amino acids as early diagnostic markers of AD. Studies have shown alterations in free amino acids in the CSF of MCI and AD patients (Kaiser *et al.*, 2010)

There are various analytical techniques for the analysis of serum amino acids with the primary classical analysis performed using IEC, which has associated long chromatography run times (Moore *et al.*, 1958, Sandlers, 2019). Later implementation of HPLC and gas chromatography with or without downstream mass spectrometry has allowed for increased throughput analysis of these analytes. However, these methods require pre-column derivatisation of samples before analysis. To allow for high sample throughput, reduced sample preparation time and high sensitivity and specificity I chose to develop a LC-MS/MS method. LC-MS/MS has the lowest requirement for sample preparation, removing the need to derivatise amino acids before analysis. In addition, the use of deuterium labelled isotopes as internal standards allowed for multiple analyte screening with high specificity. I have developed and validated this method for serum analysis and have shown that it can effectively analyse the same amino acids in CSF and cellular lysates allowing for more diverse research applications and the study of model systems.

Although LC-MS/MS amino acid analysis does not require derivatisation, direct amino acid analysis is challenging due to isobaric amino acids isoleucine, and

leucine sharing similar LC and MS properties (Yang *et al.*, 2013). When developing this method, the aim was to establish separate and distinct retention times for isoleucine and leucine and the associated deuterium labelled internal standards, allowing for the specific detection of these amino acids and in accordance with previously validated methods for dried blood spot analysis (Dietzen *et al.*, 2009). Retention times for isoleucine and leucine in my analysis were 9.13 ± 1.60 mins, 9.95 ± 2.39 mins, respectively, indicating that overlap of these analytes was possible. However, during analysis of both serum and cellular lysates distinct peaks were observed with no overlap in the calculation of peak area ratio. Furthermore, my analysis of these amino acids did not require any correction as described by Yang, thus minimising corrective errors (Yang *et al.*, 2013).

In addition to the consideration of the chromatographic separation of leucine and isoleucine when optimising for product ion transitions, through the consideration of additional non-identical transitions. However, the peak area ratios were too low to be effective for the detection of either amino acid in serum due to the inherent background. Although for unlabelled isoleucine and leucine this was the case the selection of additionally product ion transitions for the alternatively labelled amino acids allowed for specific quantification.

The extension of chromatography time to ensure this result meant that I was unable to replicate similar run times to those published by Yang, where complete elution of all amino acids, excluding glutamic acid was achieved in under six minutes (Yang *et al.*, 2013). Comparison of MRM chromatograms indicate that the use of a 3.5 µm RP18 column allows for a shorter elution time compared to a

5 µm C18 column (Figure 4.3.1 and 4.3.2). The use of a 5 µm column reduced column flow from the initial input of 0.3 mL/min to 0.18 mL/min. During method development replication of the sub-six-minute elution time was trialled using the same Waters Shield C18 column (3.5 mm, 2.16 150 mm), however, through multiple trials no distinct peak separation was observed (Figure 4.3.1). Due to this issue an alternative reverse-phase C18 column was used, with no adverse effects seen from the increase in retention times or alternate column use. Furthermore, due to the automated nature of ID-LC-MS/MS analysis, extended run time does not pose an issue as manual sample loading is not required between injections.

The optimisation of analysis parameters allowed for small sample volumes to be used with only 100 uL of serum or cellular lysate required for sample preparation and 10 µL for injection. From a clinical standpoint this is important as analysis can be achieved from either routine blood samples or without multiple collections. Through the validation process I have shown that the method is both precise and reproducible, with all amino acids except phenylalanine presenting below 5% intra-run and inter-run variation (Figure 4.3.10). However, all values were below the reported and accepted 10% coefficient of variation (Honour, 2011). This was also observed in the validation of cell lysate samples (Figure 4.3.11). Overall sample recoveries for serum were shown to be within 6% of total sample recovery. However, this method does present similar recoveries to (Yang *et al.*, 2013)

The use of this method as a diagnostic tool may require further consideration of optmisation to be effective in a clinical setting. Acetonitrile was chosen as it has a higher elution strength compared to alternative mobile phases like methanol (Lui, 2008). An increased percentage of acetonitrile reduced total run time by

reducing the elution time of phenylalanine and further increases could allow for shorter runs. This would be beneficial for clinical settings to allow for high throughput screening of samples. Additionally, the use of acetonitrile in both the mobile phase and the preparation of samples allowed for the deproteinisation before analysis in line with previously validated methods (Dietzen *et al.*, 2009). Acetonitrile also has a low analytical background compared, making it the most suitable option for serum analysis where there is a possibility of high background noise due to contaminants. However, for this analysis there are no predicted substances that could interfere with the analysis of branched chain and aromatic amino acids (Piraud *et al.*, 2003).

In conclusion, an effective ID-LC-MS/MS for the analysis of glutamic acid and the branched chain and aromatic amino acids has been developed and validated for human serum and cellular lysate. This method will be a great tool for the analysis of serum amino acids and determination of amino acid profiles in models of neurodegenerative disease.

Chapter 5

NOVEL BLOOD BIOMARKERS THAT CORRELATE WITH COGNITIVE PERFORMANCE AND HIPPOCAMPAL VOLUMETRY– POTENTIAL FOR EARLY DIAGNOSIS OF ALZHEIMER'S DISEASE DEMENTIA

Fred Hudd

REGULATION OF NEUROTRANSMITTER SYNTHESIS IN ALZHEIMER'S DISEASE – POTENTIAL FOR NOVEL DISEASE BIOMARKERS | 2019

Chapter 5 – Novel Blood Biomarkers that Correlate with Cognitive Performance and Hippocampal Volumetry – Potential for Early Diagnosis of Alzheimer's Disease Dementia

This chapter covers information, results and discussion published in Novel Blood Biomarkers that Correlate with Cognitive Performance and Hippocampal Volumetry: Potential for Early Diagnosis of Alzheimer's Disease (Hudd *et al.*, 2019). Reprinted with authorisation of ISO Press – See Reference List

5.1 – Introduction

Current criteria recognise that the biological changes observed in AD occur over several decades defined by the National Institute of Neurological and Communicative Disorders and Stroke - Alzheimer's disease and Related Disorders Association. Changes that occur as the disease progresses represents a challenge to develop new biomarkers to discriminate between disease stages and should include; (a) risk factors which present without symptomatic presentation, (b) prodromal AD dementia for those with symptomatic pre-dementia AD and (c) AD or atypical forms of AD (Dubois *et al.*, 2007).

Current clinical assessment for those presenting with memory impairment include a series of neuropsychological assessments together with relevant imaging analysis such as magnetic resonance imaging to rule out alternate causes such as tumours (Sutphen *et al.*, 2014, Viola *et al.*, 2015). Using these approaches gives an 80% positive predictive value and a 60% negative predictive value for a clinical diagnosis of AD dementia. Advancement in imaging such as MRI (Willette *et al.*, 2014), amyloid-PET (Thal *et al.*, 2014, Ito *et al.*, 2014) and SPECT (O'Brien *et al.*, 2014) allow for detection of brain atrophy, abnormalities in brain metabolism

and hypoperfusion, respectively. However, these analyses are expensive and not widely available. Furthermore, the clinical sensitivity and specificity of the combined neuropsychological assessments and imaging could be improved with the development of novel biomarkers.

Biomarker candidates to support the diagnosis of AD include CSF analysis of total tau, phosphorylated tau and amyloid-β_{42} (Khan and Alkon, 2015), plasma $A\beta_{1-42}$ and the ratio of $A\beta_{1-42}/A\beta_{1-40}$ (Jack *et al.*, 2010), plasma phospholipids (Shen *et al.*, 2018), plasma proteins (Hye *et al.*, 2014, Thambisetty *et al.*, 2010, IJsselstijn *et al.*, 2011, Schrijvers *et al.*, 2011), microRNA expression profiling (Tan *et al.*, 2014), multi-analyte platforms targeting neuroinflammatory changes (Kim *et al.*, 2014, Restrepo *et al.*, 2013) and protein panels (Hye *et al.*, 2006). In addition to these approaches, there is renewed interest in generating metabolic profiles that could be used collectively to better differentiate between MCI, AD and early disease stages.

In particular, amino acids such as the BCAAs and AAAs are plausible for neurodegenerative diseases, with studies reporting changes in the amino acid profiles of patients with AD and PD (Li *et al.*, 2010, Corso *et al.*, 2017, Fonteh *et al.*, 2007, Figura *et al.*, 2018). Figura (2018) reported significant decreases in the concentration of alanine, arginine, threonine and phenylalanine in Parkinson's disease. In addition to the BCAAs and AAAs, BCAT and its metabolite glutamate were hypothesised to have the potential to predict AD progression as new and novel biomarkers for AD. The choice of these analytes is based on the role of the BCAT proteins in regulating brain glutamate, through its function as a catalyst in

the reversible transamination of the BCAAs; leucine, isoleucine and valine to their respective branched chain α-keto acids and glutamate.

This data shows for the first time that perturbations in BCAT and glutamate metabolism observed in AD brain is reflected in serum. The data presented shows the amino acid, glutamic acid, was found to be significantly increased in the serum of AD participants. Glutamic acid and BCAT also show correlation with several neuropsychological tests and structural MRI analysis indicating that the BCAT protein and glutamic acid show promise as early diagnostic biomarkers. The intrinsic link between BCAT and the metabolic pathways that are perturbed in AD give an advantage over other blood markers in that it is associated with AD disease progression. Moreover, the predictive power of BCAT as a blood biomarker of AD was assessed to determine whether it could be increased by combining with neuropsychology and neuroimaging scores, offering a combined assessment of AD pathology.

5.2 - Specific Aims

Specific Aim 1 - To evaluate the serum profiles for glutamate, isoleucine, leucine, phenylalanine, tyrosine and valine for MCI and AD relative to control subjects.

Specific Aim 2 – Investigate if the serum hBCAT profile for MCI and AD are altered relative to control subject.

Specific Aim 3 - Compile a combined data set of neuropsychological tests results, genotype and magnetic resonance imaging data from control, MCI and AD participants.

Specific Aim 4 – To determine the clinical utility of these biomarkers and determine their potential role as biomarkers of disease pathology together neuropsychological assessments and magnetic resonance imaging.

5.3 – Results

5.3.1 – Clinical Data and ApoE Genotyping

Clinical data for each participant was determined at baseline and summarised in Table 5.3.1 with ApoE genotype for each group summarised in Figure 5.3.1. Significant differences between groups (Control/MCI/AD) were observed with respect to the age participants left school, years of education and report of head injury. The majority of patients (49%) presented with the ApoE 3/3 genotype, considered the 'neutral' genotype, 9% of patients were ApoE 4/4, which is linked to AD. The remainder of the patients were heterozygotes, with no participants expressing the ApoE 2/2 genotype, which shows a protective effect against AD but is also associated with familial type III hyperlipoproteinaemia (Wang et al, 2015).

Of participants with probable AD only one was shown to have the ApoE 4/4 genotype, with the remaining four showing a heterozygote pattern. However, there were a number of participants designated as controls that did carry the ApoE 4/4 genotype. Moreover, in some control participants, in particular those with the ApoE4 genotype, associated with a 40% greater risk of developing AD, levels of the BCAT proteins were increased indicating that these patients show common emerging profiles to participants with MCI or AD. The hypothesis in this instance is that these biomarkers may have scope as predictors for preclinical AD.

Table 5.3.1 – Clinical presentation and ApoE genotype of participants

Clinical and ApoE Data Set	Control n (%)	MCI n (%)	AD n (%)	*p*-value
Gender (female)	28 (56)	10 (46)	11 (69)	0.3603
Age, median IQR	70 (7.5)	74.5 (12.25)	75.5 (15)	0.0279
ApoE, E4 allele	4 (9)	2 (13)	1 (7)	0.9143
Years of education, median IQR	15 (5)	13 (3)	12.5 (5.5)	0.0070
Age left school, median IQR	17 (2)	16 (2)	16.5 (3)	0.0308
IQs score median (IQR)	116.4 (16)	110.7 (13.1)	122.4 (17.5)	0.1093
History of smoking	24 (48)	11 (50)	9 (56.3)	0.9500
Alcohol units per week, median (IQR)	3.5 (9.25)	2 (11.5)	3 (8.25)	0.7389
Family history of dementia (Yes)	26 (52)	6 (28)	9 (57)	0.1414
Loss of conscious (Yes)	5 (10)	2 (9)	2 (13)	0.9400
Head injury (Yes)	7 (14)	9 (41)	3 (19)	0.0364
Epilepsy (Yes)	1 (2)	0 (0)	1 (6.25)	0.3930

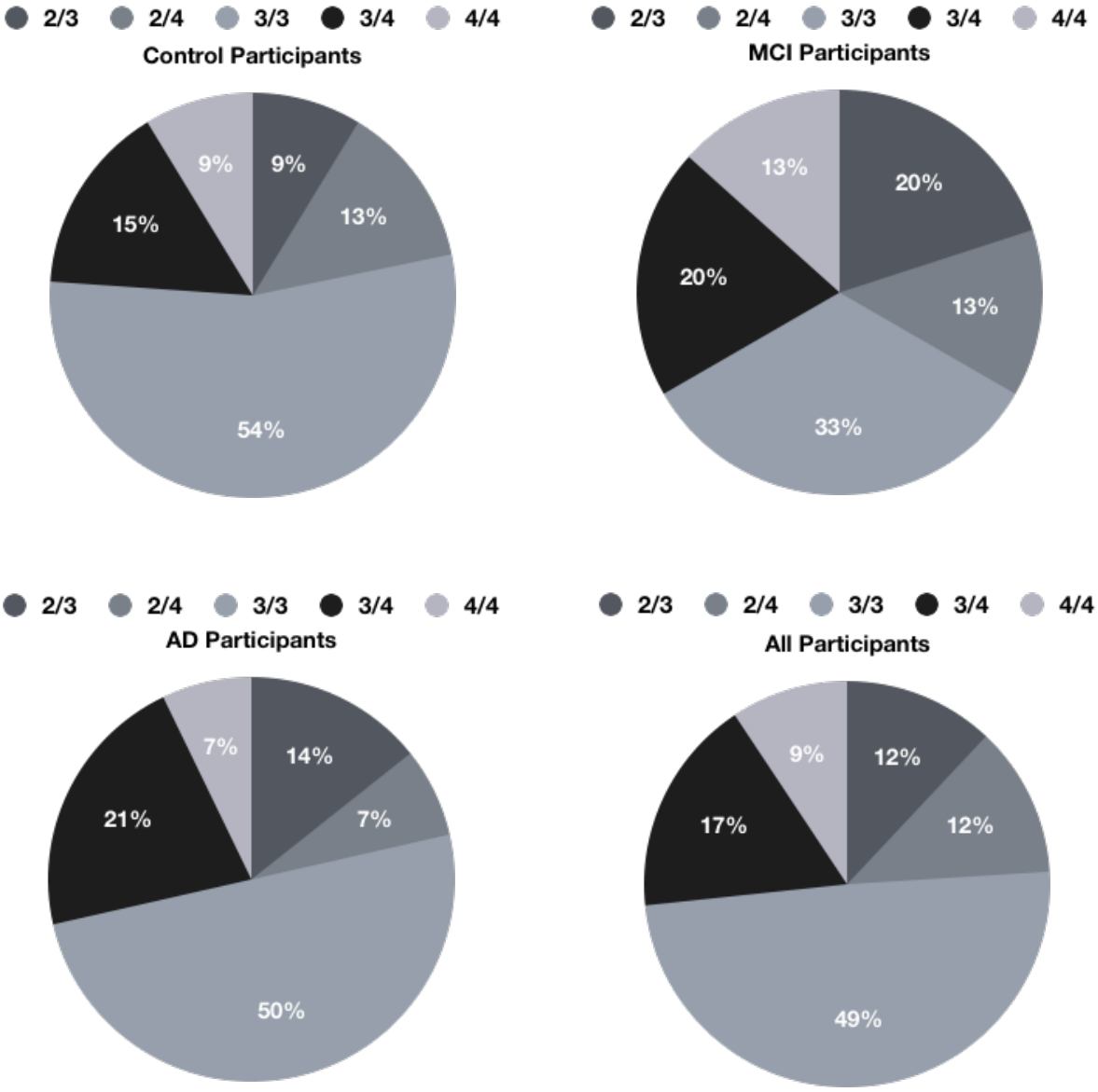

Figure 5.3.1: Distribution of ApoE genotypes between control, MCI, AD and all participants.
Percentage of ApoE genotypes 2/3, 2/4, 3/3 and 4/4 across control, MCI and AD participants. MCI participants presented the highest number of 4/4 genotypes, with the lowest percentage found in the AD participants.

5.3.2 – Increased BCAT Expression in Alzheimer's Disease Reflects Brain Patterns

Analysis of serum samples revealed increased BCAT proteins in patients with AD compared to healthy controls (p = 0.0005 and p = 0.0032, BCATc (Figure 5.3.2 A) and BCATm (Figure 5.3.2 B) respectively) with clear distinction between groups (Table 5.3.2). Data shows that in some MCI cases their blood profiles reflected changes similar to the profiles of AD participants (Figure 1A, Lane 1 (AD) and Lane 3 (MCI) respectively). Other MCI cases did not reflect this and shared typical biochemical characteristics like those of control participants (Figure 1A, Lane 4, 5 (MCI) relative to control lanes). Table 5.3.2 summarises means scores of BCAT by participant group and details the results from a one-way analysis of variance and a post-hoc application of Tukey's honestly significant differences test for each measure. Mean levels for BCATc and BCATm significantly differ between at least two patient groups ($p < 0.05$). In the sample, there is a significant difference in the level of the BCAT proteins between control and MCI (p = 0.0235 and p = 0.0084, for BCATc and BCATm, respectively) and control and ADD (p =0.0013 and p = 0.0474, BCATc and BCATm, respectively).

5.3.3 – Increased Levels of Glutamate in AD Serum Differentiate Between Groups

Serum amino acids, in particular the BCAAs, glutamate and AAAs showed an altered amino acid profile from AD participants relative to controls. In particular, there was an increase in the concentration of glutamate from control to MCI to ADD (Table 5.3.3). Table 5.3.3 summarises mean levels and within group variation for the amino acid levels. In the sample, mean levels of isoleucine, leucine, valine and tyrosine significantly differ between conditions. In this sample,

significant differences in mean levels of isoleucine, leucine, tyrosine and valine between conditions were observed. A pairwise comparison between control and MCI participants showed significant differences in isoleucine (p = 0.0077), leucine (p = 0.0141) and valine (p = 0.0063), indicating that the profile of these amino acids may be early predictors of preclinical AD (Figure 5.3.2).

5.3.4 – Differentiation Between Participant Groups

The hippocampus of AD participants displays marked atrophy compared to control (Figure 5.3.4). MRI data indicates an evident reduction of total hippocampal volume in both MCI and mild AD, with primary reduction observed in the CA1, dentate gyrus and subiculum, however tissue loss is uneven in these sub-regions. To gain understanding of the functional consequences of the described morphometric changes in the hippocampus and sub-regions versatile cognitive neuropsychology tests were administered to the same participant group (Table 5.3.4). The Montreal Cognitive Assessment test, Paired Associative Learning (PAL) and Hopkin's Verbal Learning Test Revised (HVLT) verbal learning test all discriminate between AD, MCI and healthy older groups. Table 5.3.4 summarises mean scores on cognitive assessments by patient group and the results from a one-way analysis of variance and a post hoc application of Tukey's honestly significant differences test for each measure. In each instance, sample means levels demonstrate significantly poorer cognitive ability in MCI compared to control, and significantly poorer cognitive ability in AD compared to MCI. The F-statistic indicates MoCA scores have the greatest within sample discriminatory effects. Mean levels for CA1 Volume, Dentate Gyrus, Subiculum, Hippocampal, and Entorhinal monotonically decrease with progression from

Control, to MCI, to AD, and these trends are statistically significant effects (Table 5.3.5).

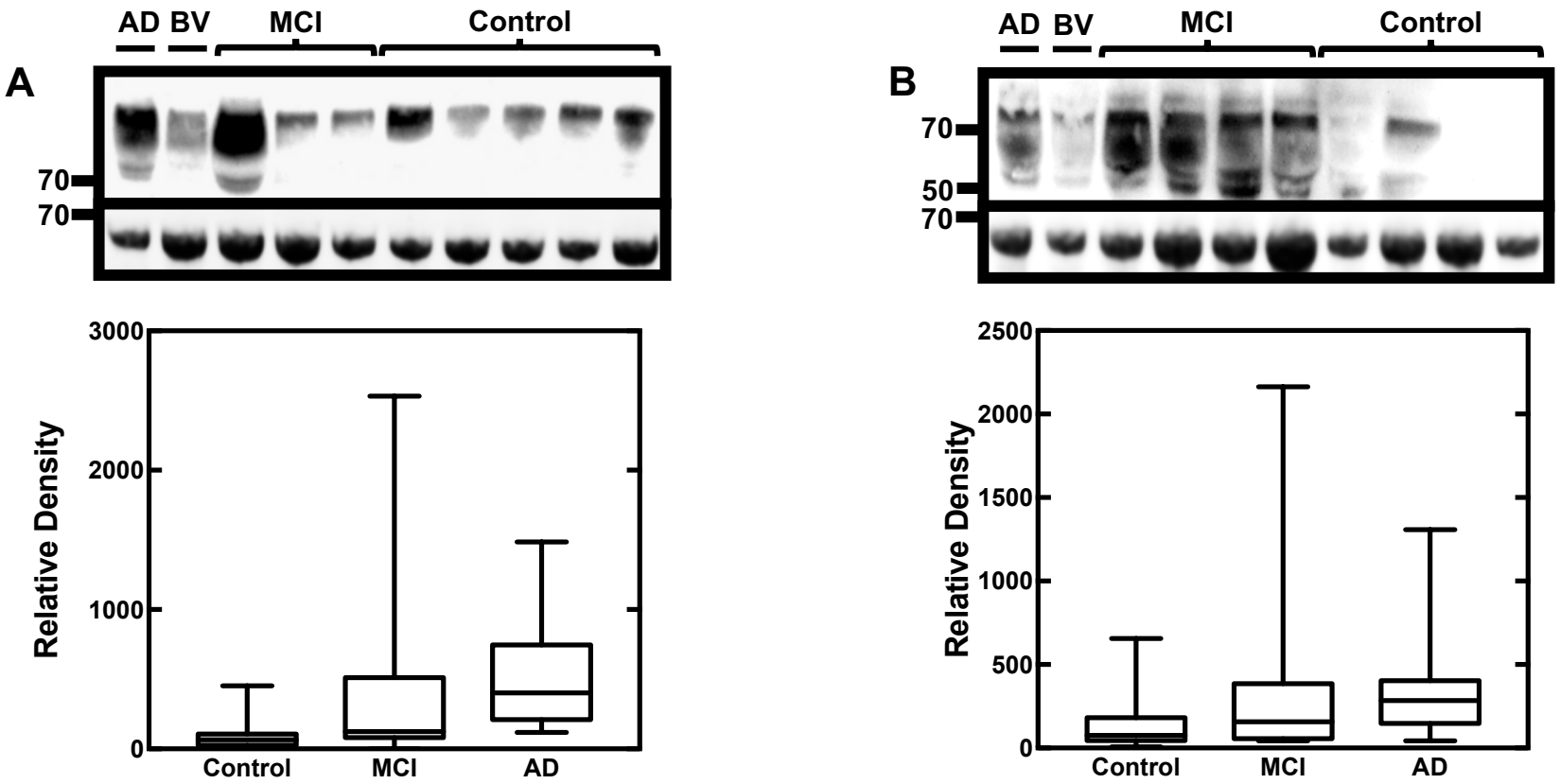

Figure 5.3.2 Western blot analysis of BCAT in serum from control, MCI and AD participants.
The protein concentration of serum samples was calculated using the Schaffner and Weissmann method (Schaffner W, 1973) and separated on a NuPAGE® Novex® 4-12% Bis-Tris followed by Western blot analysis using antibodies specific for BCATc and BCATm (1/1000 dilution). Positive bands were visualised using chemiluminescent HRP substrate and an Odyssey® Fc Imaging System (LI-COR Biosciences). Integrated area densitometry was carried out using Image Studio Ver 5.2 and the results were measured in relation the total protein. Panel A: Sample western blot analysis with box plot of BCATc from control, MCI and AD participants. Panel B: Sample western blot analysis with box plot of BCATm from control, MCI and AD. (N=75).

Table 5.3.2 – BCATc and BCATm (mean ± standard deviation) summarised by participant group

BCAT	Control (n = 45)	MCI (n = 16)	AD (n = 12)	ANOVA F (2, 7)	*p*-value	Pairwise Comparison		
						Control vs MCI	Control vs AD	MCI vs AD
BCATc	98.21 ± 113.8	366.2 ± 622	505.4 ± 402.3	8.524	0.0005	0.0235	0.0013	0.5368
BCATm	123.5 ± 123.4	441.1 ± 654.8	402.4 ± 396.4	6.239	0.0032	0.0084	0.0474	0.9562

Table 5.3.3 – Amino acid levels (µmol/L) in the serum of control, MCI and AD participants

Amino Acid	Control (n = 42)	MCI (n = 17)	AD (n = 11)	ANOVA F (2, 67)	*p*-value	Pairwise Comparison		
						Control vs MCI	Control vs AD	MCI vs AD
Glutamate	0.8436 ± 0.5192	1.791 ± 1.308	2.370 ± 2.054	10.570	0.0001	0.0103	0.0003	0.3649
Isoleucine	0.6056 ± 0.2861	0.993 ± 0.573	0.734 ± 0.634	4.837	0.0109	0.0077	0.6554	0.2792
Leucine	1.1650 ± 0.5998	1.874 ± 0.978	1.631 ± 1.369	4.620	0.0132	0.0141	0.2476	0.7420
Phenylalanine	0.5356 ± 0.2926	0.773 ± 0.416	0.599 ± 0.435	2.814	0.0670	0.0530	0.8535	0.4044
Tyrosine	0.6735 ± 0.3320	1.031 ± 0.468	1.112 ± 1.065	4.477	0.0150	0.0607	0.0490	0.9209
Valine	2.0280 ± 1.0340	3.323 ± 1.824	2.763 ± 1.940	5.347	0.0070	0.0063	0.2833	0.5669

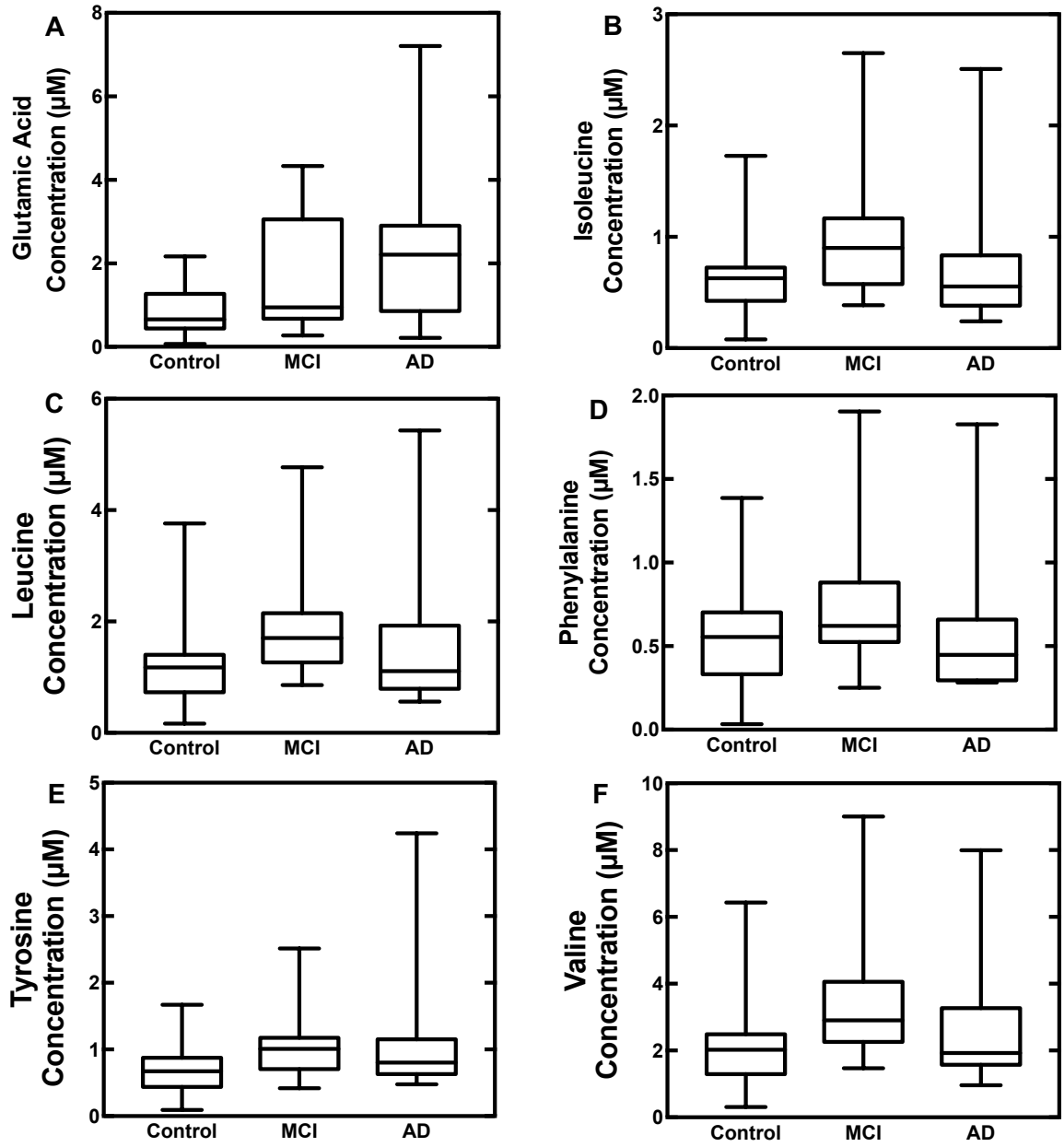

Figure 5.3.3 - Amino acid profiles of control, MCI and AD participants.
Panel A: Box plot showing serum glutamate concentration for control (n = 42; median 0.6667, range 0.07649 – 2.171), MCI (n = 17; median 0.9547, range 0.2818 – 4.341) and AD participants (n = 11; median 2.212, range 0.2203 – 7.211). **Panel B:** Box plot showing serum isoleucine concentration for control (n = 42; median 0.6291, range 0.08 – 1.728), MCI (n = 17; median 0.9008, range 0.387 – 2.651) and AD participants (n = 11; median 0.5541, range 0.242 – 2.508). **Panel C:** Box plot showing serum leucine concentration for control (n = 42; median 1.174, range 0.1649 – 3.762), MCI (n = 17; median 1.703, range 0.8577 – 4.769) and AD participants (n = 11; median, range 0.5615 – 5.429). **Panel D:** Box plot showing serum phenylalanine concentration for control (n = 42; median 0.5552, range 0.03266 – 1.386), MCI (n = 17; median 0.6218, range 0.2508 – 1.905) and AD participants (n = 11; median 0.4479, range 0.2827 – 1.828). **Panel E:** Box plot showing serum tyrosine concentration for control (n = 42; median 0.6735, range 0.09193 – 1.67), MCI (n = 17; median 1.009, range 0.4194– 2.515) and AD participants (n = 11; median 0.8049, range 0.4791 – 4.242). **Panel F:** Box plot showing serum valine concentration for control (n = 42; median 2.019, range 0.3036 – 6.422), MCI (n = 17; median 2.901, range 1.473 – 9.005) and AD participants (n = 11; median 1.928, range 0.9637 – 7.994).

In all cases for CA1 Total, CA2 Total, Dentate Gyrus, Subiculum and Hippocampal the mean levels in Control are significantly higher than MCI, and AD ($p < 0.05$), but with no significant difference between MCI and AD ($p > 0.05$). The dentate gyrus subfield showed the strongest effect within the sample.

BCATm and BCATc are both significantly correlated ($r = 0.753$, $p < 0.0001$) and are also significantly correlated with MoCA score ($r = -0.240$, $p = 0.038$ BCATm and $r = -0.329$, $p = 0.004$ BCATc). Glutamic acid levels did not significantly correlate with BCATm ($r = -0.140$, $p = 0.267$) or BCATc ($r = 0.150$, $p = 0,235$). However, glutamic acid was significantly correlated with MoCA score ($r = -0.329$, $p = 0.006$). Conversely, leucine, isoleucine, phenylalanine, tyrosine and valine are not correlated with MoCA score ($p > 0.2$ in all cases). These amino acids do form a mutually correlated system ($r > 0.85$, $p < 0.0001$) and leucine, isoleucine and valine are each significantly correlated with both BCATm and BCATc. CA1, CA2, dentate gyrus, hippocampal and entorhinal volumes are all significantly correlated with MoCA score ($r > 0.400$, $p < 0.01$) as shown in Table 5.3.6.

Multivariate discriminant analysis shows that MoCa scores alone have good and significant discriminant powers between control, MCI and AD groups (classification accuracy 81.8%; leave one-out cross validated 81.8%). This baseline discriminant model is significantly improved with the inclusion of any one of BCATc, BCATm, glutamic acid, isoleucine, leucine, phenylalanine, tyrosine or valine (shown in Table 5.3.7). Likewise,ordinal logistic regression shows that MoCA scores by themselves have good predictive powers for Control/MCI/ADD (Figure 5.3.5). However, this baseline discriminant model is not improved with the inclusion of any of the brain volume measures. MoCA scores alone are also

shown to have good predictive powers for control/MCI/AD from 15 ordinal linear regression. This baseline ordinal logistic regression model is significantly improved by the inclusion of any of, BCATm (p = 0.007), glutamic acid (p = 0.035), Leucine (p = 0.019), Valine (p = 0.008), Phenylalanine (p = 0.030), or Tyrosine (p = 0.005). Yet, this baseline inclusion of BCATc (p = 0.317), nor by the inclusion of the brain volume measures.

Multivariate discriminant analysis shows that Dentate Gyrus sub-volume was shown to have some significant discriminant powers between Control/MCI/AD (classification accuracy 61.6%; leave one-out-cross validated 61.6%). This baseline discriminant model is significantly improved with the inclusion of any one of BCATm, glutamic acid, leucine. Likewise, ordinal logistic regression shows that Dentate Gyrus volume is significantly related to outcome. Further, this baseline ordinal logistic regression model is significantly improved by the inclusion of any of, BCATm (p = 0.011), glutamic acid (p = 0.003), leucine (p = 0.045), valine (p = 0.048) but with levels of predictive accuracy notably lower when compared with the models using MoCA.

For blood markers only, BCATm and glutamic acid in combination and individually show good discriminatory powers (Table 5.3.7). For MoCA alone, sensitivity and specificity were 0.819 and 0.937 with respect to ADD. This estimate was significantly improved when combined with BCATm or the amino acids (Table 5.3.7). Of note is the measure of BCATm with MoCA which improved sensitivity to 0.903 but specificity to 1.00 indicating that this protein together with the MoCA measurement correctly categorised all participants that did not show evidence of

AD pathology into the correct group. In contrast, the MoCA models were not greatly improved by the inclusion of the Dentate Gyrus subfield volume.

Table 5.3.4 – Cognitive data (mean ± standard deviation) summarised by participant group

Cognitive Data Set	Control (n = 50)	MCI (n = 22)	AD (n = 16)	ANOVA F (2, 85)	*p*-value	Pairwise Comparison		
						Control vs MCI	Control vs AD	MCI vs AD
MoCA	27.26 ± 1.780	22.27 ± 2.84	16.44 ± 5.04	90.77	< 0.0001	< 0.0001	< 0.0001	< 0.0001
	Control (n = 47)	**MCI (n = 19)**	**AD (n = 12)**	**ANOVA F (2, 75)**	***p*-value**	**Pairwise Comparison**		
						Control vs MCI	**Control vs AD**	**MCI vs AD**
PAL Mean Reaction Time	2148 ± 454.1	3264 ± 1267	5774 ± 3341	29.73	< 0.0001	0.0176	< 0.0001	< 0.0001
PAL Total Acc	0.695 ± 0.115	0.542 ± 0.108	0.349 ± 0.102	49.80	< 0.0001	< 0.0001	< 0.0001	< 0.0001
	Control (n = 50)	**MCI (n = 22)**	**AD (n = 14)**	**ANOVA F (2, 83)**	***p*-value**	**Pairwise Comparison**		
						Control vs MCI	**Control vs AD**	**MCI vs AD**
HVLT 20 Minute Delay	9.26 ± 2.489	4.364 ± 3.170	1.000 ± 1.414	69.27	<0.0001	< 0.0001	< 0.0001	0.0007
	Control (n = 41)	**MCI (n = 17)**	**AD (n = 6)**	**ANOVA F (2, 61)**	***p*-value**	**Pairwise Comparison**		
						Control vs MCI	**Control vs AD**	**MCI vs AD**
HVLT 24 Hour Delay	8.976 ± 2.779	3.529 ± 3.204	0 ± 0	42.06	< 0.0001	< 0.0001	< 0.0001	0.0260

Table 5.3.5 – Subfield volumes for AD, MCI and control participants

Subfield	Control (n = 44)	MCI (n = 18)	AD (n = 11)	ANOVA F (2, 70)	*p*-value	Pairwise Comparison		
						Control vs MCI	Control vs AD	MCI vs AD
CA1	1.713 ± 0.2401	1.410 ± 0.3711	1.370 ± 0.4200	9.486	0.0002	0.0021	0.0040	0.9367
CA2	0.020 ± 0.0051	0.016 ± 0.0050	0.015 ± 0.0050	5.578	0.0057	0.0228	0.0343	0.9621
CA3	0.076 ± 0.0160	0.081 ± 0.0150	0.082 ± 0.0310	0.670	0.5146	0.6734	0.5992	0.9709
Dentate Gyrus	1.087 ± 0.1186	0.955 ± 0.1830	0.886 ± 0.1890	10.62	< 0.0001	0.0063	0.0004	0.4493
Subiculum	0.483 ± 0.0631	0.425 ± 0.1060	0.389 ± 0.0718	8.353	0.0006	0.0242	0.0015	0.4344
Hippocampal	3.623 ± 0.3848	3.141 ± 0.6780	3.019 ± 0.7129	9.015	0.0003	0.0046	0.0031	0.8158
Entorhinal	0.579 ± 0.0878	0.529 ± 0.1210	0.433 ± 0.1288	9.084	0.0003	0.1941	0.0002	0.0477

Table 5.3.6 – Correlation analysis with MoCA

Clinical and ApoE Data Set	*r-value*	*p*-value	Measure	*r-value*	*p*-value
CA1	0.458	< 0.0001	Glutamic Acid	-0.317	0.007
CA2	0.408	0.0001	Isoleucine	-0.056	0.643
CA3	-0.340	0.0788	Leucine	0.078	0.524
Dentate Gyrus	0.456	< 0.0001	Phenylalanine	0.083	0.492
Subiculum	0.463	< 0.0001	Tyrosine	-0.109	0.368
Hippocampal	0.450	< 0.0001	Valine	-0.017	0.887
Entorhinal	0.496	< 0.0001			

Table 5.3.7 - Percentage accuracy under leave one-out-out (L-O-O) cross-validation of baseline linear discriminant model (A) (MoCA (B) or Dentate Gyrus (C)) and extended model, along with p-value for inclusion of additional parameter in the baseline ordinal regression model. Optimal sensitivity and specificity for MCI and AD combined, and AD only using the ordinal logistic regression model.

A	Discriminant Analysis		Logistic Regression	MCI or AD	*AD*
	Accuracy	L-O-O Accuracy	*p*-value	Sensitivity and Specificity	Sensitivity and Specificity
BCATm	62.7	62.7	N/A	0.744; 0.704	0.836; 0.727
BCATm + BCATc	64.0	64.0	0.774	0.756; 0.767	0.710; 0.923
BCATm + Glu	63.6	60.6	0.003	0.704; 0.872	0.800; 0.818
BCATm + Ile	68.2	63.6	0.525	0.744; 0.741	0.818; 0.727
BCATm + Leu	62.1	62.1	0.186	0.744; 0.704	0.782; 0.727
BCATm + Phe	62.1	60.6	0.646	0.718; 0.741	0.800; 0.727
BCATm + Tyr	62.1	59.1	0.064	0.744; 0.704	0.836; 0.727
BCATm + Val	63.6	62.1	0.285	0.744; 0.741	0.800; 0.727

B	Discriminant Analysis		Logistic Regression	MCI or AD	*AD*
	Accuracy	**L-O-O Accuracy**	***p*-value**	**Sensitivity and Specificity**	**Sensitivity and Specificity**
MoCA	81.8	81.8	N/A	0.900; 0.895	0.819; 0.937
MoCA + Dentate Gyrus	81.8	81.8	0.293	0.909; 0.931	0.903; 0.909
MoCA + BCATc	83.0	83.0	0.317	0.978; 0.933	0.850; 0.923
MoCA + BCATm	86.7	84.0	0.007	0.978; 0.967	0.903; 1.000
MoCA + Glu	88.4	85.5	0.035	0.929; 0.967	0.879; 0.909
MoCA + Ile	87.0	85.5	0.044	0.976; 0.967	0.828; 0.909
MoCA + Leu	89.9	84.1	0.019	0.976; 0.967	0.828; 0.909
MoCA + Phe	88.4	85.5	0.030	0.929; 0.967	0.845; 0.909
MoCA + Tyr	87.0	85.5	0.005	0.952; 0.967	0.845; 1.000
MoCA + Val	87.0	84.1	0.008	0.976; 0.967	0.828; 0.909

C	Discriminant Analysis		Logistic Regression	MCI or AD	AD
	Accuracy	L-O-O Accuracy	*p*-value	Sensitivity and Specificity	Sensitivity and Specificity
Dentate Gyrus	61.6	61.6	N/A	0.682; 0.655	0.806; 0.727
Dentate Gyrus + MoCA	81.8	81.8	< 0.001	0.955; 0.897	0.903; 0.901
Dentate Gyrus + BCATc	63.0	63.0	0.127	0.769; 0.792	0.811; 0.800
Dentate Gyrus + BCATm	65.1	62.9	0.011	0.897; 0.708	0.887; 0.800
Dentate Gyrus + Glu	73.8	68.9	0.003	0.769; 0.818	0.923; 0.778
Dentate Gyrus + Ile	63.0	63.0	0.095	0.897; 0.727	0.769; 0.778
Dentate Gyrus + Leu	63.0	63.0	0.045	0.846; 0.818	0.731; 0.778
Dentate Gyrus + Phe	63.0	63.0	0.187	0.718; 0.818	0.788; 0.778
Dentate Gyrus + Tyr	63.0	63.0	0.087	0.897; 0.773	0.827; 0.778
Dentate Gyrus + Val	67.2	67.2	0.048	0.897; 0.673	0.846; 0.677

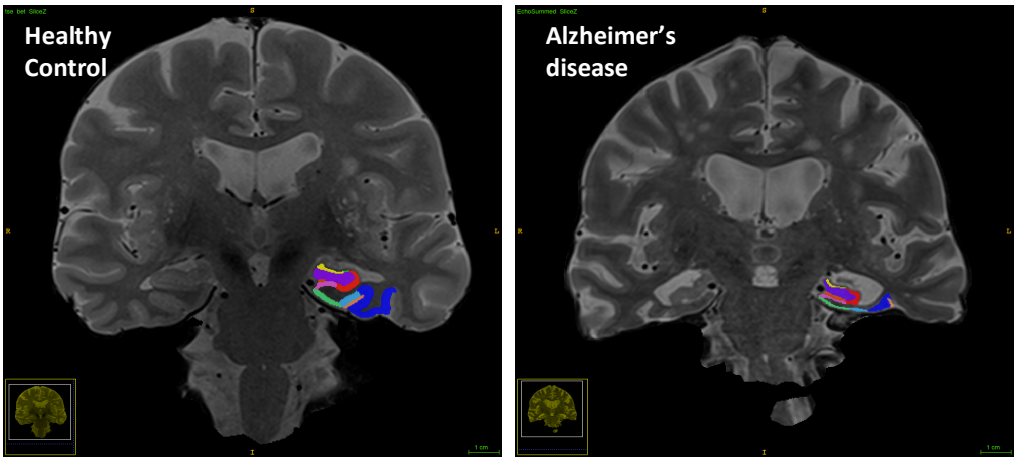

Figure 5.3.4 - T2-weighted coronal MRI images of healthy elderly control (left) and ADD patient (right).
The Hippocampus of ADD patient displays marked atrophy compared to control. Left Hippocampus and surrounding cortices is masked for each subject using ASHS protocol: Red=CA1; Purple=DG; Yellow=CA3; Lime Green=CA2; Pink=Subiculum; Pale Green=Entorhinal Cortex; Light Blue=BA35; Dark Blue=BA36; Orange=Misc; Beige=Collateral Sulcus.

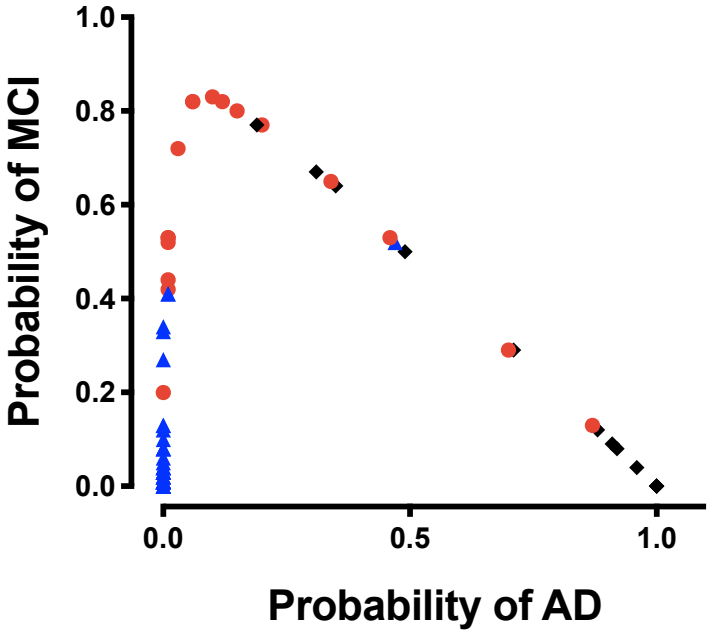

Figure 5.3.5 - Ordinal logistic model of MoCa and BCATm

5.5 – Discussion

There is a wide range of application cations for biomarkers in clinical research, drug discovery and clinical diagnosis. Validation of new and novel fluid biomarkers for dementia open possibilities for alternative or supportive diagnostic makers that through combination with other assessment modalities could hugely increase prediction values. This data suggest that the predictive power of BCAT or glutamic acid (glutamate) is increased by either structural information from MRI of vulnerable brain structures (Willette *et al.*, 2014) and/or neuropsychological tests (Dubois *et al.*, 2007). Through this three-discipline study we have begun to address the issue of early AD diagnosis, with data that shows the potential of BCAT and glutamic acid (glutamate) to predict AD.

Current guidelines address the disease on a spectrum with three specific stages; an early, preclinical stage presenting no symptoms, a middle stage of MCI and a final stage marked by symptoms of dementia (Dubois *et al.*, 2007). Formal acknowledgement in diagnostic criteria for the use of biomarkers as possible indicators of underlying AD pathology has been made (Dubois *et al.*, 2007), however, it is recommended that the use of biomarkers in this field are research focused rather than applied in a clinical setting. Previous studies by our group have shown that the levels of the BCAT proteins are increased in the hippocampus; frontal and temporal cortex in AD relative to matched control brains, with BCATm upregulation correlating with Braak stage, suggesting that the level of this enzyme is related to disease progression (Hull *et al.*, 2015, Hull *et al.*, 2012). The data has shown increased levels of serum BCAT proteins in participants with AD compared to healthy controls with clear distinction between groups (Figure 5.4.2 and Table 5.4.2). No significant difference between mean

BCAT levels in MCI compared to the more severe AD participants were observed. This argues that BCAT may reflect early pathological changes in the brain supporting the findings in brain tissue. Furthermore, the correlation of serum BCAT with MoCA score, various neuropsychological tests and several indicators of hippocampal volume reduction, suggest that BCAT is a valid measure of AD pathogenesis (Figure 5.3.5 and Table 5.3.6).

Additional studies using cell and animal models suggest that increased levels of BCATs may be initially be neuroprotective (Hull *et al.*, 2015), however, sustained increased BCAT expression could increase the production of glutamate and exacerbate neuronal excitotoxicity, potentially contributing to cell death. From the analysis of serum glutamate, the data shows a significant increase in the levels of serum glutamic acid that monotonically increased across the three groups (Figure 5.3.2 A). Interestingly, proton magnetic resonance (1H MRS) assessment of metabolites such as glutamate showed a decrease in hippocampal brain glutamate between control, MCI and AD participants (Rupsingh *et al.*, 2011). In AD, hippocampal, frontal, temporal and parietal cortex glutamatergic neurons are reported to be severely affected relative to similar neurons in the motor and sensory cortex and considered a possible early event in the pathogenesis of the disease (Francis, 2003, Revett *et al.*, 2013). A recent study has indicated that measures of the glutamatergic system correlated with MCI more so than Aβ or Tau and that there is an increase in glutamatergic synapses in individuals with MCI, supporting the theory that an increased activity of BCAT may be initially neuroprotective (Bell *et al.*, 2007). Several aspects of the glutamate/glutamine cycle are perturbed in AD brain including (a) reduced levels of VGLUT1 and 2 in the prefrontal cortex of individuals with AD (Kashani *et al.*, 2008) (b) Aβ peptides

accumulate more in VGLUT1/2-containing terminals than in non-VGLUT terminals indicating a preferential targeting of these type of neurons (Sokolow *et al.*, 2012) (c) synaptic glutamate transporter defect, an early sign in disease pathology (Cummings *et al.*, 2015), (d) low levels of glutamate synthetase in astrocytes (Yeh *et al.*, 2013, Olabarria *et al.*, 2011). This extensive evidence together with this data supports a role for BCAT and glutamate as early indicators of disease pathology.

Links have been shown between the levels of dietary amino BCAAs and reduced cognitive function, however, the mechanism by which conditions manifest is not entirely understood thus requiring further investigation. In the field of BCAA analysis there are several studies which present mixed data sets with wide variability, which is possibly linked to either study design, method or the instrumentation used (Griffin and Bradshaw, 2017). Study of the BCAAs show that levels of leucine, isoleucine and valine independently and together are lower in control relative to MCI and AD participants. Pairwise comparisons show there is a significant increase in the BCAAs in MCI relative to control, where monitoring a change over time holds promise as a predictor of AD. Genetic variants have been identified through genome-wide association study (GWAS) that carry an association with increased BCAA levels (Lotta *et al.*, 2016), with an additional study suggesting that those with a genetic predisposition to raised plasma isoleucine were positively associated with AD (Larsson and Markus, 2017). Furthermore, recent investigations have shown the predictive value of BCAAs for the development of new-onset diabetes up to 12 years after the baseline examination, which incidentally has a 50% increased risk of developing AD (McCormack *et al.*, 2013, Newgard *et al.*, 2009). Conversely, BCAA levels have

be shown to be low in other conditions such as liver disease (Itou *et al.*, 2009) and traumatic brain injury (TBI) (Vuille-Dit-Bille *et al.*, 2012, Jeter *et al.*, 2013). In TBI, decreases in brain glutamate and the plasma concentrations of the BCAAs are observed, whereas the concentrations of phenylalanine, tryptophan and tyrosine are increased and are associated with significant intracranial pressure and jugular venous oxygen saturation changes (Vuille-Dit-Bille *et al.*, 2012). Significant decreases in plasma BCAAs are also observed in Huntington's disease, which correlate with the severity of the disease over time (Mochel *et al.*, 2011, Mochel *et al.*, 2007). These clinical presentations highlight how sub-optimal or chronically high levels of BCAAs affect brain function and how the BCAT metabolic proteins and activity are important to cognitive wellbeing. Further study is required to better determine the optimal levels of BCAAs and BCAT required for optimal cognitive well-being, which in turn will help to better inform clinical practice.

In 2015 a report presented data on a patient presenting with hypervalinaemia, hyperleucine-isoleucinemia, headaches, and MCI with brain white matter lesions (Wang *et al.*, 2015). Traditional clinical diagnosis of these presentations would be related to the autosomal recessive disorder Maple Syrup Urine disease, which is caused by a BCKDC deficiency (Chuang and Chuang, 2000). Two heterogeneous BCAT2 mutations, including c.509G-A and c.790G-A, were found, indicating that when BCAT2 is mutated, BCAA metabolism is perturbed, resulting in brain lesions and cognitive impairment. Treatment with Vitamin B6 caused the symptoms to subside and the lesions to decrease, with longer term vitamin B supplementation over a period of 2 years was shown to slow accelerated brain atrophy in elderly with MCI by 30%, (Smith *et al.*, 2010).

We propose that BCAT is upregulated in a neuro-protective manner which responds to either nutritional or redox changes in the cell. However, as with most biological systems an imbalance in metabolism could generate secondary consequences, such as increased glutamate production leading to neuronal toxicity, or if oxidised could assume a moonlighting neurotoxic role (Conway and Lee, 2015). Together both the BCAT proteins and their metabolites hold promise as markers of AD pathology but also as targets for future therapy-related approaches.

In this study we took a combined approach, utilising serum analyses, advanced MRI imaging and neuropsychology tests to detect alterations in the hippocampus in MCI and AD participants. MRI data indicated a reduction of total hippocampal volume primarily in the CA1 region, dentate gyrus and subiculum and is evident in both MCI and AD brains. Administration of versatile cognitive neuropsychology tests to the same participants allowed us to gain understanding of functional consequences of morphometric changes in the hippocampus and its sub-regions. Here, morphological changes detected by MRI analysis correlated with MoCA (Table 5.3.6) indicating that these 2 measures can be used in assessment of control compared with AD participants. Using the percentage accuracy under leave one-out-out cross validation of baseline linear discriminant model (MoCA or Dentate Gyrus) showed that a combination of measuring the BCAT proteins and the amino acids with MoCA or the dentate gyrus increased the sensitivity and specificity of these tests in discerning between MCI and AD. Diagnostically the most clinically relevant assays to date include measurement of CSF $A\beta_{1\text{-}42}$, total tau, phosphorylated tau and the Aβ/total tau index (ATI). Using combinations of these biomarkers the clinical sensitivity and specificity can vary between studies

but can reach values up to 90% and 85%, respectively (Lewczuk *et al.*, 2018). However, current studies measuring these parameters in blood have not generated substantial data in support of their use diagnostically. Other studies favour multi-analyte approaches such as the Luminex-based platform that identified 30 protein markers in discriminating AD from controls (AUC=0.95) indicating that a panel approach has potential to better delineate between participant groups.

In conclusion, using this proof of concept model the measurement of BCATm and the amino acids has showed an increase in the sensitivity and specificity of MoCA analysis in correctly identifying participants free of AD pathology (100%) but also those with the disease to 90% accuracy. This analysis shows that there is a high degree of information overlap between MoCA, the MRI measures, and the amino acids. However, both BCATm and glutamate, significantly improve the predictive potential of MoCA, and significantly improve the predictive potential of the MRI measures. These findings, coupled with the underpinning of extant literature, indicate that the combined modalities show diagnostic subject to the caveats of single centre cross-sectional exploratory studies.

Chapter 6

THE EFFECT OF LEUCINE DEPRIVATION ON CELLULAR METABOLISM

Fred Hudd

REGULATION OF NEUROTRANSMITTER SYNTHESIS IN ALZHEIMER'S DISEASE – POTENTIAL FOR NOVEL DISEASE BIOMARKERS | 2019

Chapter 6 – The Effect of Leucine Deprivation on Cellular Metabolism

6.1 - Introduction

The essential dietary amino acid leucine is important for protein synthesis and maintenance of metabolic function alongside isoleucine and valine. As previously discussed, these amino acids are the key nitrogen donors for the synthesis of glutamate in the brain (LaNoue *et al.*, 2001) and are fundamental in maintaining CNS neurotransmitter homeostasis where alterations can cause neurologic dysfunction (Yudkoff, 1997). Within this, the balance of intra-neuronal and extracellular glutamate is important to allow for normal release upon depolarisation and avoid excessive build up and possible excitotoxicity respectively (Yudkoff, 1997). In AD it is hypothesised that chronic glutamate excitotoxicity leads to neuronal death and symptomatic cognitive decline (Lewerenz and Maher, 2015), however the exact mechanisms are yet to be determined. Increased understanding of the effect of altered leucine levels in the brain may shed light on the mechanisms by which these altered neurotransmitter profiles occur.

In addition to increasing our understanding of the role of leucine as a precursor to neurotransmitter synthesis, further understanding of its role as an activator of mTOR (Jewell *et al.*, 2013) and the relation to autophagy pathway would help to determine some of the mechanistic underpinning of neurodegenerative disease development and progression. Under normal physiological conditions the mTOR pathway is responsible for neural development and circuit formation (Lipton and Sahin, 2014), and the regulation of autophagy (Jung *et al.*, 2010). mTOR acts as

a sensor of cellular nutritional status whereby reduction in cellular growth factors or conditions of nutrient starvation results in the inhibition of mTOR, leading to autophagy (Jung *et al.*, 2010). In AD there is a strong implication that dysregulated autophagy has a role on the disease pathogenesis (Saxton and Sabatini, 2017), with reports of early disease state alteration of mTOR1 activity and lysosomal dysfunction (Uddin *et al.*, 2019), which could subsequently lead to increased accumulation of aggregates (Perez *et al.*, 2015). However, there is still uncertainty in this field as to whether increased mTOR activation or reduced levels of BCAAs are beneficial in disease state.

In contrast to reports of reduced BCAA being beneficial, a review of studies into BCAA supplementation showed that there is a therapeutic benefit in the supplementation of BCAAs in cases of severe TBI (Sharma *et al.*, 2018), whereby improved cognition was noted after treatment. Although these accounts appear to be conflicting it is more likely due to the fact that it is the balance of BCAAs is important i.e. excess or limiting is toxic. Therefore, a greater understanding of these pathways will be an important avenue for identification of new and novel therapeutic targets.

This work has shown that in leucine deprived conditions intracellular glutamic acid is decreased significantly compared to controls. Interestingly, the level of BCATc was shown to be significantly increase in response to LD conditions which correlated with an increase in autophagy markers Beclin 1 and LC3 are shown to be significantly increased. This finding may indicate a possible interaction of hBCAT with the autophagy pathway. Finally, this work has shown significant metabolic perturbation in conditions of acute leucine deprivation when compared

to controls and in line with complete nutrient deprivation of cellular models. Overall, these findings indicate that leucine deprivation has a widespread effect on intracellular mechanisms in neuronal cells, which may have possible influence cognition and AD pathology.

6.2 – Specific Aims

Specific Aim 1 – To evaluate the glutamic acid, BCAA and AAA profiles in cellular model SH-SY5Y under leucine deprived and nutrient deprived conditions in addition to the response to leucine supplementation

Specific Aim 2 – Analyse key markers of autophagy, Beclin 1, LC3, mTOR and Phospho mTOR to determine the effect of leucine deprivation and the possible role or interaction of BCAT with the autophagy pathway

Specific Aim 3 – Determine the metabolic profile of SH-SY5Y cells under leucine deprived and nutrient deprived conditions

6.3 – Results

6.3.1 – Perturbations in the Levels of Glutamic Acid, BCAAs and AAAs in Leucine and Nutrient Deprived Conditions

Glutamic acid, isoleucine, leucine, phenylalanine, tyrosine and valine levels in the cellular lysate of SH-SY5Y cells was determined by ID-LC-MS/MS after treatment under leucine deprived, nutrient deprived conditions for 12, 24, 48 and 72 hours. In response to leucine deprivation for 24 hr there was a significant decrease in the concentration of glutamate relative to control (*p value* = <0.0001) with concentrations lower than nutrient deprivation reported, indicating that leucine is fundamentally important to glutamate regulation. Of the amino acids measured glutamate alone was shown to significantly decrease under control, leucine deprived and nutrient deprived conditions over a 72 hour period (Figure 6.3.1). Furthermore, there was a significant increase in all other amino acids except leucine observed at 12 hours (Summarised in Table 6.3.1) relative to control or nutrient deprived conditions suggesting that these other amino acids are taken up in the absence of leucine. However, over time the concentration of these amino acids also significantly decreased relative to control conditions (Tables 6.3.2-6.3.5).

6.3.1 – The Effect of Leucine and Nutrient Deprivation on Autophagy and the Expression of hBCATc

Under conditions described above the expression profiles of Beclin 1, LC3I/II, mTOR, and hBCATc were assessed by Western blot analysis in cellular lysates of SH-SY5Y cells. All measurements were normalised against the loading control α-tubulin and statistically analysed using an unpaired t-test.

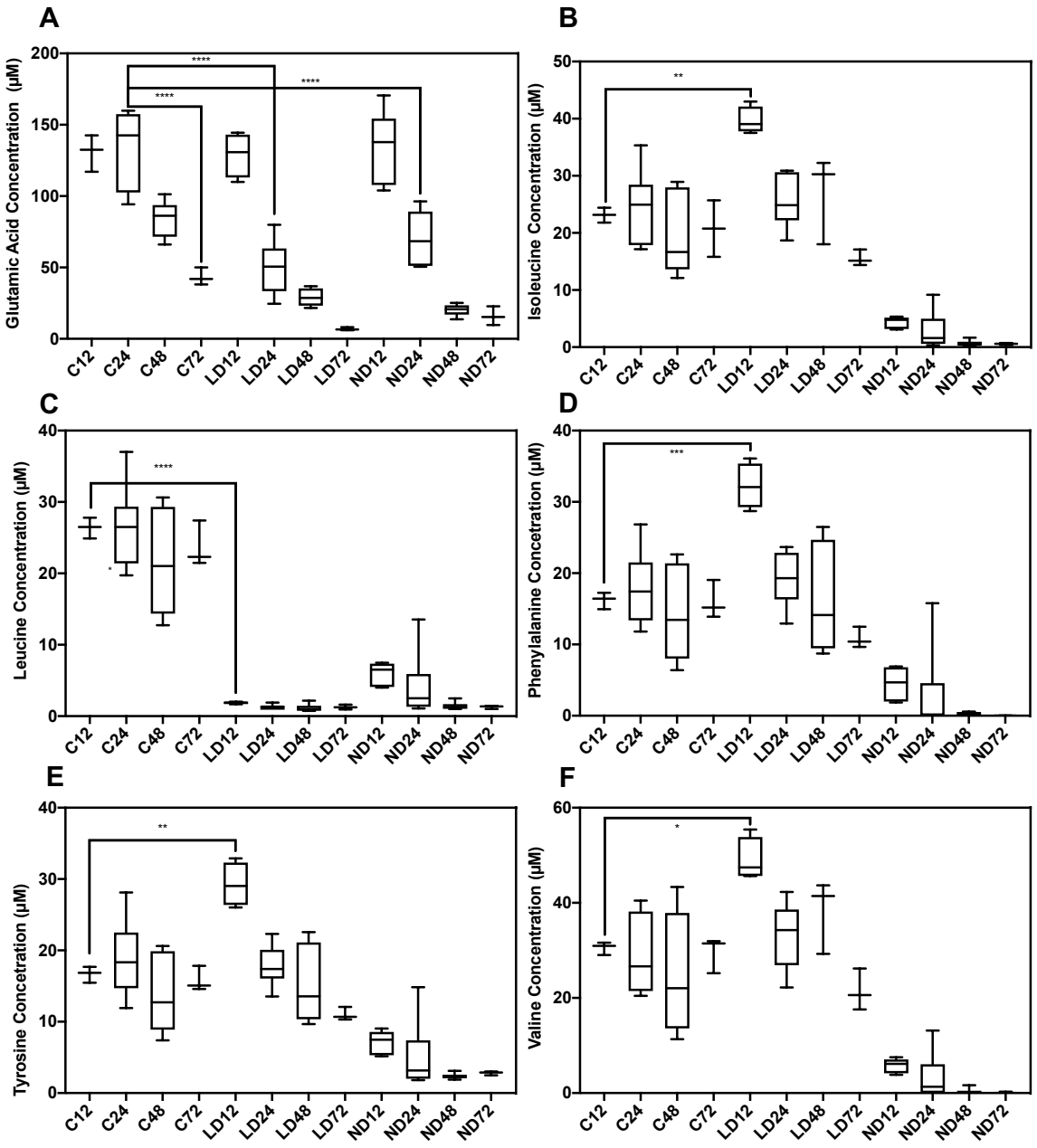

Figure 6.3.1 – Box and whisker plots of cellular lysate Glu, Ile, Leu, Phe, Tyr and Val changes under leucine deprived, nutrient deprived and control conditions over a 72-hour period.

Cellular lysate amino acids levels were analysed using our validated ID-LC-MS/MS method Significant changes in all amino acids were noted in response to both leucine and nutrient deprivation. **A** – Glutamic acid concentration was shown to decrease significantly under control conditions between 12 and 72 hours (*p value* = <0.0001). Additionally, a highly significant decrease was observed between control and leucine deprived cells and control and nutrient deprived cells at 24 hours *p value* = <0.0001 and 0.0001 respectively. **B, D, E and F** – Significant increases in isoleucine, phenylalanine, tyrosine and valine were seen in leucine deprived cells after 12 hours *p value* = 0.0079 (Ile) and <0.0001 (Phe, Tyr and Val). Analysis additionally showed that in nutrient deprivation all amino acids are significantly decreased. **C** – Leucine deprivation was shown to have an immediate impact on the levels of intracellular leucine with a significant difference between leucine concentration under leucine deprivation and nutrient deprivation at 12 hours (*p value* = <0.0035)

Table 6.3.1 – Pairwise comparison of Glu, Ile, Leu, Phe, Tyr and Val under control and leucine deprived condition at 12-hour and 24-hour time points.

Amino Acid	C12	C24	LD12	LD24	Pairwise Comparison		
					C12 vs C24	LD12 vs LD24	C24 vs LD24
Glutamate	130.7 ± 7.402	133.2 ± 10.02	129.0 ± 7.896	49.36 ± 6.102	0.9980	<0.0001	<0.0001
Amino Acid	**C12**	**C24**	**LD12**	**LD24**	**Pairwise Comparison**		
					C12 vs C24	**LD12 vs LD24**	**C12 vs LD12**
Isoleucine	23.13 ± 0.752	24.42 ± 2.209	36.51 ± 3.283	25.53 ± 1.905	0.9787	0.0016	0.0018
Leucine	26.40 ± 0.839	26.64 ± 1.954	1.867 ± 0.013	1.245 ± 0.112	<0.0001	0.9891	<0.0001
Phenylalanine	16.21 ± 0.674	18.04 ± 1.757	32.24 ± 1.581	19.20 ± 1.582	0.9086	0.0006	0.0004
Tyrosine	16.68 ± 0.652	18.70 ± 1.828	29.24 ± 1.548	17.81 ± 1.188	0.8695	0.0016	0.0031
Valine	30.54 ± 0.778	28.83 ± 2.827	48.68 ± 2.295	33.14 ± 2.961	0.9816	0.0101	0.0114

Table 6.3.2 – Pairwise comparison Glu, Ile, Leu, Phe, Tyr and Val under control, leucine deprived and nutrient deprived conditions analysed at 12 hours.

Amino Acid	C12	LD12	ND12	ANOVA F (2,9)	*p*-value	Pairwise Comparison		
						C12 vs LD12	C24 vs ND12	LD12 vs ND12
Glutamate	130.7 ± 7.402	129.0 ± 7.896	132.4 ± 11.75	0.03080	0.9698	0.9933	0.9931	0.9668
Isoleucine	23.13 ± 0.752	36.51 ± 3.283	4.295 ± 0.468	58.47	<0.0001	0.0079	0.0007	<0.0001
Leucine	26.40 ± 0.839	1.867 ± 0.013	5.885 ± 0.747	33.1	<0.0001	<0.0001	<0.0001	0.0035
Phenylalanine	16.21 ± 0.674	32.24 ± 1.581	4.456 ± 1.079	137.9	<0.0001	<0.0001	0.0003	<0.0001
Tyrosine	16.68 ± 0.652	29.24 ± 1.548	7.037 ± 0.754	115.5	<0.0001	<0.0001	0.0005	<0.0001
Valine	30.54 ± 0.778	48.68 ± 2.295	5.712 ± 0.685	249.8	<0.0001	<0.0001	<0.0001	<0.0001

C12 – Control 12 Hours, LD12 – Leucine Deprived 12 Hours and ND12 – Nutrient Deprived 12 Hours

Table 6.3.3 – Pairwise comparison Glu, Ile, Leu, Phe, Tyr and Val under control, leucine deprived and nutrient deprived conditions analysed at 24 hours.

Amino Acid	C24	LD24	ND24	ANOVA F (2,19)	*p*-value	Pairwise Comparison		
						C24 vs LD24	C24 vs ND24	LD24 vs ND24
Glutamate	133.2 ± 10.02	49.36 ± 6.102	70.30 ± 7.959	31.05	<0.0001	<0.0001	0.0001	0.1817
Isoleucine	24.42 ± 2.209	25.53 ± 1.905	3.141 ± 0.918	67.66	<0.0001	0.8979	<0.0001	<0.0001
Leucine	26.64 ± 1.954	1.245 ± 0.112	4.659 ± 1.293	101.0	<0.0001	<0.0001	<0.0001	0.1589
Phenylalanine	18.04 ± 1.757	19.20 ± 1.582	3.853 ± 5.828	24.96	<0.0001	0.9089	<0.0001	<0.0001
Tyrosine	18.70 ± 1.828	17.81 ± 1.188	5.815 ± 1.435	23.29	<0.0001	0.9306	<0.0001	<0.0001
Valine	28.83 ± 2.827	33.14 ± 2.961	3.857 ± 1.415	53.10	<0.0001	0.4502	<0.0001	<0.0001

C24 – Control 24 Hours, LD24 – Leucine Deprived 24 Hours and ND24 – Nutrient Deprived 24 Hours

Table 6.3.4 – Pairwise comparison Glu, Ile, Leu, Phe, Tyr and Val under control, leucine deprived and nutrient deprived conditions analysed at 48 hours.

Amino Acid	C48	LD48	ND48	ANOVA F (2,14)	*p*-value	Pairwise Comparison		
						C48 vs LD48	C48 vs ND48	LD48 vs ND48
Glutamate	84.06 ± 5.161	29.17 ± 2.805	20.22 ± 1.683	94.73	<0.0001	<0.0001	<0.0001	0.2349
Isoleucine	19.36 ± 2.918	26.84 ± 4.456	0.659 ± 0.211	27.62	<0.0001	0.1836	0.0002	<0.0001
Leucine	21.53 ± 3.038	1.117 ± 0.218	1.410 ± 0.223	44.03	<0.0001	<0.0001	<0.0001	0.9924
Phenylalanine	14.25 ± 2.742	16.20 ± 3.025	0.208 ± 0.109	13.68	0.0004	0.8283	0.0021	0.0007
Tyrosine	13.75 ± 2.326	15.09 ± 2.169	2.348 ± 0.171	14.50	0.0003	0.8643	0.0015	0.0005
Valine	24.86 ± 5.227	38.12 ± 4.477	0.274 ± 0.271	21.53	0.0001	0.1279	0.0012	0.0002

C48 – Control 48 Hours, LD48 – Leucine Deprived 48 Hours and ND48 – Nutrient Deprived 48 Hours

Table 6.3.5 – Pairwise comparison Glu, Ile, Leu, Phe, Tyr and Val under control, leucine deprived and nutrient deprived conditions analysed at 72 hours.

Amino Acid	C72	LD72	ND72	ANOVA F (2,6	*p*-value	Pairwise Comparison		
						C72 vs LD72	C72 vs ND72	LD72 vs ND72
Glutamate	43.34 ± 3.513	6.910 ± 0.663	15.89 ± 3.185	39.53	0.0004	0.0003	0.0016	0.1690
Isoleucine	20.75 ± 2.860	15.55 ± 0.810	0.562 ± 0.101	37.27	0.0004	0.1614	0.0004	0.0020
Leucine	23.73 ± 1.857	1.265 ± 0.1953	1.272 ± 0.131	144.1	<0.0001	<0.0001	<0.0001	>0.9999
Phenylalanine	16.04 ± 1.552	10.84 ± 0.847	0.008 ± 0.008	64.18	<0.0001	0.0265	<0.0001	0.0007
Tyrosine	15.84 ± 1.011	11.03 ± 0.537	2.794 ± 0.158	97.78	<0.0001	0.0054	<0.0001	0.0003
Valine	29.53 ± 2.175	21.45 ± 2.524	0.090 ± 0.090	62.51	<0.0001	0.0566	<0.0001	0.0006

C72 – Control 72 Hours, LD72 – Leucine Deprived 72 Hours and ND72 – Nutrient Deprived 72 Hours

Significant increases in the levels of hBCATc, Beclin 1 and LC3 lipidation were reported in leucine deprived cells *p value* = 0.0460, 0.0259 and 0.0399, respectively (Table 6.3.6). Representative Western blots for each proteins and bar charts of relative densities are shown in Figure 6.3.2. Analysis of hBCATc, LC3I/II, pmTOR and mTOR over a period of 72 hours indicates that under leucine deprived conditions levels of hBCATc increase relative to LC3I/II lipidation from 24 to 72 hours compared to controls, supporting a role for leucine and BCATc in regulating autophagy (Figure 6.3.2 and 6.3.3). Moreover, there is a concomitant decrease in the level of activated mTOR indicating that protein synthesis is decreased supporting a role for BCATc in crosstalk between pathways.

6.3. - Assessment of Mitochondrial Function in Neuronal Model SH-SY5Y under Conditions of Leucine Deprivation, Nutrient Deprivation and in Response to Leucine Supplementation

The effects of leucine deprivation, nutrient deprivation and leucine supplementation on mitochondrial respiration in SH-SY5Y cells was determined using an Agilent Seahorse XFe24 Analyser and the application of the Agilent Seahorse XF Mito Stress Kit. Differences in baseline respiration and respiration following the injection of; complex IV inhibitor oligomycin, mitochondrial uncoupler carbonyl cyanide 4-(trifluoromethoxy)phenylhydrazone (FCCP) and complex I and II inhibitors rotenone and antimycin A were assessed by repeated measurement one-way analysis of variance with the application of the Geisser-Greenhouse correction and a post-hoc application of Tukey's honestly significant differences test for each measure. Respiratory graph plots for oxygen consumption rate and extracellular acidification rate are shown in Figure 6.3.4

and 6.3.5 respectively. Figure 6.3.4 shows that leucine deprivation for 24 hours causes perturbations in oxygen consumption rate when compared to control at 24 hours. Additionally, significant decreases in extracellular oxygen consumption rate were observed between control and leucine deprived groups at 24 hours. Similar perturbations were observed when cells were deprived of nutrients for 24 hours with significant differences to control cells at the matched time points. Significant differences are also observed between cells deprived of leucine for 48 hours and 72 hours when compared to nutrient deprived cells at 24 and 72 hours and cells supplemented with leucine.

Within treatment groups significant differences in oxygen consumption rate were seen for leucine deprivation between 24 hours and 48 hours and between nutrient deprived cells at 48 and 72 hours compared to nutrient deprivation for 24 hours. Pairwise comparison and mean values of each experimental condition are summarised in Table 6.3.7.

Table 6.3.6 – Expression levels of BCATc, Beclin 1 and LC3 in cell maintained under control and leucine deprived conditions

Protein	**Control (n = 3)**	**Leucine Deprived (n = 3)**	**Unpaired t-test *p value***
BCATc	6.910 ± 0.701	40.50 ± 11.73	0.0460
Beclin 1	1.582 ± 0.158	13.18 ± 3.353	0.0259
LC3	0.1681 ± 0.035	3.885 ± 1.238	0.0399

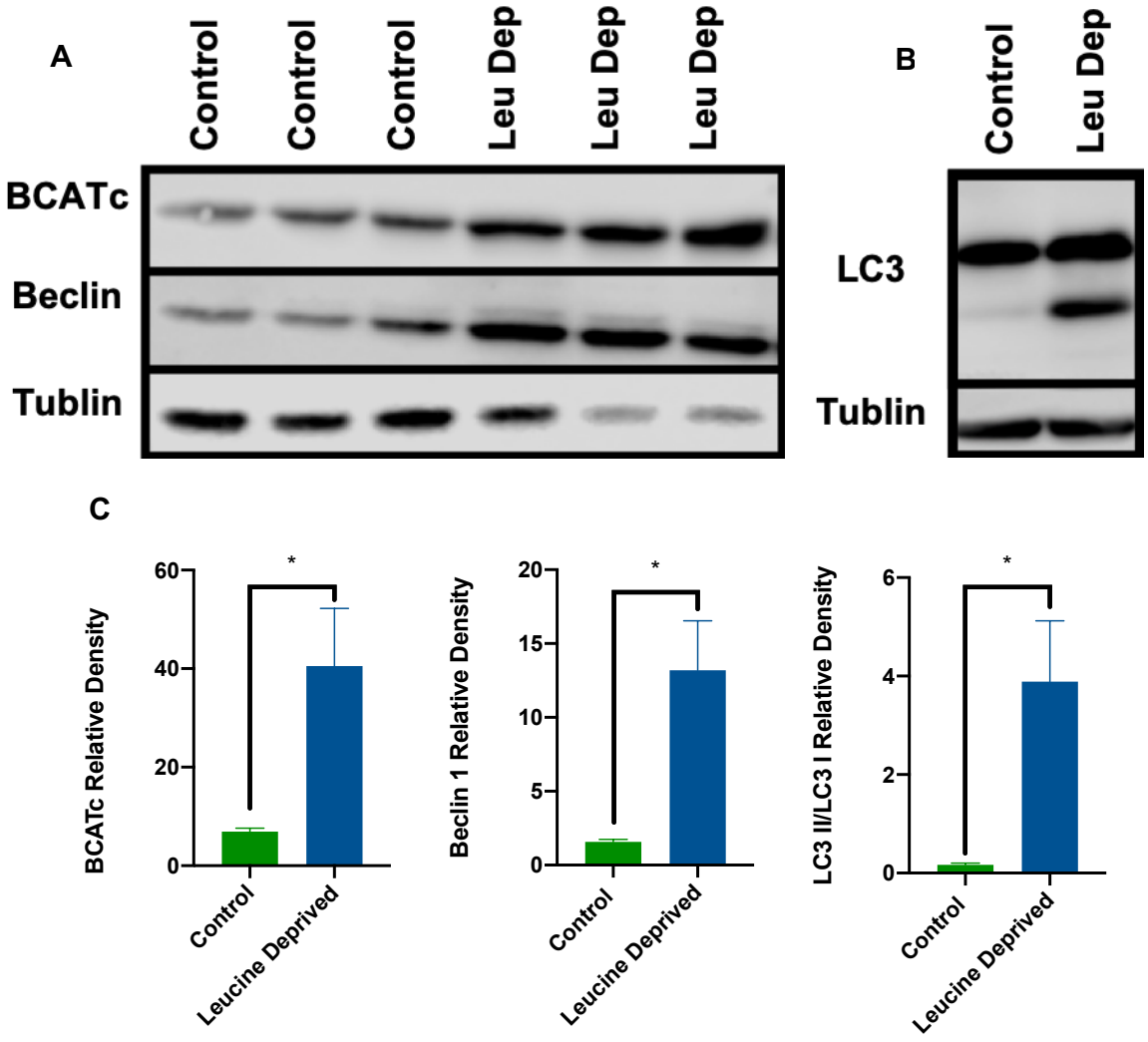

Figure 6.3.2 – Western blot analysis of BCATc, Beclin 1 and LC3 in the cellular lysate of SH-SY5Y cells maintained under leucine deprived conditions.
The protein concentration of cellular lysate samples was calculated using the Schaffner and Weissmann method (Schaffner W, 1973) and separated on a NuPAGE® Novex® 4-12% Bis-Tris followed by Western blot analysis using antibodies specific for BCATc, Beclin 1 and LC3 BCATm (1/1000, 1/1000 and 1/500 dilution respectively). Positive bands were visualised using chemiluminescent HRP substrate and an Odyssey® Fc Imaging System (LI-COR Biosciences). Integrated area densitometry was carried out using Image Studio Ver 5.2 and the results were measured in relation the α-tubulin loading control. **A**: Sample western blot analysis of BCATc and Beclin 1 under control and leucine deprived conditions (n = 3). **B**: Sample western blot analysis of LC3 under control and leucine deprived conditions (n=3). **C**: Bar charts of the relative density of BCATc, Beclin 1 and LC3 under maintained under control and leucine deprived conditions. Significant differences were seen in the expression of each protein; BCATc *p value* = 0.0460, Beclin 1 *p value* = 0.0259 and LC3 *p value* = 0.0399. *Leu Dep = Leucine Deprived

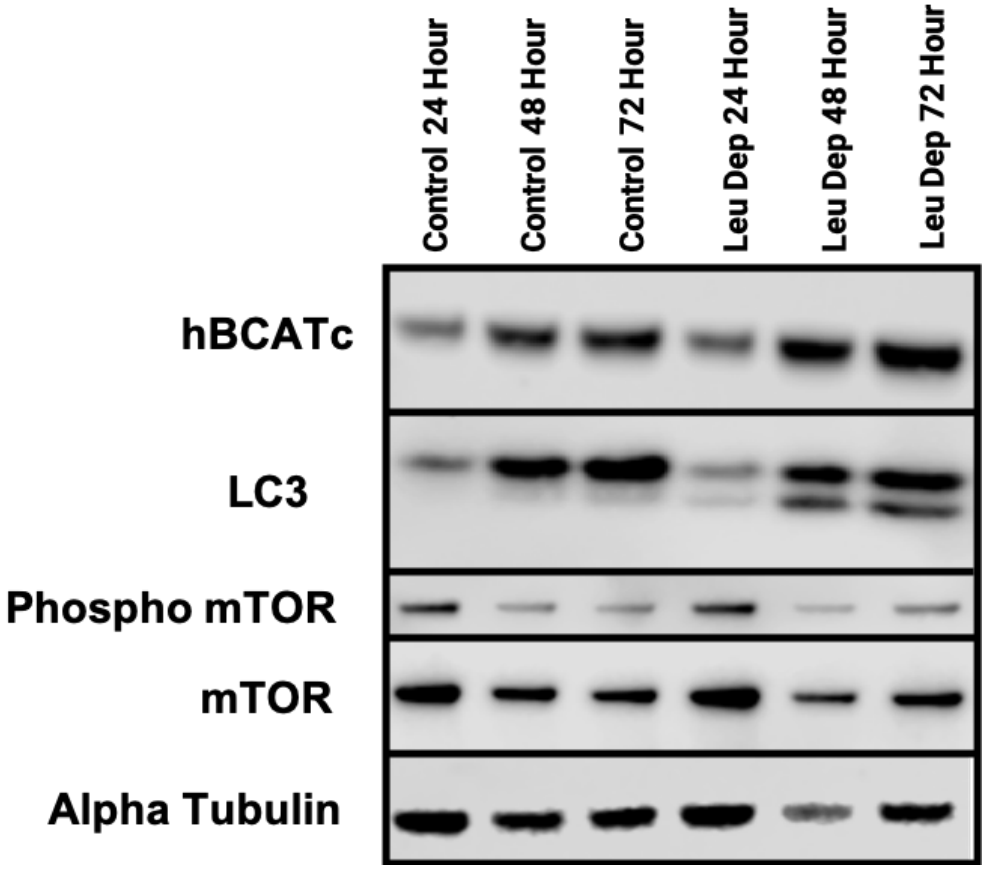

Figure 6.3.3 – Western blot analysis of BCATc, LC3I/II, pmTOR and mTOR in the cellular lysate of SH-SY5Y cells maintained under leucine deprived conditions over 72 hours. The protein concentration of cellular lysate samples was calculated using the Schaffner and Weissmann method (Schaffner W, 1973) and separated on a NuPAGE® Novex® 4-12% Bis-Tris followed by Western blot analysis using antibodies specific for hBCATc, LC3I/II pmTOR and mTOR. Positive bands were visualised using chemiluminescent HRP substrate and an Odyssey® Fc Imaging System (LI-COR Biosciences). (n =2).

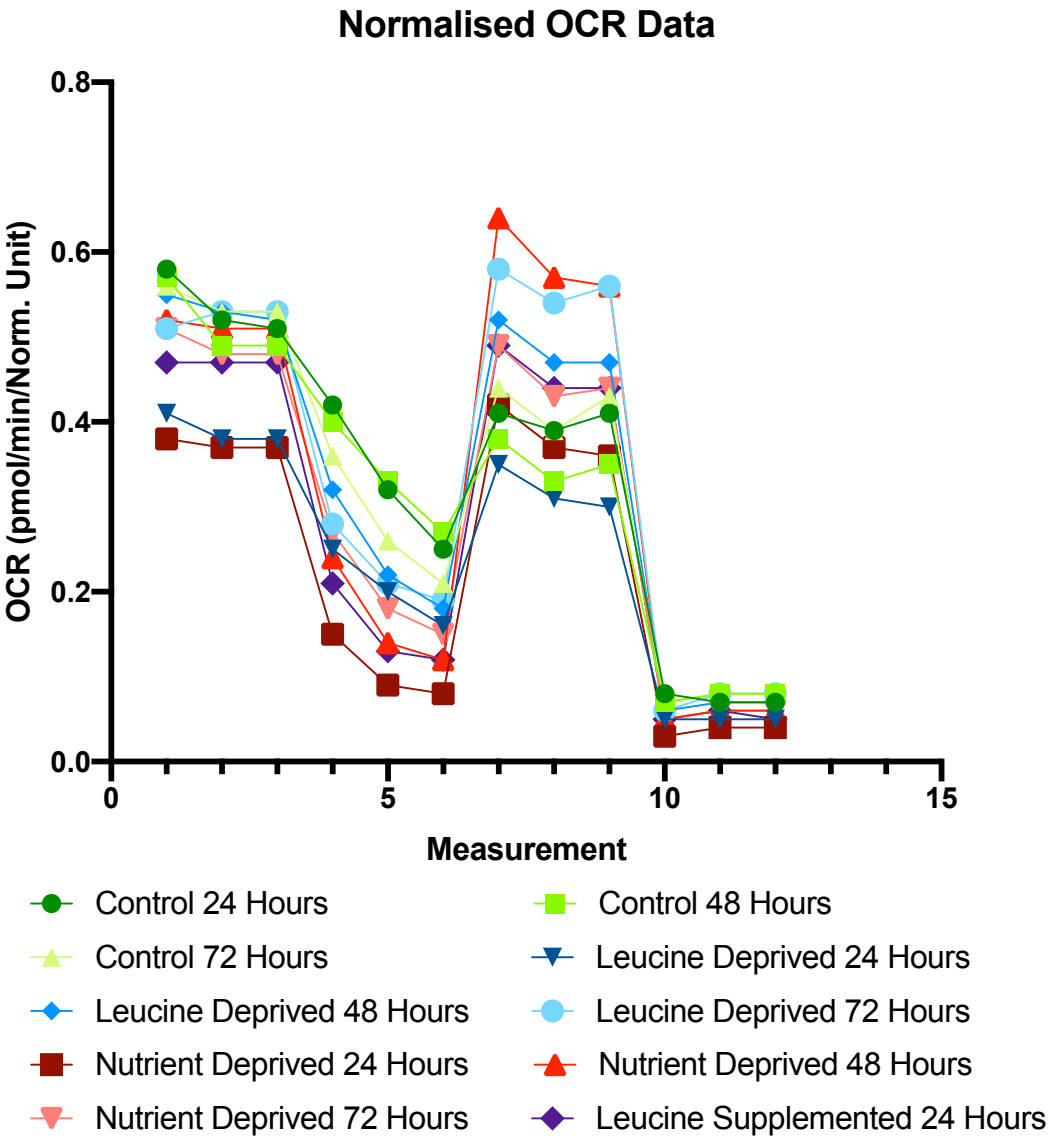

Figure 6.3.4 – Normalised oxygen consumption rate data from analysis of SH-SY5Y cells under normal, leucine deprived, nutrient deprived and leucine supplemented conditions.
Oxygen consumption rate was measured using an Agilent Seahorse XFe24 Analyser with the Seahorse XF Cell Mito Stress Test Kit. Cells were mere grown and treated according to the methods described in 3.5.21, 3.5.22, 3.5.23 and 3.5.24. Oxygen consumption rate was normalised against crystal violet staining of cells post-analysis (3.5.29) (n=3).

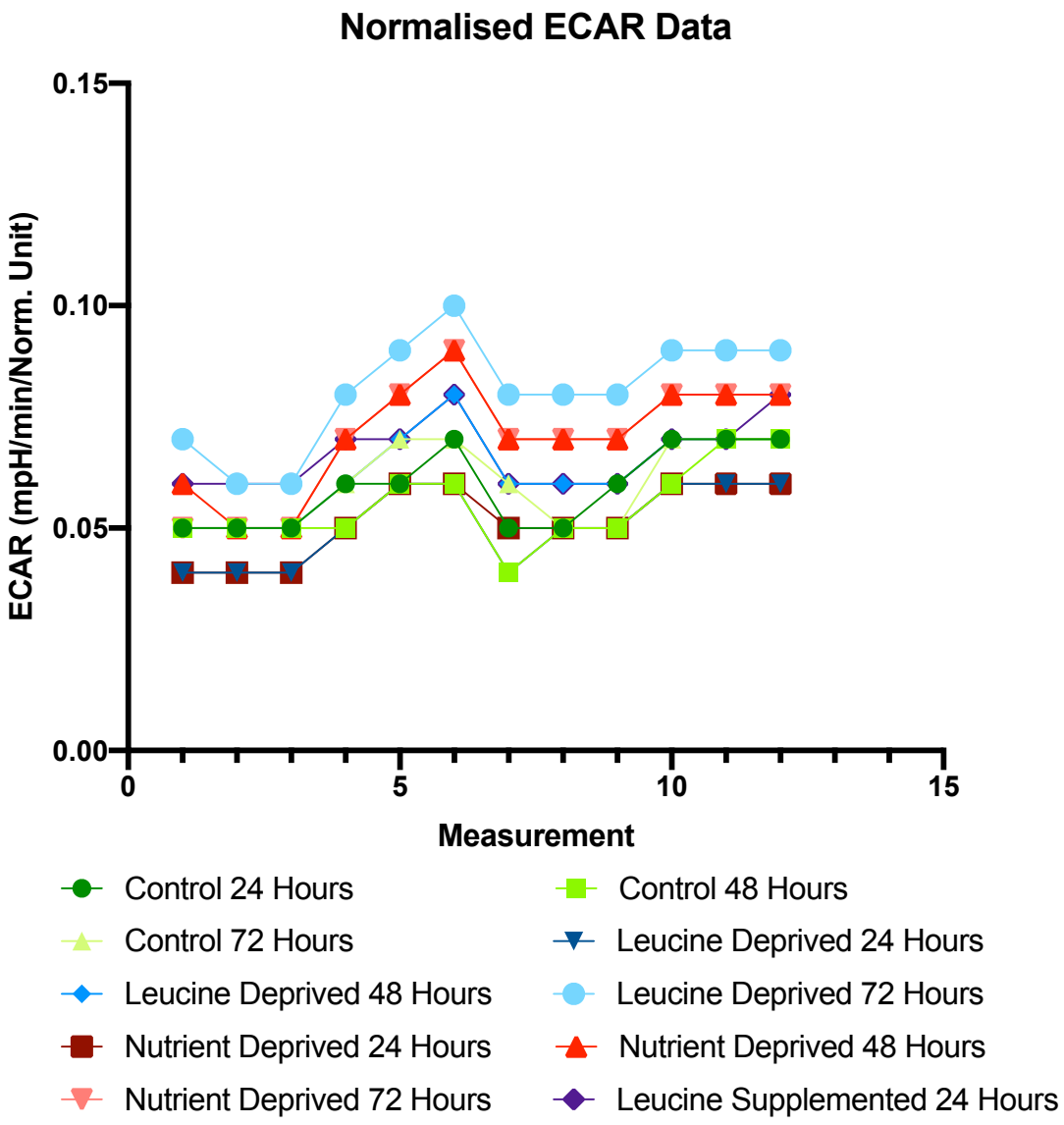

Figure 6.3.5 – Normalised extracellular acidification rate data from analysis of SH-SY5Y cells under normal, leucine deprived, nutrient deprived and leucine supplemented conditions.
Extracellular acidification rate was measured using an Agilent Seahorse XFe24 Analyser with the Seahorse XF Cell Mito Stress Test Kit. Cells were mere grown and treated according to the methods described in 3.5.21, 3.5.22, 3.5.23 and 3.5.24. extracellular acidification rate was normalised against crystal violet staining of cells post-analysis (3.5.29) (n=3).

Table 6.3.7 – Pairwise comparison of oxygen consumption rate and extracellular acidification rate of SH-SY5Y cells maintained under normal (control), leucine deprived, nutrient deprived or leucine supplemented conditions.

Cell Treatments - Pairwise Comparison	*p-values*	
	OCR	**ECAR**
Control 24 Hours vs. Control 48 Hours	0.5740	0.2425
Control 24 Hours vs. Control 72 Hours	0.9958	0.9998
Control 24 Hours vs. Leucine Deprived 24 Hours	0.0020	0.0004
Control 24 Hours vs. Leucine Deprived 48 Hours	>0.9999	0.4312
Control 24 Hours vs. Leucine Deprived 72 Hours	>0.9999	<0.0001
Control 24 Hours vs. Nutrient Deprived 24 Hours	0.0360	0.0031
Control 24 Hours vs. Nutrient Deprived 48 Hours	>0.9999	0.0037
Control 24 Hours vs. Nutrient Deprived 72 Hours	0.7406	0.0137
Control 24 Hours vs. Supplemented 24 Hours	0.6179	0.0031
Control 48 Hours vs. Control 72 Hours	0.9997	0.3294
Control 48 Hours vs. Leucine Deprived 24 Hours	0.0082	0.2425
Control 48 Hours vs. Leucine Deprived 48 Hours	>0.9999	0.0962
Control 48 Hours vs. Leucine Deprived 72 Hours	0.9983	<0.0001
Control 48 Hours vs. Nutrient Deprived 24 Hours	0.1514	0.7392
Control 48 Hours vs. Nutrient Deprived 48 Hours	>0.9999	0.0044
Control 48 Hours vs. Nutrient Deprived 72 Hours	0.9972	0.0128
Control 48 Hours vs. Supplemented 24 Hours	0.9612	0.0006
Control 72 Hours vs. Leucine Deprived 24 Hours	0.0020	0.0018
Control 72 Hours vs. Leucine Deprived 48 Hours	>0.9999	0.6623
Control 72 Hours vs. Leucine Deprived 72 Hours	0.9976	<0.0001
Control 72 Hours vs. Nutrient Deprived 24 Hours	0.0089	0.0004
Control 72 Hours vs. Nutrient Deprived 48 Hours	>0.9999	0.0038
Control 72 Hours vs. Nutrient Deprived 72 Hours	0.4915	0.0146
Control 72 Hours vs. Supplemented 24 Hours	0.3910	0.0146
Leucine Deprived 24 Hours vs. Leucine Deprived 48 Hours	0.0181	<0.0001
Leucine Deprived 24 Hours vs. Leucine Deprived 72 Hours	0.0550	<0.0001

Cell Treatments - Pairwise Comparison Continued	*p-values*	
	OCR	**ECAR**
Leucine Deprived 24 Hours vs. Nutrient Deprived 24 Hours	0.9920	0.9859
Leucine Deprived 24 Hours vs. Nutrient Deprived 48 Hours	0.3508	<0.0001
Leucine Deprived 24 Hours vs. Nutrient Deprived 72 Hours	0.1214	<0.0001
Leucine Deprived 24 Hours vs. Supplemented 24 Hours	0.6404	<0.0001
Leucine Deprived 48 Hours vs. Leucine Deprived 72 Hours	0.9540	<0.0001
Leucine Deprived 48 Hours vs. Nutrient Deprived 24 Hours	0.0006	<0.0001
Leucine Deprived 48 Hours vs. Nutrient Deprived 48 Hours	>0.9999	0.0004
Leucine Deprived 48 Hours vs. Nutrient Deprived 72 Hours	0.0003	0.0031
Leucine Deprived 48 Hours vs. Supplemented 24 Hours	0.0072	0.2425
Leucine Deprived 72 Hours vs. Nutrient Deprived 24 Hours	0.0003	<0.0001
Leucine Deprived 72 Hours vs. Nutrient Deprived 48 Hours	0.9297	<0.0001
Leucine Deprived 72 Hours vs. Nutrient Deprived 72 Hours	0.0458	<0.0001
Leucine Deprived 72 Hours vs. Supplemented 24 Hours	0.0011	0.0017
Nutrient Deprived 24 Hours vs. Nutrient Deprived 48 Hours	0.0116	<0.0001
Nutrient Deprived 24 Hours vs. Nutrient Deprived 72 Hours	0.0010	<0.0001
Nutrient Deprived 24 Hours vs. Supplemented 24 Hours	0.0014	<0.0001
Nutrient Deprived 48 Hours vs. Nutrient Deprived 72 Hours	0.8102	0.9859
Nutrient Deprived 48 Hours vs. Supplemented 24 Hours	0.1655	0.7140
Nutrient Deprived 72 Hours vs. Supplemented 24 Hours	0.3400	0.9339
Leucine Deprived 24 Hours vs. Nutrient Deprived 72 Hours	0.5740	0.2425

6.4 Discussion

The multifaceted cellular role of leucine as a nutrient and signalling amino acid presents itself as an interesting target with respect to disease pathology. Here, the study was focused on the role of leucine as a nitrogen donor in neurotransmitter synthesis, leucine regulator of mTOR and its role in autophagy. Importantly, for the first time there is evidence that BCAT plays an important conduit in regulating the interplay between these two pathways. This data has shown that perturbations in the levels of available leucine has significant effects on intracellular amino acid levels, activation of the autophagy pathway and cellular metabolism. Furthermore, an increase in the expression of hBCATc in line with autophagy markers in response to leucine deprived conditions was observed, supporting a key role for BCAT in regulating autophagy.

The maintenance of cellular homeostasis relies on effective cellular synthesis and degradation, which are often perturbed in disease. Autophagy is the major system by which cellular clearance is achieved, with roles in the degradation of whole organelles or protein aggregates and removal of cytosolic proteins in a chaperone mediated fashion (Cuervo and Wong, 2014, Choi *et al.*, 2013). In instances of cellular stress, such as nutrient deprivation, autophagy has a function as a cellular survival mechanism acting to prevent cell death (Choi *et al.*, 2013). The function of autophagy is especially important in neuronal cells, as damaged organelles cannot be redistributed, which if left uncleared can lead to neurotoxicity through intracellular build-up (Wong and Cuervo, 2010, Winslow and Rubinsztein, 2008).

The initiation of autophagy is controlled by two protein complexes ULK1 and the Beclin1-class III phosphatidylinositol 3-kinase (PI3KC3) with nutrient signalling as

the driving factor. PI3KC3 is essential for the formation of autophagosome formation (Rabanal-Ruiz *et al.*, 2017) and the initiation of autophagy through the generation of phosphatidylinositol 3-phosphate . Within this mechanism the activity of Beclin 1 is mediated by its interaction with binding partners (Xie *et al.*, 2016), with its pro-autophagic function inhibited through binding with Bcl-2 (Pattingre *et al.*, 2005). These interactions highlight other possible target for Beclin 1, which may play a role in the regulation of autophagy. In this study significant increases in hBCATc in response to leucine deprivation together with markers of autophagy, Beclin and LC3I/II (Figure 6.3.2 and 6.3.3) were observed. This correlated increase could indicate a possible interaction between hBCATc and Beclin 1 resulting in activation of the autophagy pathway. The increase in these markers indicate that there is an increase in autophagosome synthesis rather than increased flux.

The other primary regulator of the initiation of autophagy is mTOR1, which under fed conditions suppresses autophagy through the phosphorylation of ULK1 and Atg13 and promotes protein synthesis, cellular growth and proliferation by phosphorylation of s6 kinase and 4E-BP (Rabanal-Ruiz *et al.*, 2017). In nutrient deprivation ULK1 is activated to induce autophagy. Previous studies have explored the potential indirect contribution of glutamate dehydrogenase to autophagy and its effect on mTOR1 (Meijer and Codogno, 2008). A study reported that in combination, glutamine and leucine activate mTOR1 through enhanced α-ketoglutarate production (Duran *et al.*, 2012). However, the upstream involvement of BCAT was not considered. Here, it is shown that activation of mTOR is reduced in response to leucine deprivation suggesting that BCATc may be an important scaffold protein between these two signalling pathways. Furthermore, there is a

relationship with dysregulated autophagy in neurodegenerative disorders contributing to the pathogenic accumulation of protein aggregates, in addition accelerated lysosome accumulation in AD (Nixon *et al.*, 2005). In AD brain, both autophagic vacuoles and dystrophic neurites were found to be significantly increased in AD brain. This accelerated accumulation may occur by an increase in synthesis or perturbation of the autophagosome pathway resulting in the autophagosome-lysosome fusion disruption (Orr and Oddo, 2013). Moreover, these studies showed a correlation between the levels of Aβ and γ-secretase and these autophagic vacuoles indicating that this imbalanced clearance could contribute to elevated Aβ in the brain. This imbalance between autophagosome formation and clearance is considered an early event in AD pathogenesis.

Related studies by our group have shown the rapamycin, a positive regulator of autophagy and inhibitor of mTOR also increase the level of BCATc. Moreover, in this study an increase in the level of Aβ generated (Harris *et al.*, 2020) through increased autophagosome synthesis was shown. Interestingly, this increase in Aβ was alleviated through incubation with leucine. Together this data shows that in addition to leucine and BCAT regulating glutamate it also plays a key role in autophagy. As discussed, the levels of BCATc are significantly increased in AD brain relative to matched controls (Hull *et al.*, 2015). I propose that this increased level of BCAT could contribute to increased autophagosome synthesis. As autophagosome clearance is impaired this sustained activity by BCAT will promote aggregate accumulation contributing to pathology.

The mechanisms by which hBCAT regulates autophagy could be through its redox-active CXXC motif. The hBCAT proteins are unique amongst the

aminotransferase proteins with respect to their regulation by changes in the redox environment. In response to oxidation (Conway *et al.*, 2004, Conway *et al.*, 2003) S-nitrosation (Conway *et al.*, 2008)or S-glutathionylation the hBCAT proteins are differentially inactivated dependent on the modification. Our group has demonstrated that the reactive thiol is the N-terminal redox sensor and the C-terminal cysteine is the resolving cysteine, permitting reversible regulation. Previous work has also shown that *in vitro* the BCAT proteins have novel thiol oxidoreductase activity that can accelerate the refolding of reduced and denatured RNase, in particular when S-glutathionylated (Hull *et al.*, 2015). This intriguing regulatory feature of BCAT was also shown to govern their interaction with protein disulphide isomerase, a thiol disulphide isomerase, where BCAT was shown to increase the rate of refolding by PDI supporting a chaperone role for BCAT in protein folding (Hull *et al.*, 2015). Several other metabolic proteins, isolated from neuronal IMR32 cells, were also shown to have peroxide-mediated redox associations with BCAT (Coles *et al.*, 2009). These proteins have either known reactive cysteine residues or proteins with phosphorylation sites that are directly involved or controlled by G protein cell signalling, known to be modulated by peroxide. Therefore, as indicated in other studies BCAT may have roles as a chaperone or for scaffolding in regulating autophagy facilitating crosstalk with the mTOR pathway. Understanding how leucine supplementation reverses or control autophagy mediated Aβ generation will be an interesting target for future therapies.

In conclusion this work has shown that leucine and nutrient deprivation causes a significant decrease in intracellular glutamic acid and causes increased expression of markers of autophagy Beclin 1 and LC3. Furthermore, these

findings further support previously seen trends by our group and highlight a role for BCAT in autophagy. Metabolic analysis has additionally shown that in cases of acute leucine deprivation cellular metabolism is significantly altered. Moving forward additional research into the role of leucine in disease and the effect of leucine deprivation on cellular metabolism could give rise to promising diagnostic and therapeutic targets for not only neurodegenerative disease but conditions where altered autophagy is present.

Chapter 7

FUTURE WORK

Chapter 7 – Future Work

7.1 – Expansion of Biomarker Data Set

The promising findings through the analysis of serum hBCAT, branched chain and aromatic amino acids have shown that increased reseaerch in this area could yield a viable, novel and differential biomarker for AD and MCI. Through our collaboration we have currently collected samples from additional cohorts, which include those with subjective cognitive impairment and additional MCI participants. These participants have been tested using an alternative cognitive assessment, the Rivermead Behavioural Mental Test and have also been ApoE genotyped. These additional data sets will allow for the model generated from the first study to be tested on larger population and further assess the predictive power of these analytes as biomarkers.

7.2 – Evaluating the Effect of hBCAT Knockdown and Overexpression Under Leucine Deprived Conditions

The study of the effect of hBCAT overexpression and knockdown under control and leucine deprived conditions would allow for the further exploration of the role of hBCAT proteins in BCAA metabolism and their effect on the autophagy pathway. Our group has previously used siRNA and mammalian expression vectors to knockdown and overexpress hBCAT respectively. The aim would be to develop a lentiviral, selectable system to allow for alteration of the protein expression and generation of stable cell lines. This system would additionally allow for the knockdown of wildtype BCAT and expression of thiol mutated forms of the protein.

Bibliography

REFERENCED WORK

Fred Hudd

REGULATION OF NEUROTRANSMITTER SYNTHESIS IN ALZHEIMER'S DISEASE – POTENTIAL FOR NOVEL DISEASE BIOMARKERS | 2019

Bibliography:

Agarwal-Mawal, A., Qureshi, H. Y., Cafferty, P. W., Yuan, Z., Han, D., Lin, R. & Paudel, H. K. 2003. 14-3-3 connects glycogen synthase kinase-3 beta to tau within a brain microtubule-associated tau phosphorylation complex. *J Biol Chem,* 278**,** 12722-8.

Albert, M. S., Dekosky, S. T., Dickson, D., Dubois, B., Feldman, H. H., Fox, N. C., Gamst, A., Holtzman, D. M., Jagust, W. J., Petersen, R. C., Snyder, P. J., Carrillo, M. C., Thies, B. & Phelps, C. H. 2011. The diagnosis of mild cognitive impairment due to Alzheimer's disease: recommendations from the National Institute on Aging-Alzheimer's Association workgroups on diagnostic guidelines for Alzheimer's disease. *Alzheimers Dement,* 7**,** 270-9.

Alegret, M., Rodriguez, O., Espinosa, A., Ortega, G., Sanabria, A., Valero, S., Hernandez, I., Rosende-Roca, M., Vargas, L., Abdelnour, C., Mauleon, A., Gailhajanet, A., Martin, E., Tarraga, L., Rentz, D. M., Amariglio, R. E., Ruiz, A. & Boada, M. 2015. Concordance between Subjective and Objective Memory Impairment in Volunteer Subjects. *J Alzheimers Dis,* 48**,** 1109-17.

Alonso, A. C., Grundke-Iqbal, I. & Iqbal, K. 1996. Alzheimer's disease hyperphosphorylated tau sequesters normal tau into tangles of filaments and disassembles microtubules. *Nat Med,* 2**,** 783-7.

Alonso, A. C., Zaidi, T., Grundke-Iqbal, I. & Iqbal, K. 1994. Role of abnormally phosphorylated tau in the breakdown of microtubules in Alzheimer disease. *Proc Natl Acad Sci U S A,* 91**,** 5562-6.

Alzheimer's, A. 2015. 2015 Alzheimer's disease facts and figures. *Alzheimers Dement,* 11**,** 332-84.

Aquilani, R., Viglio, S., Iadarola, P., Opasich, C., Testa, A., Dioguardi, F. S. & Pasini, E. 2008. Oral amino acid supplements improve exercise capacities in elderly patients with chronic heart failure. *Am J Cardiol,* 101**,** 104E-110E.

Axe, E. L., Walker, S. A., Manifava, M., Chandra, P., Roderick, H. L., Habermann, A., Griffiths, G. & Ktistakis, N. T. 2008. Autophagosome formation from membrane compartments enriched in phosphatidylinositol 3-phosphate and dynamically connected to the endoplasmic reticulum. *J Cell Biol,* 182**,** 685-701.

Bancher, C., Brunner, C., Lassmann, H., Budka, H., Jellinger, K., Wiche, G., Seitelberger, F., Grundke-Iqbal, I., Iqbal, K. & Wisniewski, H. M. 1989. Accumulation of abnormally phosphorylated tau precedes the formation of neurofibrillary tangles in Alzheimer's disease. *Brain Res,* 477**,** 90-9.

Bartus, R. T., Dean, R. L., 3rd, Beer, B. & Lippa, A. S. 1982. The cholinergic hypothesis of geriatric memory dysfunction. *Science,* 217**,** 408-14.

Bekris, L. M., Yu, C. E., Bird, T. D. & Tsuang, D. W. 2010. Genetics of Alzheimer disease. *J Geriatr Psychiatry Neurol,* 23**,** 213-27.

Bell, K. F., Bennett, D. A. & Cuello, A. C. 2007. Paradoxical upregulation of glutamatergic presynaptic boutons during mild cognitive impairment. *J Neurosci,* 27**,** 10810-7.

Bell, K. F., Ducatenzeiler, A., Ribeiro-Da-Silva, A., Duff, K., Bennett, D. A. & Cuello, A. C. 2006. The amyloid pathology progresses in a neurotransmitter-specific manner. *Neurobiol Aging,* 27**,** 1644-57.

Bennett, D. A., Wilson, R. S., Schneider, J. A., Evans, D. A., Mendes De Leon, C. F., Arnold, S. E., Barnes, L. L. & Bienias, J. L. 2003. Education modifies the relation of AD pathology to level of cognitive function in older persons. *Neurology,* 60**,** 1909-15.

Bishop, G. M. & Robinson, S. R. 2002. The amyloid hypothesis: let sleeping dogmas lie? *Neurobiol Aging,* 23**,** 1101-5.

Blokland, A., Honig, W. & Raaijmakers, W. G. 1992. Effects of intra-hippocampal scopolamine injections in a repeated spatial acquisition task in the rat. *Psychopharmacology (Berl),* 109**,** 373-6.

Boado, R. J., Li, J. Y., Nagaya, M., Zhang, C. & Pardridge, W. M. 1999. Selective expression of the large neutral amino acid transporter at the blood-brain barrier. *Proc Natl Acad Sci U S A,* 96**,** 12079-84.

Bobinski, M., De Leon, M. J., Wegiel, J., Desanti, S., Convit, A., Saint Louis, L. A., Rusinek, H. & Wisniewski, H. M. 2000. The histological validation of post mortem magnetic resonance imaging-determined hippocampal volume in Alzheimer's disease. *Neuroscience,* 95**,** 721-5.

Boccia, M. M., Blake, M. G., Acosta, G. B. & Baratti, C. M. 2003. Atropine, an anticholinergic drug, impairs memory retrieval of a high consolidated avoidance response in mice. *Neurosci Lett,* 345**,** 97-100.

Braak, H. & Braak, E. 1991. Neuropathological stageing of Alzheimer-related changes. *Acta Neuropathol,* 82**,** 239-59.

Brautigam, C. A., Wynn, R. M., Chuang, J. L., Machius, M., Tomchick, D. R. & Chuang, D. T. 2006. Structural insight into interactions between dihydrolipoamide dehydrogenase (E3) and E3 binding protein of human pyruvate dehydrogenase complex. *Structure,* 14**,** 611-21.

Bredesen, D. E. 2009. Neurodegeneration in Alzheimer's disease: caspases and synaptic element interdependence. *Mol Neurodegener,* 4**,** 27.

Brothers, H. M., Gosztyla, M. L. & Robinson, S. R. 2018. The Physiological Roles of Amyloid-beta Peptide Hint at New Ways to Treat Alzheimer's Disease. *Front Aging Neurosci,* 10**,** 118.

Buchhave, P., Minthon, L., Zetterberg, H., Wallin, A. K., Blennow, K. & Hansson, O. 2012. Cerebrospinal fluid levels of beta-amyloid 1-42, but not of tau, are fully changed already 5 to 10 years before the onset of Alzheimer dementia. *Arch Gen Psychiatry,* 69**,** 98-106.

Canada, A. S. O. 2019. *Lewy body dementia | Alzheimer Society of Canada* [Online]. Available: https://alzheimer.ca/en/Home/About-dementia/Dementias/Lewy-Body-Dementia [Accessed].

Carlsson, A. & Lindqvist, M. 1978. Dependence of 5-HT and catecholamine synthesis on concentrations of precursor amino-acids in rat brain. *Naunyn Schmiedebergs Arch Pharmacol,* 303**,** 157-64.

Cataldo, A. M., Peterhoff, C. M., Troncoso, J. C., Gomez-Isla, T., Hyman, B. T. & Nixon, R. A. 2000. Endocytic pathway abnormalities precede amyloid beta deposition in sporadic Alzheimer's disease and Down syndrome: differential effects of APOE genotype and presenilin mutations. *Am J Pathol,* 157**,** 277-86.

Chan, E. Y., Longatti, A., Mcknight, N. C. & Tooze, S. A. 2009. Kinase-inactivated ULK proteins inhibit autophagy via their conserved C-terminal domains using an Atg13-independent mechanism. *Mol Cell Biol,* 29**,** 157-71.

Chen, R., Zou, Y., Mao, D., Sun, D., Gao, G., Shi, J., Liu, X., Zhu, C., Yang, M., Ye, W., Hao, Q., Li, R. & Yu, L. 2014. The general amino acid control pathway regulates mTOR and autophagy during serum/glutamine starvation. *J Cell Biol,* 206**,** 173-82.

Chertkow, H., Feldman, H. H., Jacova, C. & Massoud, F. 2013. Definitions of dementia and predementia states in Alzheimer's disease and vascular cognitive impairment: consensus from the Canadian conference on diagnosis of dementia. *Alzheimers Res Ther,* 5**,** S2.

Cho, J. H. & Johnson, G. V. 2003. Glycogen synthase kinase 3beta phosphorylates tau at both primed and unprimed sites. Differential impact on microtubule binding. *J Biol Chem,* 278**,** 187-93.

Choi, A. M., Ryter, S. W. & Levine, B. 2013. Autophagy in human health and disease. *N Engl J Med,* 368**,** 651-62.

Choi, D. W. 1985. Glutamate neurotoxicity in cortical cell culture is calcium dependent. *Neurosci Lett,* 58**,** 293-7.

Choi, D. W. 1988. Calcium-mediated neurotoxicity: relationship to specific channel types and role in ischemic damage. *Trends Neurosci,* 11**,** 465-9.

Chow, V. W., Mattson, M. P., Wong, P. C. & Gleichmann, M. 2010. An overview of APP processing enzymes and products. *Neuromolecular Med,* 12**,** 1-12.

Christensen, H., Mackinnon, A., Jorm, A. F., Korten, A., Jacomb, P., Hofer, S. M. & Henderson, S. 2004. The Canberra Longitudinal Study: Design, Aims, Methodology, Outcomes and Recent Empirical Investigations. *Aging, Neuropsychology, and Cognition,* 11**,** 169-195.

Chuang, D. T., Chuang, J. L. & Wynn, R. M. 2006. Lessons from genetic disorders of branched-chain amino acid metabolism. *J Nutr,* 136**,** 243S-9S.

Chuang, J. L. & Chuang, D. T. 2000. Diagnosis and mutational analysis of maple syrup urine disease using cell cultures. *Methods Enzymol,* 324**,** 413-23.

Cirrito, J. R., Yamada, K. A., Finn, M. B., Sloviter, R. S., Bales, K. R., May, P. C., Schoepp, D. D., Paul, S. M., Mennerick, S. & Holtzman, D. M. 2005. Synaptic activity regulates interstitial fluid amyloid-beta levels in vivo. *Neuron,* 48**,** 913-22.

Cole, J. T., Mitala, C. M., Kundu, S., Verma, A., Elkind, J. A., Nissim, I. & Cohen, A. S. 2010. Dietary branched chain amino acids ameliorate injury-induced cognitive impairment. *Proc Natl Acad Sci U S A,* 107**,** 366-71.

Coles, S. J., Easton, P., Sharrod, H., Hutson, S. M., Hancock, J., Patel, V. B. & Conway, M. E. 2009. S-Nitrosoglutathione inactivation of the mitochondrial and cytosolic BCAT proteins: S-nitrosation and S-thiolation. *Biochemistry,* 48**,** 645-56.

Collingridge, G. L. & Singer, W. 1990. Excitatory amino acid receptors and synaptic plasticity. *Trends Pharmacol Sci,* 11**,** 290-6.

Conway, M. E., Coles, S. J., Islam, M. M. & Hutson, S. M. 2008. Regulatory control of human cytosolic branched-chain aminotransferase by oxidation and S-glutathionylation and its interactions with redox sensitive neuronal proteins. *Biochemistry,* 47**,** 5465-79.

Conway, M. E. & Lee, C. 2015. The redox switch that regulates molecular chaperones. *Biomol Concepts,* 6**,** 269-84.

Conway, M. E., Poole, L. B. & Hutson, S. M. 2004. Roles for cysteine residues in the regulatory CXXC motif of human mitochondrial branched chain aminotransferase enzyme. *Biochemistry,* 43**,** 7356-64.

Conway, M. E., Yennawar, N., Wallin, R., Poole, L. B. & Hutson, S. M. 2003. Human mitochondrial branched chain aminotransferase: structural basis for substrate specificity and role of redox active cysteines. *Biochim Biophys Acta,* 1647**,** 61-5.

Cooper, C., Li, R., Lyketsos, C. & Livingston, G. 2013. Treatment for mild cognitive impairment: systematic review. *Br J Psychiatry,* 203**,** 255-64.

Cooper, C., Sommerlad, A., Lyketsos, C. G. & Livingston, G. 2015. Modifiable predictors of dementia in mild cognitive impairment: a systematic review and meta-analysis. *Am J Psychiatry,* 172**,** 323-34.

Corder, E. H., Saunders, A. M., Risch, N. J., Strittmatter, W. J., Schmechel, D. E., Gaskell, P. C., Jr., Rimmler, J. B., Locke, P. A., Conneally, P. M., Schmader, K. E. & Et Al. 1994. Protective effect of apolipoprotein E type 2 allele for late onset Alzheimer disease. *Nat Genet,* 7**,** 180-4.

Corder, E. H., Saunders, A. M., Strittmatter, W. J., Schmechel, D. E., Gaskell, P. C., Small, G. W., Roses, A. D., Haines, J. L. & Pericak-Vance, M. A. 1993. Gene dose of apolipoprotein E type 4 allele and the risk of Alzheimer's disease in late onset families. *Science,* 261**,** 921-3.

Corso, G., Cristofano, A., Sapere, N., La marca, G., Angiolillo, A., Vitale, M., Fratangelo, R., Lombardi, T., Porcile, C., Intrieri, M. & Di costanzo, A. 2017. Serum Amino Acid Profiles in Normal Subjects and in Patients with or at Risk of Alzheimer Dementia. *Dementia and Geriatric Cognitive Disorders Extra,* 7**,** 143-159.

Csapó, J., Albert, C., Lóki, K. & Csapó-Kiss, Z. 2008. Separation and determination of the amino acids by ion exchange column chromatography applying postcolumn derivatization. *Acta Universitatis Sapientiae - Alimentaria,* 1**,** 5-29.

Cuervo, A. M. & Wong, E. 2014. Chaperone-mediated autophagy: roles in disease and aging. *Cell Res,* 24**,** 92-104.

Cullen, K. M., Kocsi, Z. & Stone, J. 2006. Microvascular pathology in the aging human brain: evidence that senile plaques are sites of microhaemorrhages. *Neurobiol Aging,* 27**,** 1786-96.

Cummings, D. M., Liu, W., Portelius, E., Bayram, S., Yasvoina, M., Ho, S. H., Smits, H., Ali, S. S., Steinberg, R., Pegasiou, C. M., James, O. T., Matarin, M., Richardson, J. C., Zetterberg, H., Blennow, K., Hardy, J. A., Salih, D. A. & Edwards, F. A. 2015. First effects of rising amyloid-beta in transgenic mouse brain: synaptic transmission and gene expression. *Brain,* 138**,** 1992-2004.

Daneman, R. & Prat, A. 2015. The blood-brain barrier. *Cold Spring Harb Perspect Biol,* 7**,** a020412.

Davies, P. & Maloney, A. J. 1976. Selective loss of central cholinergic neurons in Alzheimer's disease. *Lancet,* 2**,** 1403.

De Ferrari, G. V., Canales, M. A., Shin, I., Weiner, L. M., Silman, I. & Inestrosa, N. C. 2001. A structural motif of acetylcholinesterase that promotes amyloid beta-peptide fibril formation. *Biochemistry,* 40**,** 10447-57.

Deane, R., Sagare, A., Hamm, K., Parisi, M., Lane, S., Finn, M. B., Holtzman, D. M. & Zlokovic, B. V. 2008. apoE isoform-specific disruption of amyloid beta peptide clearance from mouse brain. *J Clin Invest,* 118**,** 4002-13.

Denk, J., Boelmans, K., Siegismund, C., Lassner, D., Arlt, S. & Jahn, H. 2015. MicroRNA Profiling of CSF Reveals Potential Biomarkers to Detect Alzheimer`s Disease. *PLoS One,* 10**,** e0126423.

Denk, J., Oberhauser, F., Kornhuber, J., Wiltfang, J., Fassbender, K., Schroeter, M. L., Volk, A. E., Diehl-Schmid, J., Prudlo, J., Danek, A., Landwehrmeyer, B., Lauer, M., Otto, M., Jahn, H. & Group, F. T. S. 2018. Specific serum and CSF microRNA profiles distinguish sporadic behavioural variant of frontotemporal dementia compared with Alzheimer patients and cognitively healthy controls. *PLoS One,* 13**,** e0197329.

Dietzen, D. J., Rinaldo, P., Whitley, R. J., Rhead, W. J., Hannon, W. H., Garg, U. C., Lo, S. F. & Bennett, M. J. 2009. National academy of clinical biochemistry laboratory medicine practice guidelines: follow-up testing for metabolic disease identified by expanded newborn screening using tandem mass spectrometry; executive summary. *Clin Chem,* 55**,** 1615-26.

Dillon, S. E., Tsivos, D., Knight, M., Mccann, B., Pennington, C., Shiel, A. I., Conway, M. E., Newson, M. A., Kauppinen, R. A. & Coulthard, E. J. 2017. The impact of ageing reveals distinct roles for human dentate gyrus and CA3 in pattern separation and object recognition memory. *Sci Rep,* 7**,** 14069.

Dubois, B., Feldman, H. H., Jacova, C., Cummings, J. L., Dekosky, S. T., Barberger-Gateau, P., Delacourte, A., Frisoni, G., Fox, N. C., Galasko, D., Gauthier, S., Hampel, H., Jicha, G. A., Meguro, K., O'brien, J., Pasquier, F., Robert, P., Rossor, M., Salloway, S., Sarazin, M., De Souza, L. C., Stern, Y., Visser, P. J. & Scheltens, P. 2010. Revising the definition of Alzheimer's disease: a new lexicon. *Lancet Neurol,* 9**,** 1118-27.

Dubois, B., Feldman, H. H., Jacova, C., Dekosky, S. T., Barberger-Gateau, P., Cummings, J., Delacourte, A., Galasko, D., Gauthier, S., Jicha, G., Meguro, K., O'brien, J., Pasquier, F., Robert, P., Rossor, M., Salloway, S., Stern, Y., Visser, P. J. & Scheltens, P. 2007. Research criteria for the diagnosis of Alzheimer's disease: revising the NINCDS-ADRDA criteria. *Lancet Neurol,* 6**,** 734-46.

Dugger, B. N. & Dickson, D. W. 2017. Pathology of Neurodegenerative Diseases. *Cold Spring Harb Perspect Biol,* 9.

Duong, S., Patel, T. & Chang, F. 2017. Dementia: What pharmacists need to know. *Can Pharm J (Ott),* 150**,** 118-129.

Duran, R. V., Oppliger, W., Robitaille, A. M., Heiserich, L., Skendaj, R., Gottlieb, E. & Hall, M. N. 2012. Glutaminolysis activates Rag-mTORC1 signaling. *Mol Cell,* 47**,** 349-58.

Fagan, A. M., Mintun, M. A., Mach, R. H., Lee, S. Y., Dence, C. S., Shah, A. R., Larossa, G. N., Spinner, M. L., Klunk, W. E., Mathis, C. A., Dekosky, S. T., Morris, J. C. & Holtzman, D. M. 2006. Inverse relation between in vivo amyloid imaging load and cerebrospinal fluid Abeta42 in humans. *Ann Neurol,* 59**,** 512-9.

Farrer, L. A., Cupples, L. A., Haines, J. L., Hyman, B., Kukull, W. A., Mayeux, R., Myers, R. H., Pericak-Vance, M. A., Risch, N. & Van Duijn, C. M. 1997. Effects of age, sex, and ethnicity on the association between apolipoprotein E genotype and Alzheimer disease. A meta-analysis. APOE and Alzheimer Disease Meta Analysis Consortium. *JAMA,* 278**,** 1349-56.

Fernstrom, J. D. 1990. Aromatic amino acids and monoamine synthesis in the central nervous system: influence of the diet. *J Nutr Biochem,* 1**,** 508-17.

Fernstrom, J. D. 2005. Branched-chain amino acids and brain function. *J Nutr,* 135**,** 1539S-46S.

Fernstrom, J. D. 2013. Large neutral amino acids: dietary effects on brain neurochemistry and function. *Amino Acids,* 45**,** 419-30.

Ferreira-Vieira, T. H., Guimaraes, I. M., Silva, F. R. & Ribeiro, F. M. 2016. Alzheimer's disease: Targeting the Cholinergic System. *Curr Neuropharmacol,* 14**,** 101-15.

Figura, M., Kuśmierska, K., Bucior, E., Szlufik, S., Koziorowski, D., Jamrozik, Z. & Janik, P. 2018. Serum amino acid profile in patients with Parkinson’s disease. *PLOS ONE,* 13**,** e0191670.

Folstein, M. F., Folstein, S. E. & Mchugh, P. R. 1975. "Mini-mental state". A practical method for grading the cognitive state of patients for the clinician. *J Psychiatr Res,* 12**,** 189-98.

Fonteh, A. N., Harrington, R. J., Tsai, A., Liao, P. & Harrington, M. G. 2007. Free amino acid and dipeptide changes in the body fluids from Alzheimer's disease subjects. *Amino Acids,* 32**,** 213-24.

Francis, P. T. 2003. Glutamatergic systems in Alzheimer's disease. *Int J Geriatr Psychiatry,* 18**,** S15-21.

French, D. 2017. Chapter Five - Advances in Clinical Mass Spectrometry. *In:* MAKOWSKI, G. S. (ed.) *Advances in Clinical Chemistry.* Elsevier.

Galluzzi, L., Pietrocola, F., Levine, B. & Kroemer, G. 2014. Metabolic control of autophagy. *Cell,* 159**,** 1263-76.

Garthwaite, J., Charles, S. L. & Chess-Williams, R. 1988. Endothelium-derived relaxing factor release on activation of NMDA receptors suggests role as intercellular messenger in the brain. *Nature,* 336**,** 385-8.

Gartside, S. E., Cowen, P. J. & Sharp, T. 1992. Evidence that the large neutral amino acid L-valine decreases electrically-evoked release of 5-HT in rat hippocampus in vivo. *Psychopharmacology (Berl),* 109**,** 251-3.

Gatz, M., Reynolds, C. A., Fratiglioni, L., Johansson, B., Mortimer, J. A., Berg, S., Fiske, A. & Pedersen, N. L. 2006. Role of genes and environments for explaining Alzheimer disease. *Arch Gen Psychiatry,* 63**,** 168-74.

Gelfand, R. A., Glickman, M. G., Jacob, R., Sherwin, R. S. & Defronzo, R. A. 1986. Removal of infused amino acids by splanchnic and leg tissues in humans. *Am J Physiol,* 250**,** E407-13.

Glenner, G. G. & Wong, C. W. 2012. Alzheimer's disease: initial report of the purification and characterization of a novel cerebrovascular amyloid protein. 1984. *Biochem Biophys Res Commun,* 425**,** 534-9.

Glick, D., Barth, S. & Macleod, K. F. 2010. Autophagy: cellular and molecular mechanisms. *J Pathol,* 221**,** 3-12.

Glymour, M. M., Weuve, J., Berkman, L. F., Kawachi, I. & Robins, J. M. 2005. When is baseline adjustment useful in analyses of change? An example with education and cognitive change. *Am J Epidemiol,* 162**,** 267-78.

Goedert, M. & Crowther, R. A. 1989. Amyloid plaques, neurofibrillary tangles and their relevance for the study of Alzheimer's disease. *Neurobiol Aging,* 10**,** 405-6; discussion 412-4.

Goedert, M., Spillantini, M. G., Jakes, R., Rutherford, D. & Crowther, R. A. 1989. Multiple isoforms of human microtubule-associated protein tau: sequences and localization in neurofibrillary tangles of Alzheimer's disease. *Neuron,* 3**,** 519-26.

Gosche, K. M., Mortimer, J. A., Smith, C. D., Markesbery, W. R. & Snowdon, D. A. 2002. Hippocampal volume as an index of Alzheimer neuropathology: findings from the Nun Study. *Neurology,* 58**,** 1476-82.

Griffin, J. W. & Bradshaw, P. C. 2017. Amino Acid Catabolism in Alzheimer's Disease Brain: Friend or Foe? *Oxid Med Cell Longev,* 2017**,** 5472792.

Grimmer, T., Riemenschneider, M., Forstl, H., Henriksen, G., Klunk, W. E., Mathis, C. A., Shiga, T., Wester, H. J., Kurz, A. & Drzezga, A. 2009. Beta amyloid in Alzheimer's disease: increased deposition in brain is reflected in reduced concentration in cerebrospinal fluid. *Biol Psychiatry,* 65**,** 927-34.

Grundke-Iqbal, I., Iqbal, K., Tung, Y. C., Quinlan, M., Wisniewski, H. M. & Binder, L. I. 1986. Abnormal phosphorylation of the microtubule-associated protein tau (tau) in Alzheimer cytoskeletal pathology. *Proc Natl Acad Sci U S A,* 83**,** 4913-7.

Harris, M., El Hindy, M., Usmari-Moraes, M., Hudd, F., Shafei, M., Dong, M., Hezwani, M., Clark, P., House, M., Forshaw, T., Kehoe, P. & Conway, M. E. 2020. BCAT-induced autophagy regulates Abeta load through an interdependence of redox state and PKC phosphorylation-implications in Alzheimer's disease. *Free Radic Biol Med*.

Harris, R. A., Hawes, J. W., Popov, K. M., Zhao, Y., Shimomura, Y., Sato, J., Jaskiewicz, J. & Hurley, T. D. 1997. Studies on the regulation of the mitochondrial alpha-ketoacid dehydrogenase complexes and their kinases. *Adv Enzyme Regul,* 37**,** 271-93.

Harris, R. A., Joshi, M., Jeoung, N. H. & Obayashi, M. 2005. Overview of the molecular and biochemical basis of branched-chain amino acid catabolism. *J Nutr,* 135**,** 1527S-30S.

Hensley, K. & Harris-White, M. E. 2015a. Redox regulation of autophagy in healthy brain and neurodegeneration. *Neurobiol Dis*.

Hensley, K. & Harris-White, M. E. 2015b. Redox regulation of autophagy in healthy brain and neurodegeneration. *Neurobiol Dis,* 84**,** 50-9.

Hernandez, F., Perez, M., Lucas, J. J., Mata, A. M., Bhat, R. & Avila, J. 2004. Glycogen synthase kinase-3 plays a crucial role in tau exon 10 splicing and intranuclear distribution of SC35. Implications for Alzheimer's disease. *J Biol Chem,* 279**,** 3801-6.

Hollmann, M. & Heinemann, S. 1994. Cloned glutamate receptors. *Annu Rev Neurosci,* 17**,** 31-108.

Honour, J. W. 2011. Development and validation of a quantitative assay based on tandem mass spectrometry. *Ann Clin Biochem,* 48**,** 97-111.

Huang, X., Atwood, C. S., Hartshorn, M. A., Multhaup, G., Goldstein, L. E., Scarpa, R. C., Cuajungco, M. P., Gray, D. N., Lim, J., Moir, R. D., Tanzi, R. E. & Bush, A. I. 1999. The Aβ Peptide of Alzheimer's Disease Directly Produces Hydrogen Peroxide through Metal Ion Reduction. *Biochemistry,* 38**,** 7609-7616.

Hudd, F., Shiel, A., Harris, M., Bowdler, P., Mccann, B., Tsivos, D., Wearn, A., Knight, M., Kauppinen, R., Coulthard, E., White, P. & Conway, M. E. 2019. Novel Blood Biomarkers that Correlate with Cognitive Performance and Hippocampal Volumetry: Potential for Early Diagnosis of Alzheimer's Disease. *J Alzheimers Dis,* 67**,** 931-947.

Hull, J., Hindy, M. E., Kehoe, P. G., Chalmers, K., Love, S. & Conway, M. E. 2012. Distribution of the branched chain aminotransferase proteins in the human brain and their role in glutamate regulation. *J Neurochem,* 123**,** 997-1009.

Hull, J., Patel, V., El Hindy, M., Lee, C., Odeleye, E., Hezwani, M., Love, S., Kehoe, P., Chalmers, K. & Conway, M. 2015. Regional Increase in the Expression of the BCAT Proteins in Alzheimer's Disease Brain: Implications in Glutamate Toxicity. *J Alzheimers Dis,* 45**,** 891-905.

Hutson, S. 2001. Structure and function of branched chain aminotransferases. *Prog Nucleic Acid Res Mol Biol,* 70**,** 175-206.

Huynh, T. V., Davis, A. A., Ulrich, J. D. & Holtzman, D. M. 2017. Apolipoprotein E and Alzheimer's disease: the influence of apolipoprotein E on amyloid-beta and other amyloidogenic proteins. *J Lipid Res,* 58**,** 824-836.

Hye, A., Lynham, S., Thambisetty, M., Causevic, M., Campbell, J., Byers, H. L., Hooper, C., Rijsdijk, F., Tabrizi, S. J., Banner, S., Shaw, C. E., Foy, C., Poppe, M., Archer, N., Hamilton, G., Powell, J., Brown, R. G., Sham, P., Ward, M. & Lovestone, S. 2006. Proteome-based plasma biomarkers for Alzheimer's disease. *Brain,* 129**,** 3042-50.

Hye, A., Riddoch-Contreras, J., Baird, A. L., Ashton, N. J., Bazenet, C., Leung, R., Westman, E., Simmons, A., Dobson, R., Sattlecker, M., Lupton, M., Lunnon, K., Keohane, A., Ward, M., Pike, I., Zucht, H. D., Pepin, D., Zheng, W., Tunnicliffe, A., Richardson, J., Gauthier, S., Soininen, H., Kloszewska, I., Mecocci, P., Tsolaki, M., Vellas, B. & Lovestone, S. 2014. Plasma proteins predict conversion to dementia from prodromal disease. *Alzheimers Dement,* 10**,** 799-807 e2.

Ijsselstijn, L., Dekker, L. J., Koudstaal, P. J., Hofman, A., Sillevis Smitt, P. A., Breteler, M. M. & Luider, T. M. 2011. Serum clusterin levels are not increased in presymptomatic Alzheimer's disease. *J Proteome Res,* 10**,** 2006-10.

Ikonomovic, M. D., Klunk, W. E., Abrahamson, E. E., Mathis, C. A., Price, J. C., Tsopelas, N. D., Lopresti, B. J., Ziolko, S., Bi, W., Paljug, W. R., Debnath, M. L., Hope, C. E., Isanski, B. A., Hamilton, R. L. & Dekosky, S. T. 2008. Post-mortem correlates of in vivo PiB-PET amyloid imaging in a typical case of Alzheimer's disease. *Brain,* 131**,** 1630-45.

Iqbal, K., Liu, F., Gong, C. X. & Grundke-Iqbal, I. 2010. Tau in Alzheimer disease and related tauopathies. *Curr Alzheimer Res,* 7**,** 656-64.

Irvine, G. B., El-Agnaf, O. M., Shankar, G. M. & Walsh, D. M. 2008. Protein aggregation in the brain: the molecular basis for Alzheimer's and Parkinson's diseases. *Mol Med,* 14**,** 451-64.

Ito, H., Shimada, H., Shinotoh, H., Takano, H., Sasaki, T., Nogami, T., Suzuki, M., Nagashima, T., Takahata, K., Seki, C., Kodaka, F., Eguchi, Y., Fujiwara, H., Kimura, Y., Hirano, S., Ikoma, Y., Higuchi, M., Kawamura, K., Fukumura, T., Boo, E. L., Farde, L. & Suhara, T. 2014. Quantitative Analysis of Amyloid Deposition in Alzheimer Disease Using PET and the Radiotracer (1)(1)C-AZD2184. *J Nucl Med,* 55**,** 932-8.

Itou, M., Kawaguchi, T., Taniguchi, E., Oku, Y., Fukushima, N., Ando, E., Oriishi, T., Uchida, Y., Otsuka, M., Tanaka, S., Iwasaki, S., Torii, M., Yoshida, K., Adachi, Y., Suga, M., Yoshiyama, M., Ibi, R., Akiyama, Y., Takakura, M., Mitsuyama, K., Tsuruta, O. & Sata, M. 2009. Branched-chain amino acid supplements reduced ascites and increased the quality of life in a patient with liver cirrhosis: A case report. *Mol Med Rep,* 2**,** 977-81.

Jack, C. R., Jr., Dickson, D. W., Parisi, J. E., Xu, Y. C., Cha, R. H., O'brien, P. C., Edland, S. D., Smith, G. E., Boeve, B. F., Tangalos, E. G., Kokmen, E. & Petersen, R. C. 2002. Antemortem MRI findings correlate with hippocampal neuropathology in typical aging and dementia. *Neurology,* 58**,** 750-7.

Jack, C. R., Jr., Knopman, D. S., Jagust, W. J., Shaw, L. M., Aisen, P. S., Weiner, M. W., Petersen, R. C. & Trojanowski, J. Q. 2010. Hypothetical model of dynamic biomarkers of the Alzheimer's pathological cascade. *Lancet Neurol,* 9**,** 119-28.

Jagust, W. J., Landau, S. M., Shaw, L. M., Trojanowski, J. Q., Koeppe, R. A., Reiman, E. M., Foster, N. L., Petersen, R. C., Weiner, M. W., Price, J. C., Mathis, C. A. & Alzheimer's Disease Neuroimaging, I. 2009. Relationships between biomarkers in aging and dementia. *Neurology,* 73**,** 1193-9.

Janelidze, S., Zetterberg, H., Mattsson, N., Palmqvist, S., Vanderstichele, H., Lindberg, O., Van Westen, D., Stomrud, E., Minthon, L., Blennow, K., Swedish Bio, F. S. G. & Hansson, O. 2016. CSF Abeta42/Abeta40 and Abeta42/Abeta38 ratios: better diagnostic markers of Alzheimer disease. *Ann Clin Transl Neurol,* 3**,** 154-65.

Jeter, C. B., Hergenroeder, G. W., Ward, N. H., 3rd, Moore, A. N. & Dash, P. K. 2013. Human mild traumatic brain injury decreases circulating branched-chain amino acids and their metabolite levels. *J Neurotrauma,* 30**,** 671-9.

Jewell, J. L., Russell, R. C. & Guan, K.-L. 2013. Amino acid signalling upstream of mTOR. *Nature Reviews Molecular Cell Biology,* 14**,** 133-139.

Jiang, Q., Lee, C. Y., Mandrekar, S., Wilkinson, B., Cramer, P., Zelcer, N., Mann, K., Lamb, B., Willson, T. M., Collins, J. L., Richardson, J. C., Smith, J. D., Comery, T. A., Riddell, D., Holtzman, D. M., Tontonoz, P. & Landreth, G. E. 2008. ApoE promotes the proteolytic degradation of Abeta. *Neuron,* 58**,** 681-93.

Johnson, K. A., Fox, N. C., Sperling, R. A. & Klunk, W. E. 2012. Brain imaging in Alzheimer disease. *Cold Spring Harb Perspect Med,* 2**,** a006213.

Jung, C. H., Ro, S. H., Cao, J., Otto, N. M. & Kim, D. H. 2010. mTOR regulation of autophagy. *FEBS Lett,* 584**,** 1287-95.

Kaiser, E., Schoenknecht, P., Kassner, S., Hildebrandt, W., Kinscherf, R. & Schroeder, J. 2010. Cerebrospinal fluid concentrations of functionally important amino acids and metabolic compounds in patients with mild cognitive impairment and Alzheimer's disease. *Neurodegener Dis,* 7**,** 251-9.

Kamenetz, F., Tomita, T., Hsieh, H., Seabrook, G., Borchelt, D., Iwatsubo, T., Sisodia, S. & Malinow, R. 2003. APP processing and synaptic function. *Neuron,* 37**,** 925-37.

Kashani, A., Lepicard, E., Poirel, O., Videau, C., David, J. P., Fallet-Bianco, C., Simon, A., Delacourte, A., Giros, B., Epelbaum, J., Betancur, C. & El Mestikawy, S. 2008. Loss of VGLUT1 and VGLUT2 in the prefrontal cortex is correlated with cognitive decline in Alzheimer disease. *Neurobiol Aging,* 29**,** 1619-30.

Khan, T. K. & Alkon, D. L. 2015. Alzheimer's Disease Cerebrospinal Fluid and Neuroimaging Biomarkers: Diagnostic Accuracy and Relationship to Drug Efficacy. *J Alzheimers Dis,* 46**,** 817-36.

Khatoon, S., Grundke-Iqbal, I. & Iqbal, K. 1992. Brain levels of microtubule-associated protein tau are elevated in Alzheimer's disease: a radioimmuno-slot-blot assay for nanograms of the protein. *J Neurochem,* 59**,** 750-3.

Kim, E., Jung, Y. S., Kim, H., Kim, J. S., Park, M., Jeong, J., Lee, S. K., Yoon, H. G., Hwang, G. S. & Namkoong, K. 2014. Metabolomic signatures in peripheral blood associated with Alzheimer's disease amyloid-beta-induced neuroinflammation. *J Alzheimers Dis,* 42**,** 421-33.

Kopke, E., Tung, Y. C., Shaikh, S., Alonso, A. C., Iqbal, K. & Grundke-Iqbal, I. 1993. Microtubule-associated protein tau. Abnormal phosphorylation of a non-paired helical filament pool in Alzheimer disease. *J Biol Chem,* 268**,** 24374-84.

Ksiezak-Reding, H., Binder, L. I. & Yen, S. H. 1988. Immunochemical and biochemical characterization of tau proteins in normal and Alzheimer's disease brains with Alz 50 and Tau-1. *J Biol Chem,* 263**,** 7948-53.

Kwong, K. K., Belliveau, J. W., Chesler, D. A., Goldberg, I. E., Weisskoff, R. M., Poncelet, B. P., Kennedy, D. N., Hoppel, B. E., Cohen, M. S., Turner, R. & Et Al. 1992. Dynamic magnetic resonance imaging of human brain activity during primary sensory stimulation. *Proc Natl Acad Sci U S A,* 89**,** 5675-9.

Laforce, R., Jr., Buteau, J. P., Paquet, N., Verret, L., Houde, M. & Bouchard, R. W. 2010. The value of PET in mild cognitive impairment, typical and atypical/unclear dementias: A retrospective memory clinic study. *Am J Alzheimers Dis Other Demen,* 25**,** 324-32.

Lanoue, K. F., Berkich, D. A., Conway, M., Barber, A. J., Hu, L. Y., Taylor, C. & Hutson, S. 2001. Role of specific aminotransferases in de novo glutamate synthesis and redox shuttling in the retina. *J Neurosci Res,* 66**,** 914-22.

Larsson, S. C. & Markus, H. S. 2017. Branched-chain amino acids and Alzheimer's disease: a Mendelian randomization analysis. *Sci Rep,* 7**,** 13604.

Leinonen, V., Alafuzoff, I., Aalto, S., Suotunen, T., Savolainen, S., Nagren, K., Tapiola, T., Pirttila, T., Rinne, J., Jaaskelainen, J. E., Soininen, H. & Rinne, J. O. 2008. Assessment of beta-amyloid in a frontal cortical brain biopsy specimen and by positron emission tomography with carbon 11-labeled Pittsburgh Compound B. *Arch Neurol,* 65**,** 1304-9.

Lewczuk, P., Riederer, P., O'bryant, S. E., Verbeek, M. M., Dubois, B., Visser, P. J., Jellinger, K. A., Engelborghs, S., Ramirez, A., Parnetti, L., Jack, C. R., Jr., Teunissen, C. E., Hampel, H., Lleo, A., Jessen, F., Glodzik, L., De Leon, M. J., Fagan, A. M., Molinuevo, J. L., Jansen, W. J., Winblad, B., Shaw, L. M.,

Andreasson, U., Otto, M., Mollenhauer, B., Wiltfang, J., Turner, M. R., Zerr, I., Handels, R., Thompson, A. G., Johansson, G., Ermann, N., Trojanowski, J. Q., Karaca, I., Wagner, H., Oeckl, P., Van Waalwijk Van Doorn, L., Bjerke, M., Kapogiannis, D., Kuiperij, H. B., Farotti, L., Li, Y., Gordon, B. A., Epelbaum, S., Vos, S. J. B., Klijn, C. J. M., Van Nostrand, W. E., Minguillon, C., Schmitz, M., Gallo, C., Lopez Mato, A., Thibaut, F., Lista, S., Alcolea, D., Zetterberg, H., Blennow, K., Kornhuber, J. & Members of the Wfsbp Task Force Working on This Topic: Peter Riederer, C. G. D. K. a. L. M. F. T. 2018. Cerebrospinal fluid and blood biomarkers for neurodegenerative dementias: An update of the Consensus of the Task Force on Biological Markers in Psychiatry of the World Federation of Societies of Biological Psychiatry. *World J Biol Psychiatry,* 19**,** 244-328.

Lewerenz, J. & Maher, P. 2015. Chronic Glutamate Toxicity in Neurodegenerative Diseases-What is the Evidence? *Front Neurosci,* 9**,** 469.

Li, B., Chohan, M. O., Grundke-Iqbal, I. & Iqbal, K. 2007. Disruption of microtubule network by Alzheimer abnormally hyperphosphorylated tau. *Acta Neuropathol,* 113**,** 501-11.

Li, N.-J., Liu, W.-T., Li, W., Li, S.-Q., Chen, X.-H., Bi, K.-S. & He, P. 2010. Plasma metabolic profiling of Alzheimer's disease by liquid chromatography/mass spectrometry. *Clinical Biochemistry,* 43**,** 992-997.

Li, Q. X., Berndt, M. C., Bush, A. I., Rumble, B., Mackenzie, I., Friedhuber, A., Beyreuther, K. & Masters, C. L. 1994. Membrane-associated forms of the beta A4 amyloid protein precursor of Alzheimer's disease in human platelet and brain: surface expression on the activated human platelet. *Blood,* 84**,** 133-42.

Lipton, J. O. & Sahin, M. 2014. The neurology of mTOR. *Neuron,* 84**,** 275-91.

Lipton, S. A. & Rosenberg, P. A. 1994. Excitatory amino acids as a final common pathway for neurologic disorders. *N Engl J Med,* 330**,** 613-22.

Lista, S., Faltraco, F., Prvulovic, D. & Hampel, H. 2013. Blood and plasma-based proteomic biomarker research in Alzheimer's disease. *Prog Neurobiol,* 101-102**,** 1-17.

Liu, F., Liang, Z., Shi, J., Yin, D., El-Akkad, E., Grundke-Iqbal, I., Iqbal, K. & Gong, C. X. 2006. PKA modulates GSK-3beta- and cdk5-catalyzed phosphorylation of tau in site- and kinase-specific manners. *FEBS Lett,* 580**,** 6269-74.

Lloret, A., Badia, M. C., Giraldo, E., Ermak, G., Alonso, M. D., Pallardo, F. V., Davies, K. J. & Vina, J. 2011. Amyloid-beta toxicity and tau hyperphosphorylation are linked via RCAN1 in Alzheimer's disease. *J Alzheimers Dis,* 27**,** 701-9.

Lopez, O. L., Kuller, L. H., Becker, J. T., Dulberg, C., Sweet, R. A., Gach, H. M. & Dekosky, S. T. 2007. Incidence of dementia in mild cognitive impairment in the cardiovascular health study cognition study. *Arch Neurol,* 64**,** 416-20.

Lotta, L. A., Scott, R. A., Sharp, S. J., Burgess, S., Luan, J., Tillin, T., Schmidt, A. F., Imamura, F., Stewart, I. D., Perry, J. R., Marney, L., Koulman, A., Karoly, E. D., Forouhi, N. G., Sjogren, R. J., Naslund, E., Zierath, J. R., Krook, A., Savage, D. B., Griffin, J. L., Chaturvedi, N., Hingorani, A. D., Khaw, K. T., Barroso, I., Mccarthy, M. I., O'rahilly, S., Wareham, N. J. & Langenberg, C. 2016. Genetic Predisposition to an Impaired Metabolism of the Branched-Chain Amino Acids and Risk of Type 2 Diabetes: A Mendelian Randomisation Analysis. *PLoS Med,* 13**,** e1002179.

Lui, S.-H. 2008. Quality Evaluation of HPLC-Grade Acetonitrile.

Lyketsos, C. G., Chen, L. S. & Anthony, J. C. 1999. Cognitive decline in adulthood: an 11.5-year follow-up of the Baltimore Epidemiologic Catchment Area study. *Am J Psychiatry,* 156**,** 58-65.

Ma, T., Hoeffer, C. A., Capetillo-Zarate, E., Yu, F., Wong, H., Lin, M. T., Tampellini, D., Klann, E., Blitzer, R. D. & Gouras, G. K. 2010. Dysregulation of the mTOR pathway mediates impairment of synaptic plasticity in a mouse model of Alzheimer's disease. *PLoS One,* 5.

Magistretti, P. J. 2006. Neuron-glia metabolic coupling and plasticity. *J Exp Biol,* 209**,** 2304-11.

Mangialasche, F., Solomon, A., Winblad, B., Mecocci, P. & Kivipelto, M. 2010. Alzheimer's disease: clinical trials and drug development. *Lancet Neurol,* 9**,** 702-16.

Mattson, M. P. & Chan, S. L. 2003. Neuronal and glial calcium signaling in Alzheimer's disease. *Cell Calcium,* 34**,** 385-97.

Mccormack, S. E., Shaham, O., Mccarthy, M. A., Deik, A. A., Wang, T. J., Gerszten, R. E., Clish, C. B., Mootha, V. K., Grinspoon, S. K. & Fleischman, A. 2013. Circulating branched-chain amino acid concentrations are associated with obesity and future insulin resistance in children and adolescents. *Pediatr Obes,* 8**,** 52-61.

Mckhann, G., Drachman, D., Folstein, M., Katzman, R., Price, D. & Stadlan, E. M. 1984. Clinical diagnosis of Alzheimer's disease: report of the NINCDS-ADRDA Work Group under the auspices of Department of Health and Human Services Task Force on Alzheimer's Disease. *Neurology,* 34**,** 939-44.

Meijer, A. J. & Codogno, P. 2008. Nutrient sensing: TOR's Ragtime. *Nat Cell Biol,* 10**,** 881-3.

Menkes, J. H. 1962. Maple syrup disease and other disorders of keto acid metabolism. *Res Publ Assoc Res Nerv Ment Dis,* 40**,** 69-93.

Mielke, M. M., Hagen, C. E., Wennberg, A. M. V., Airey, D. C., Savica, R., Knopman, D. S., Machulda, M. M., Roberts, R. O., Jack, C. R., Jr., Petersen, R. C. & Dage, J. L. 2017. Association of Plasma Total Tau Level With Cognitive Decline and Risk of Mild Cognitive Impairment or Dementia in the Mayo Clinic Study on Aging. *JAMA Neurol,* 74**,** 1073-1080.

Mielke, M. M., Hagen, C. E., Xu, J., Chai, X., Vemuri, P., Lowe, V. J., Airey, D. C., Knopman, D. S., Roberts, R. O., Machulda, M. M., Jack, C. R., Jr., Petersen, R. C. & Dage, J. L. 2018. Plasma phospho-tau181 increases with Alzheimer's disease clinical severity and is associated with tau- and amyloid-positron emission tomography. *Alzheimers Dement,* 14**,** 989-997.

Minati, L., Edginton, T., Bruzzone, M. G. & Giaccone, G. 2009. Current concepts in Alzheimer's disease: a multidisciplinary review. *Am J Alzheimers Dis Other Demen,* 24**,** 95-121.

Mochel, F., Benaich, S., Rabier, D. & Durr, A. 2011. Validation of plasma branched chain amino acids as biomarkers in Huntington disease. *Arch Neurol,* 68**,** 265-7.

Mochel, F., Charles, P., Seguin, F., Barritault, J., Coussieu, C., Perin, L., Le Bouc, Y., Gervais, C., Carcelain, G., Vassault, A., Feingold, J., Rabier, D. & Durr, A. 2007. Early energy deficit in Huntington disease: identification of a plasma biomarker traceable during disease progression. *PLoS One,* 2**,** e647.

Moore, S., Spackman, D. H. & Stein, W. H. 1958. Chromatography of Amino Acids on Sulfonated Polystyrene Resins. An Improved System. *Analytical Chemistry,* 30**,** 1185-1190.

Moraes, M. U. & Gaudet, T. J. 2018. Immunotherapeutic and pharmacological approaches for the treatment of Alzheimer's disease. *Bioscience Horizons: The International Journal of Student Research,* 11.

Morley, J. E. & Farr, S. A. 2014. The role of amyloid-beta in the regulation of memory. *Biochem Pharmacol,* 88**,** 479-85.

Mosconi, L., Tsui, W. H., Herholz, K., Pupi, A., Drzezga, A., Lucignani, G., Reiman, E. M., Holthoff, V., Kalbe, E., Sorbi, S., Diehl-Schmid, J., Perneczky, R., Clerici, F., Caselli, R., Beuthien-Baumann, B., Kurz, A., Minoshima, S. & De Leon, M. J. 2008. Multicenter standardized 18F-FDG PET diagnosis of mild cognitive impairment, Alzheimer's disease, and other dementias. *J Nucl Med,* 49**,** 390-8.

Motter, R., Vigo-Pelfrey, C., Kholodenko, D., Barbour, R., Johnson-Wood, K., Galasko, D., Chang, L., Miller, B., Clark, C., Green, R. & Et Al. 1995. Reduction of beta-amyloid peptide42 in the cerebrospinal fluid of patients with Alzheimer's disease. *Ann Neurol,* 38**,** 643-8.

Murakami, T., Matsuo, M., Shimizu, A. & Shimomura, Y. 2005. Dissociation of branched-chain alpha-keto acid dehydrogenase kinase (BDK) from branched-chain alpha-keto acid dehydrogenase complex (BCKDC) by BDK inhibitors. *J Nutr Sci Vitaminol (Tokyo),* 51**,** 48-50.

Murman, D. L. 2015. The Impact of Age on Cognition. *Semin Hear,* 36**,** 111-21.

Murphy, M. P. & Levine, H., 3rd 2010. Alzheimer's disease and the amyloid-beta peptide. *J Alzheimers Dis,* 19**,** 311-23.

Nakamura, A., Kaneko, N., Villemagne, V. L., Kato, T., Doecke, J., Dore, V., Fowler, C., Li, Q. X., Martins, R., Rowe, C., Tomita, T., Matsuzaki, K., Ishii, K., Ishii, K., Arahata, Y., Iwamoto, S., Ito, K., Tanaka, K., Masters, C. L. & Yanagisawa, K. 2018. High performance plasma amyloid-beta biomarkers for Alzheimer's disease. *Nature,* 554**,** 249-254.

Nakashima, H., Ishihara, T., Suguimoto, P., Yokota, O., Oshima, E., Kugo, A., Terada, S., Hamamura, T., Trojanowski, J. Q., Lee, V. M. & Kuroda, S. 2005. Chronic lithium treatment decreases tau lesions by promoting ubiquitination in a mouse model of tauopathies. *Acta Neuropathol,* 110**,** 547-56.

Naoi, M. & Maruyama, W. 1999. Cell death of dopamine neurons in aging and Parkinson's disease. *Mech Ageing Dev,* 111**,** 175-88.

Narayan, S. B., Ditewig-Meyers, G., Graham, K. S., Scott, R. & Bennett, M. J. 2011. Measurement of plasma amino acids by Ultraperformance(R) Liquid Chromatography. *Clin Chem Lab Med,* 49**,** 1177-85.

Newgard, C. B., An, J., Bain, J. R., Muehlbauer, M. J., Stevens, R. D., Lien, L. F., Haqq, A. M., Shah, S. H., Arlotto, M., Slentz, C. A., Rochon, J., Gallup, D., Ilkayeva, O., Wenner, B. R., Yancy, W. S., Jr., Eisenson, H., Musante, G., Surwit, R. S., Millington, D. S., Butler, M. D. & Svetkey, L. P. 2009. A branched-chain amino acid-related metabolic signature that differentiates obese and lean humans and contributes to insulin resistance. *Cell Metab,* 9**,** 311-26.

Niikura, T., Tajima, H. & Kita, Y. 2006. Neuronal cell death in Alzheimer's disease and a neuroprotective factor, humanin. *Curr Neuropharmacol,* 4**,** 139-47.

Nilsson, P. & Saido, T. C. 2014. Dual roles for autophagy: degradation and secretion of Alzheimer's disease Abeta peptide. *Bioessays,* 36**,** 570-8.

Nixon, R. A. 2007. Autophagy, amyloidogenesis and Alzheimer disease. *J Cell Sci,* 120**,** 4081-91.

Nixon, R. A., Wegiel, J., Kumar, A., Yu, W. H., Peterhoff, C., Cataldo, A. & Cuervo, A. M. 2005. Extensive Involvement of Autophagy in Alzheimer Disease: An Immuno-Electron Microscopy Study. *Journal of Neuropathology & Experimental Neurology,* 64**,** 113-122.

Noble, W., Planel, E., Zehr, C., Olm, V., Meyerson, J., Suleman, F., Gaynor, K., Wang, L., Lafrancois, J., Feinstein, B., Burns, M., Krishnamurthy, P., Wen, Y., Bhat, R., Lewis, J., Dickson, D. & Duff, K. 2005. Inhibition of glycogen synthase kinase-3 by lithium correlates with reduced tauopathy and degeneration in vivo. *Proc Natl Acad Sci U S A,* 102**,** 6990-5.

O'brien, J. T., Firbank, M. J., Davison, C., Barnett, N., Bamford, C., Donaldson, C., Olsen, K., Herholz, K., Williams, D. & Lloyd, J. 2014. 18F-FDG PET and perfusion SPECT in the diagnosis of Alzheimer and Lewy body dementias. *J Nucl Med,* 55**,** 1959-65.

Ogawa, S., Lee, T. M., Kay, A. R. & Tank, D. W. 1990. Brain magnetic resonance imaging with contrast dependent on blood oxygenation. *Proc Natl Acad Sci U S A,* 87**,** 9868-72.

Olabarria, M., Noristani, H. N., Verkhratsky, A. & Rodriguez, J. J. 2011. Age-dependent decrease in glutamine synthetase expression in the hippocampal astroglia of the triple transgenic Alzheimer's disease mouse model: mechanism for deficient glutamatergic transmission? *Mol Neurodegener,* 6**,** 55.

Olsson, B., Blennow, K. & Zetterberg, H. 2016. The clinical value of fluid biomarkers for dementia diagnosis - Authors' reply. *Lancet Neurol,* 15**,** 1204-1205.

Orr, M. E. & Oddo, S. 2013. Autophagic/lysosomal dysfunction in Alzheimer's disease. *Alzheimers Res Ther,* 5**,** 53.

Ovod, V., Ramsey, K. N., Mawuenyega, K. G., Bollinger, J. G., Hicks, T., Schneider, T., Sullivan, M., Paumier, K., Holtzman, D. M., Morris, J. C., Benzinger, T., Fagan, A. M., Patterson, B. W. & Bateman, R. J. 2017. Amyloid beta concentrations and stable isotope labeling kinetics of human plasma specific to central nervous system amyloidosis. *Alzheimers Dement,* 13**,** 841-849.

Parisi, J. M., Rebok, G. W., Xue, Q.-L., Fried, L. P., Seeman, T. E., Tanner, E. K., Gruenewald, T. L., Frick, K. D. & Carlson, M. C. 2012. The Role of Education and Intellectual Activity on Cognition. *Journal of Aging Research,* 2012**,** 9.

Pase, M. P., Beiser, A. S., Himali, J. J., Satizabal, C. L., Aparicio, H. J., Decarli, C., Chene, G., Dufouil, C. & Seshadri, S. 2019. Assessment of Plasma Total Tau Level as a Predictive Biomarker for Dementia and Related Endophenotypes. *JAMA Neurol,* 76**,** 598-606.

Pattingre, S., Tassa, A., Qu, X., Garuti, R., Liang, X. H., Mizushima, N., Packer, M., Schneider, M. D. & Levine, B. 2005. Bcl-2 antiapoptotic proteins inhibit Beclin 1-dependent autophagy. *Cell,* 122**,** 927-39.

Perez, S. E., He, B., Nadeem, M., Wuu, J., Ginsberg, S. D., Ikonomovic, M. D. & Mufson, E. J. 2015. Hippocampal endosomal, lysosomal, and autophagic dysregulation in mild cognitive impairment: correlation with abeta and tau pathology. *J Neuropathol Exp Neurol,* 74**,** 345-58.

Petersen, R. C. 2004. Mild cognitive impairment as a diagnostic entity. *J Intern Med,* 256**,** 183-94.

Petersen, R. C. 2007. The current status of mild cognitive impairment--what do we tell our patients? *Nat Clin Pract Neurol,* 3**,** 60-1.

Petersen, R. C., Smith, G. E., Waring, S. C., Ivnik, R. J., Tangalos, E. G. & Kokmen, E. 1999. Mild cognitive impairment: clinical characterization and outcome. *Arch Neurol,* 56**,** 303-8.

Peterson, T. R., Laplante, M., Thoreen, C. C., Sancak, Y., Kang, S. A., Kuehl, W. M., Gray, N. S. & Sabatini, D. M. 2009. DEPTOR is an mTOR inhibitor frequently overexpressed in multiple myeloma cells and required for their survival. *Cell,* 137**,** 873-86.

Pickford, F., Masliah, E., Britschgi, M., Lucin, K., Narasimhan, R., Jaeger, P. A., Small, S., Spencer, B., Rockenstein, E., Levine, B. & Wyss-Coray, T. 2008. The autophagy-related protein beclin 1 shows reduced expression in early Alzheimer disease and regulates amyloid beta accumulation in mice. *J Clin Invest,* 118**,** 2190-9.

Piraud, M., Vianey-Saban, C., Petritis, K., Elfakir, C., Steghens, J.-P. & Bouchu, D. 2005. Ion-pairing reversed-phase liquid chromatography/electrospray ionization mass spectrometric analysis of 76 underivatized amino acids of biological interest: a new tool for the diagnosis of inherited disorders of amino acid metabolism. *Rapid Communications in Mass Spectrometry,* 19**,** 1587-1602.

Piraud, M., Vianey-Saban, C., Petritis, K., Elfakir, C., Steghens, J.-P., Morla, A. & Bouchu, D. 2003. ESI-MS/MS analysis of underivatised amino acids: a new tool for the diagnosis of inherited disorders of amino acid metabolism. Fragmentation study of 79 molecules of biological interest in positive and negative ionisation mode. *Rapid Communications in Mass Spectrometry,* 17**,** 1297-1311.

Platell, C., Kong, S. E., Mccauley, R. & Hall, J. C. 2000. Branched-chain amino acids. *J Gastroenterol Hepatol,* 15**,** 706-17.

Prince, M., Comas-Herrera, A., Knapp, M., Guerchet, M. L. & Karagiannidou, M. 2016. World Alzheimer report 2016: improving healthcare for people living with dementia: coverage, quality and costs now and in the future. *Alzheimer's Disease International*.

Puig, K. L. & Combs, C. K. 2013. Expression and function of APP and its metabolites outside the central nervous system. *Exp Gerontol,* 48**,** 608-11.

Puzzo, D. & Arancio, O. 2013. Amyloid-beta peptide: Dr. Jekyll or Mr. Hyde? *J Alzheimers Dis,* 33 Suppl 1**,** S111-20.

Rabanal-Ruiz, Y., Otten, E. G. & Korolchuk, V. I. 2017. mTORC1 as the main gateway to autophagy. *Essays Biochem,* 61**,** 565-584.

Rees, T. M. & Brimijoin, S. 2003. The role of acetylcholinesterase in the pathogenesis of Alzheimer's disease. *Drugs Today (Barc),* 39**,** 75-83.

Restrepo, L., Stafford, P. & Johnston, S. A. 2013. Feasibility of an early Alzheimer's disease immunosignature diagnostic test. *J Neuroimmunol,* 254**,** 154-60.

Revett, T. J., Baker, G. B., Jhamandas, J. & Kar, S. 2013. Glutamate system, amyloid ss peptides and tau protein: functional interrelationships and relevance to Alzheimer disease pathology. *J Psychiatry Neurosci,* 38**,** 6-23.

Rice, L. & Bisdas, S. 2017. The diagnostic value of FDG and amyloid PET in Alzheimer's disease-A systematic review. *Eur J Radiol,* 94**,** 16-24.

Riedel, G., Platt, B. & Micheau, J. 2003. Glutamate receptor function in learning and memory. *Behav Brain Res,* 140**,** 1-47.

Rocher, A. B., Chapon, F., Blaizot, X., Baron, J. C. & Chavoix, C. 2003. Resting-state brain glucose utilization as measured by PET is directly related to regional synaptophysin levels: a study in baboons. *Neuroimage,* 20**,** 1894-8.

Rohn, T. T., Wirawan, E., Brown, R. J., Harris, J. R., Masliah, E. & Vandenabeele, P. 2011. Depletion of Beclin-1 due to proteolytic cleavage by caspases in the Alzheimer's disease brain. *Neurobiol Dis,* 43**,** 68-78.

Rombouts, S. A., Barkhof, F., Veltman, D. J., Machielsen, W. C., Witter, M. P., Bierlaagh, M. A., Lazeron, R. H., Valk, J. & Scheltens, P. 2000. Functional MR imaging in Alzheimer's disease during memory encoding. *AJNR Am J Neuroradiol,* 21**,** 1869-75.

Rupsingh, R., Borrie, M., Smith, M., Wells, J. L. & Bartha, R. 2011. Reduced hippocampal glutamate in Alzheimer disease. *Neurobiol Aging,* 32**,** 802-10.

Saftig, P., Beertsen, W. & Eskelinen, E. L. 2008. LAMP-2: a control step for phagosome and autophagosome maturation. *Autophagy,* 4**,** 510-2.

Sandlers, Y. 2019. Amino Acids Profiling for the Diagnosis of Metabolic Disorders [Online First]. *IntechOpen* [Online].

Sattler, R. & Tymianski, M. 2000. Molecular mechanisms of calcium-dependent excitotoxicity. *J Mol Med (Berl),* 78**,** 3-13.

Saunders, A. M., Strittmatter, W. J., Schmechel, D., George-Hyslop, P. H., Pericak-Vance, M. A., Joo, S. H., Rosi, B. L., Gusella, J. F., Crapper-Maclachlan, D. R., Alberts, M. J. & Et Al. 1993. Association of apolipoprotein E allele epsilon 4 with late-onset familial and sporadic Alzheimer's disease. *Neurology,* 43**,** 1467-72.

Saxton, R. A. & Sabatini, D. M. 2017. mTOR Signaling in Growth, Metabolism, and Disease. *Cell,* 168**,** 960-976.

Schrijvers, E. M., Koudstaal, P. J., Hofman, A. & Breteler, M. M. 2011. Plasma clusterin and the risk of Alzheimer disease. *JAMA,* 305**,** 1322-6.

Selkoe, D. J. 2001. Alzheimer's disease: genes, proteins, and therapy. *Physiol Rev,* 81**,** 741-66.

Selkoe, D. J. 2002. Alzheimer's disease is a synaptic failure. *Science,* 298**,** 789-91.

Seubert, P., Vigo-Pelfrey, C., Esch, F., Lee, M., Dovey, H., Davis, D., Sinha, S., Schlossmacher, M., Whaley, J., Swindlehurst, C. & Et Al. 1992. Isolation and quantification of soluble Alzheimer's beta-peptide from biological fluids. *Nature,* 359**,** 325-7.

Shafei, M. A., Harris, M. & Conway, M. E. 2017. Divergent Metabolic Regulation of Autophagy and mTORC1—Early Events in Alzheimer’s Disease? *Frontiers in Aging Neuroscience,* 9.

Sharma, B., Lawrence, D. W. & Hutchison, M. G. 2018. Branched Chain Amino Acids (BCAAs) and Traumatic Brain Injury: A Systematic Review. *J Head Trauma Rehabil,* 33**,** 33-45.

Sharp, T., Bramwell, S. R. & Grahame-Smith, D. G. 1992. Effect of acute administration of L-tryptophan on the release of 5-HT in rat hippocampus in relation

to serotoninergic neuronal activity: an in vivo microdialysis study. *Life Sci,* 50**,** 1215-23.

Shen, Y., Wang, H., Sun, Q., Yao, H., Keegan, A. P., Mullan, M., Wilson, J., Lista, S., Leyhe, T., Laske, C., Rujescu, D., Levey, A., Wallin, A., Blennow, K., Li, R. & Hampel, H. 2018. Increased Plasma Beta-Secretase 1 May Predict Conversion to Alzheimer's Disease Dementia in Individuals With Mild Cognitive Impairment. *Biol Psychiatry,* 83**,** 447-455.

Shivamurthy, V. K., Tahari, A. K., Marcus, C. & Subramaniam, R. M. 2015. Brain FDG PET and the diagnosis of dementia. *AJR Am J Roentgenol,* 204**,** W76-85.

Shoji, M., Matsubara, E., Kanai, M., Watanabe, M., Nakamura, T., Tomidokoro, Y., Shizuka, M., Wakabayashi, K., Igeta, Y., Ikeda, Y., Mizushima, K., Amari, M., Ishiguro, K., Kawarabayashi, T., Harigaya, Y., Okamoto, K. & Hirai, S. 1998. Combination assay of CSF tau, A beta 1-40 and A beta 1-42(43) as a biochemical marker of Alzheimer's disease. *J Neurol Sci,* 158**,** 134-40.

Small, S. A. & Petsko, G. A. 2015. Retromer in Alzheimer disease, Parkinson disease and other neurological disorders. *Nature Reviews Neuroscience,* 16**,** 126.

Smith, A. D., Smith, S. M., De Jager, C. A., Whitbread, P., Johnston, C., Agacinski, G., Oulhaj, A., Bradley, K. M., Jacoby, R. & Refsum, H. 2010. Homocysteine-lowering by B vitamins slows the rate of accelerated brain atrophy in mild cognitive impairment: a randomized controlled trial. *PLoS One,* 5**,** e12244.

Sokolow, S., Luu, S. H., Nandy, K., Miller, C. A., Vinters, H. V., Poon, W. W. & Gylys, K. H. 2012. Preferential accumulation of amyloid-beta in presynaptic glutamatergic terminals (VGluT1 and VGluT2) in Alzheimer's disease cortex. *Neurobiol Dis,* 45**,** 381-7.

Sontag, E., Nunbhakdi-Craig, V., Lee, G., Bloom, G. S. & Mumby, M. C. 1996. Regulation of the phosphorylation state and microtubule-binding activity of Tau by protein phosphatase 2A. *Neuron,* 17**,** 1201-7.

Sontag, E., Nunbhakdi-Craig, V., Lee, G., Brandt, R., Kamibayashi, C., Kuret, J., White, C. L., 3rd, Mumby, M. C. & Bloom, G. S. 1999. Molecular interactions among protein phosphatase 2A, tau, and microtubules. Implications for the regulation of tau phosphorylation and the development of tauopathies. *J Biol Chem,* 274**,** 25490-8.

Stern, Y. 2009. Cognitive reserve. *Neuropsychologia,* 47**,** 2015-28.

Stern, Y., Gurland, B., Tatemichi, T. K., Tang, M. X., Wilder, D. & Mayeux, R. 1994. Influence of education and occupation on the incidence of Alzheimer's disease. *JAMA,* 271**,** 1004-10.

Stoothoff, W. H. & Johnson, G. V. 2005. Tau phosphorylation: physiological and pathological consequences. *Biochim Biophys Acta,* 1739**,** 280-97.

Sutphen, C. L., Fagan, A. M. & Holtzman, D. M. 2014. Progress update: fluid and imaging biomarkers in Alzheimer's disease. *Biol Psychiatry,* 75**,** 520-6.

Tampellini, D., Rahman, N., Gallo, E. F., Huang, Z., Dumont, M., Capetillo-Zarate, E., Ma, T., Zheng, R., Lu, B., Nanus, D. M., Lin, M. T. & Gouras, G. K. 2009. Synaptic activity reduces intraneuronal Abeta, promotes APP transport to synapses, and protects against Abeta-related synaptic alterations. *J Neurosci,* 29**,** 9704-13.

Tan, L., Yu, J. T., Tan, M. S., Liu, Q. Y., Wang, H. F., Zhang, W., Jiang, T. & Tan, L. 2014. Genome-wide serum microRNA expression profiling identifies serum biomarkers for Alzheimer's disease. *J Alzheimers Dis,* 40**,** 1017-27.

Tatebe, H., Kasai, T., Ohmichi, T., Kishi, Y., Kakeya, T., Waragai, M., Kondo, M., Allsop, D. & Tokuda, T. 2017. Quantification of plasma phosphorylated tau to use as a biomarker for brain Alzheimer pathology: pilot case-control studies including patients with Alzheimer's disease and down syndrome. *Mol Neurodegener,* 12**,** 63.

Thal, D. R., Attems, J. & Ewers, M. 2014. Spreading of amyloid, tau, and microvascular pathology in Alzheimer's disease: findings from neuropathological and neuroimaging studies. *J Alzheimers Dis,* 42 Suppl 4**,** S421-9.

Thambisetty, M., Simmons, A., Velayudhan, L., Hye, A., Campbell, J., Zhang, Y., Wahlund, L. O., Westman, E., Kinsey, A., Guntert, A., Proitsi, P., Powell, J., Causevic, M., Killick, R., Lunnon, K., Lynham, S., Broadstock, M., Choudhry, F., Howlett, D. R., Williams, R. J., Sharp, S. I., Mitchelmore, C., Tunnard, C., Leung, R., Foy, C., O'brien, D., Breen, G., Furney, S. J., Ward, M., Kloszewska, I., Mecocci, P., Soininen, H., Tsolaki, M., Vellas, B., Hodges, A., Murphy, D. G., Parkins, S., Richardson, J. C., Resnick, S. M., Ferrucci, L., Wong, D. F., Zhou, Y., Muehlboeck, S., Evans, A., Francis, P. T., Spenger, C. & Lovestone, S. 2010. Association of plasma clusterin concentration with severity, pathology, and progression in Alzheimer disease. *Arch Gen Psychiatry,* 67**,** 739-48.

Tolboom, N., Van Der Flier, W. M., Yaqub, M., Boellaard, R., Verwey, N. A., Blankenstein, M. A., Windhorst, A. D., Scheltens, P., Lammertsma, A. A. & Van Berckel, B. N. 2009. Relationship of cerebrospinal fluid markers to 11C-PiB and 18F-FDDNP binding. *J Nucl Med,* 50**,** 1464-70.

Trotti, D., Aoki, M., Pasinelli, P., Berger, U. V., Danbolt, N. C., Brown, R. H., Jr. & Hediger, M. A. 2001. Amyotrophic lateral sclerosis-linked glutamate transporter mutant has impaired glutamate clearance capacity. *J Biol Chem,* 276**,** 576-82.

Tschanz, J. T., Welsh-Bohmer, K. A., Lyketsos, C. G., Corcoran, C., Green, R. C., Hayden, K., Norton, M. C., Zandi, P. P., Toone, L., West, N. A., Breitner, J. C. & Cache County, I. 2006. Conversion to dementia from mild cognitive disorder: the Cache County Study. *Neurology,* 67**,** 229-34.

U.S. Department of Agriculture, A. R. S. 2004. USDA National Nutrient Database for Standard Reference. Nutrient Data Laboratory Home Page.

Uddin, M. S., Mamun, A. A., Labu, Z. K., Hidalgo-Lanussa, O., Barreto, G. E. & Ashraf, G. M. 2019. Autophagic dysfunction in Alzheimer's disease: Cellular and molecular mechanistic approaches to halt Alzheimer's pathogenesis. *J Cell Physiol,* 234**,** 8094-8112.

Van Cauwenberghe, C., Van Broeckhoven, C. & Sleegers, K. 2016. The genetic landscape of Alzheimer disease: clinical implications and perspectives. *Genet Med,* 18**,** 421-30.

Viola, K. L., Sbarboro, J., Sureka, R., De, M., Bicca, M. A., Wang, J., Vasavada, S., Satpathy, S., Wu, S., Joshi, H., Velasco, P. T., Macrenaris, K., Waters, E. A., Lu, C., Phan, J., Lacor, P., Prasad, P., Dravid, V. P. & Klein, W. L. 2015. Towards non-invasive diagnostic imaging of early-stage Alzheimer's disease. *Nat Nanotechnol,* 10**,** 91-8.

Vuille-Dit-Bille, R. N., Ha-Huy, R. & Stover, J. F. 2012. Changes in plasma phenylalanine, isoleucine, leucine, and valine are associated with significant changes in intracranial pressure and jugular venous oxygen saturation in patients with severe traumatic brain injury. *Amino Acids,* 43**,** 1287-96.

W.H.O. 2019. *Dementia* [Online]. Available: https://www.who.int/news-room/fact-sheets/detail/dementia [Accessed].

Walker, V. & Mills, G. A. 1995. Quantitative methods for amino acid analysis in biological fluids. *Ann Clin Biochem,* 32 (Pt 1)**,** 28-57.

Wallin, A. K., Blennow, K., Zetterberg, H., Londos, E., Minthon, L. & Hansson, O. 2010. CSF biomarkers predict a more malignant outcome in Alzheimer disease. *Neurology,* 74**,** 1531-7.

Walsh, D. M. & Selkoe, D. J. 2007. A beta oligomers - a decade of discovery. *J Neurochem,* 101**,** 1172-84.

Wang, R. & Reddy, P. H. 2017. Role of Glutamate and NMDA Receptors in Alzheimer's Disease. *J Alzheimers Dis,* 57**,** 1041-1048.

Wang, X. L., Li, C. J., Xing, Y., Yang, Y. H. & Jia, J. P. 2015. Hypervalinemia and hyperleucine-isoleucinemia caused by mutations in the branched-chain-amino-acid aminotransferase gene. *J Inherit Metab Dis,* 38**,** 855-61.

Weigand, S. D., Vemuri, P., Wiste, H. J., Senjem, M. L., Pankratz, V. S., Aisen, P. S., Weiner, M. W., Petersen, R. C., Shaw, L. M., Trojanowski, J. Q., Knopman, D. S., Jack, C. R., Jr. & Alzheimer's Disease Neuroimaging, I. 2011. Transforming cerebrospinal fluid Abeta42 measures into calculated Pittsburgh Compound B units of brain Abeta amyloid. *Alzheimers Dement,* 7**,** 133-41.

Weingarten, M. D., Lockwood, A. H., Hwo, S. Y. & Kirschner, M. W. 1975. A protein factor essential for microtubule assembly. *Proc Natl Acad Sci U S A,* 72**,** 1858-62.

Willette, A. A., Calhoun, V. D., Egan, J. M., Kapogiannis, D. & Alzheimers Disease Neuroimaging, I. 2014. Prognostic classification of mild cognitive impairment and Alzheimer's disease: MRI independent component analysis. *Psychiatry Res,* 224**,** 81-8.

Wilson, R. S., Hebert, L. E., Scherr, P. A., Barnes, L. L., Mendes De Leon, C. F. & Evans, D. A. 2009. Educational attainment and cognitive decline in old age. *Neurology,* 72**,** 460-5.

Winslow, A. R. & Rubinsztein, D. C. 2008. Autophagy in neurodegeneration and development. *Biochim Biophys Acta,* 1782**,** 723-9.

Witgen, B. M., Lifshitz, J., Smith, M. L., Schwarzbach, E., Liang, S. L., Grady, M. S. & Cohen, A. S. 2005. Regional hippocampal alteration associated with cognitive

deficit following experimental brain injury: a systems, network and cellular evaluation. *Neuroscience,* 133**,** 1-15.

Wolk, D. A. & Dickerson, B. 2019. *Clinical features and diagnosis of Alzheimer disease - UpToDate* [Online]. Available: https://www.uptodate.com/contents/clinical-features-and-diagnosis-of-alzheimer-disease [Accessed].

Wolozin, B. & Davies, P. 1987. Alzheimer-related neuronal protein A68: specificity and distribution. *Ann Neurol,* 22**,** 521-6.

Wong, E. & Cuervo, A. M. 2010. Autophagy gone awry in neurodegenerative diseases. *Nat Neurosci,* 13**,** 805-11.

Wood, B., Knight, M. J., Tsivos, D., Oliver, R., Coulthard, E. & Kauppinen, R. 2015. Magnetic resonance scanning and segmentation procedure at 3T for volumetry of human hippocampal subfields. *Biomedical Spectroscopy and Imaging,* 4**,** 197-208.

Woolf, N. J. & Butcher, L. L. 2011. Cholinergic systems mediate action from movement to higher consciousness. *Behav Brain Res,* 221**,** 488-98.

Xie, Y., Kang, R. & Tang, D. 2016. Chapter 2 - Role of the Beclin 1 Network in the Cross-Regulation Between Autophagy and Apoptosis. *In:* HAYAT, M. A. (ed.) *Autophagy: Cancer, Other Pathologies, Inflammation, Immunity, Infection, and Aging.* San Diego: Academic Press.

Xie, Z. & Klionsky, D. J. 2007. Autophagosome formation: core machinery and adaptations. *Nat Cell Biol,* 9**,** 1102-9.

Yang, A. J., Chandswangbhuvana, D., Margol, L. & Glabe, C. G. 1998. Loss of endosomal/lysosomal membrane impermeability is an early event in amyloid Abeta1-42 pathogenesis. *J Neurosci Res,* 52**,** 691-8.

Yang, R., Dong, J., Guo, H., Li, H., Wang, S., Zhao, H., Zhou, W., Yu, S., Wang, M. & Chen, W. 2013. Rapid and precise measurement of serum branched-chain and aromatic amino acids by isotope dilution liquid chromatography tandem mass spectrometry. *PLoS One,* 8**,** e81144.

Yeh, C. Y., Verkhratsky, A., Terzieva, S. & Rodriguez, J. J. 2013. Glutamine synthetase in astrocytes from entorhinal cortex of the triple transgenic animal model

of Alzheimer's disease is not affected by pathological progression. *Biogerontology,* 14**,** 777-87.

Yu, W. H., Cuervo, A. M., Kumar, A., Peterhoff, C. M., Schmidt, S. D., Lee, J. H., Mohan, P. S., Mercken, M., Farmery, M. R., Tjernberg, L. O., Jiang, Y., Duff, K., Uchiyama, Y., Naslund, J., Mathews, P. M., Cataldo, A. M. & Nixon, R. A. 2005. Macroautophagy--a novel Beta-amyloid peptide-generating pathway activated in Alzheimer's disease. *J Cell Biol,* 171**,** 87-98.

Yudkoff, M. 1997. Brain metabolism of branched-chain amino acids. *Glia,* 21**,** 92-8.

Yudkoff, M., Daikhin, Y., Nissim, I., Horyn, O., Luhovyy, B., Lazarow, A. & Nissim, I. 2005. Brain amino acid requirements and toxicity: the example of leucine. *J Nutr,* 135**,** 1531S-8S.

Zahodne, L. B., Stern, Y. & Manly, J. J. 2015. Differing effects of education on cognitive decline in diverse elders with low versus high educational attainment. *Neuropsychology,* 29**,** 649-57.

Zetterberg, H. & Burnham, S. C. 2019. Blood-based molecular biomarkers for Alzheimer's disease. *Mol Brain,* 12**,** 26.

Zetterberg, H., Wilson, D., Andreasson, U., Minthon, L., Blennow, K., Randall, J. & Hansson, O. 2013. Plasma tau levels in Alzheimer's disease. *Alzheimers Res Ther,* 5**,** 9.

Zhang, K. & Kaufman, R. J. 2006. The unfolded protein response: a stress signaling pathway critical for health and disease. *Neurology,* 66**,** S102-9.

Zlokovic, B. V. 2008. The blood-brain barrier in health and chronic neurodegenerative disorders. *Neuron,* 57**,** 178-201.

Zumwalt, R. W., Desgres, J., Kuo, K. C., Pautz, J. E. & Gehrke, C. W. 1987. Amino acid analysis by capillary gas chromatography. *J Assoc Off Anal Chem,* 70**,** 253-62.

Zupancic, M., Mahajan, A. & Handa, K. 2011. Dementia with lewy bodies: diagnosis and management for primary care providers. *Prim Care Companion CNS Disord,* 13.